Tetrathiafulvalenes, Oligoacenenes, and Their Buckminsterfullerene Derivatives: The Brick and Mortar of Organic Electronics

Michael Bendikov* and Fred Wudl*

Department of Chemistry and Biochemistry and Exotic Materials Institute, University of California, Los Angeles, California 90095

Dmitrii F. Perepichka*

Centre Énergie, Matériaux et Télécommunications, Institut National de la Recherche Scientifique, 1650 Blvd. Lionel-Boulet, Varennes, Québec J3X 1S2, Canada

Received May 17, 2004

Contents

* To whom correspondence should be addressed. Michael Bendikov: present address, Department of Organic Chemistry, Weizmann Institute of Science, 76100 Rehovot, Israel; telephone, +972-8-9346028; fax, +972-8-9344142; e-mail, michael.bendikov@weizmann.ac.il. Fred Wudl: phone, (310) 206-0941; fax, (310) 825-0767; e-mail, wudl@chem.ucla.edu. Dmitrii F. Perepichka: phone, (450) 929 8152; fax, (450) 929 8102; e-mail, perepichka@inrs-emt.uquebec.ca.

1. Introduction

As follows from their name, the application of electronic materials is based on special behavior of electrons in such media. For organic (molecular) electronic materials, the behavior of a single electron, including electron transfer/transport, n-/p-doping processes, and so forth, depends primarily on the energy of the highest occupied molecular orbital (HOMO) and lowest unoccupied molecular orbital (LUMO) levels and the orbital interactions. By designing molecules with tunable HOMO and LUMO levels, one can achieve control over the properties of materials and the performance of the electronic devices based on them. The molecules with low HOMO/LUMO gaps are of particular importance due to their ability to easily donate (from HOMO) or accept (on LUMO) an electron, which is the basic process in all organic electronic devices. Although any molecule can, in theory, act as an electron donor and electron acceptor, only a few, so-called electrochemically amphoteric compounds, can do both within a readily accessible potential window, forming stable redox states. The value of the band gap (in organic semiconductors) and the conductance band formation (in organic metals) are directly connected with the position of HOMO/LUMO levels in individual molecules (as well as with intermolecular interactions in the solid). Finally, the molecules with a controlled

10.1021/cr030666m CCC: $48.50
Published on Web 10/26/2004

Michael Bendikov was born in 1971 in Kharkov, Ukraine. He moved to Israel in 1991, where he obtained a B.A. in Chemistry from Technion—Israel Institute of Technology. He received his M.Sc. (1996) and Ph.D. (2001) also from Technion, studying the chemistry of organosilicon compounds with Professor Y. Apeloig. During his Ph.D. studies he won The Israel Chemical Society Prize and the Wolf Foundation Prize for Ph.D. students. In 2001 he joined the group of Professor F. Wudl at UCLA as a postdoctoral research associate, and in June 2004 he started his independent research as a Senior Scientist at The Weizmann Institute of Science, Israel. His research interests include physical organic chemistry of novel electronic materials and computational chemistry.

Fred Wudl is the Dean M. Willard Professor of Chemistry and Materials and the Director of the Exotic Materials Institute at the University of California, Los Angeles. He was born in Cochabamba, Bolivia, in 1941 and moved to the United States in 1958. He received his B.S. (1964) and Ph.D. (1967) degrees in Chemistry at UCLA, where his dissertation work was done with Professor Donald J. Cram. After postdoctoral research with R. B. Woodward at Harvard, he joined the faculty of the State University of New York at Buffalo. He then moved, first in 1972 to AT&T Bell Laboratories and, subsequently, to the University of California, Santa Barbara, in 1982 and then on to UCLA in 1997. He is most widely known for his work on organic conductors and superconductors. He discovered the electronic conductivity of the precursor to the first organic metal and superconductor. In the recent past he has been interested in electronically conducting polymers, where he discovered the first transparent organic conductor and the first self-doped polymers. Currently he is interested in the optical and electrooptical properties of processable conjugated polymers as well as in the organic chemistry of fullerenes and the design and synthesis of self-mending polymers.

HOMO/LUMO gap are the prime targets for unimolecular electronic applications.

There are two basic strategies to endow a low HOMO/LUMO gap (or high electrochemical amphotericity) in organics: (i) by extending π-conjugation in the molecule and (ii) by construction of covalent D−A compounds (where D is a π-electron donor and A is a π-electron acceptor) in which the HOMO and

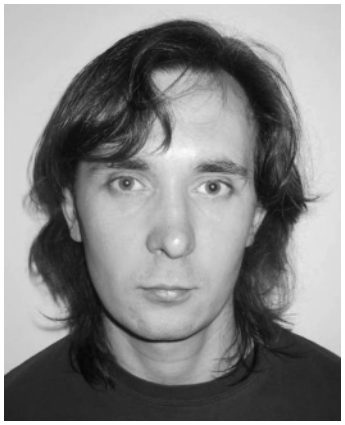

Dmitrii Perepichka was born in Ukraine in 1972. He received his Ph.D. in 1999 from the Institute of Physical Organic Chemistry (Ukrainian National Academy of Sciences) under Prof. A. F. Popov, for work on π-electron acceptors with push–pull functionality. Starting in 1999, he spent two years as a postdoctoral researcher with Prof. Martin Bryce at the University of Durham (U.K.), working on covalent linkage of strong electron acceptors and electron donors (such as TTF–TCNQ diads) for molecular electronics applications. In 2001 he joined the group of Prof. Fred Wudl at UCLA, where he was engaged in a number of projects, including synthesis of conjugated polymers and functionalization of carbon nanotubes. In 2003 Dr. Perepichka was appointed as an Assistant Professor at INRS-Énergie, Matériaux et Télécommunications (Québec), where he is developing research programs in the areas of molecular devices, nanostructured conjugated polymers, and the chemistry of carbon nanotubes.

LUMO orbitals can be tuned relatively independently. Both principles have been successfully realized in the design of π-conjugated polymers. For small closed-shell molecules, a narrow HOMO−LUMO gap is a rare characteristic, although it has been achieved, on the basis of the first strategy, in oligo(acenes) and in fullerene materials. There are also many examples of tuning the HOMO−LUMO gap on the basis of the second strategy, as exemplified by various tetrathiafulvalene−A derivatives.

Numerous derivatives of the sulfur heterocycle 2,2′-bis(1,3-dithiolylidene), mislabeled tetrathiafulvalene (TTF), are the subject of this review. The discovery, in the early 1970s (see below), of the unusual stability and solid-state properties of the radical cation resulting from a single-electron oxidation of the parent molecule led to subsequent formation of organic metals and eventually organic superconductors. Essentially all of these molecular solids are based on copious derivatives of TTF that were synthesized by clever organic chemists throughout the world in the last 30 years. Besides substitution of the peripheral hydrogen atoms by a myriad of groups, modifications include exchanging the sulfur atoms for selenium[1,2] and tellurium.[3−5] Clearly, with the large number of publications on TTF and its derivatives, it would be nearly impossible to cover the field as one article in *Chemical Reviews*. In what follows we will see only a glimpse into the fecundity of the field with coverage of synthetic design of small HOMO−LUMO gaps. The following classes of compounds are described: π-extended TTFs including TTF−acenes, conjugated TTF−acceptor compounds (TTF−σ-A), and, particularly, TTF−σ-fullerene systems.

The second section is devoted to oligo(acene) materials which are the focus of recent major research activities of chemists, physicists, and materials sci-

entists, primarily due to their application in organic field-effect transistors (OFETs). Reflecting the very limited number of review articles available in this field, we will present a general overview of the chemistry and physics of oligo(acene)s, although, within the scope of this *Chemical Reviews* article, particular attention will be given to the concept of small HOMO/LUMO gap and coverage of across-field materials: oligo(acene)-based sulfur heterocycles (except TTF−acenes) and oligo(acene)-fullerene conjugates.

2. Reducing the HOMO/LUMO Gap in TTF Derivatives

Since discovering the first organic conductors based on tetrathiafulvalene (TTF, **1**), [TTF]Cl in 1972[6] and metal TTF−TCNQ in 1973,[7] tetrathiafulvalene has been among the most studied heterocyclic systems.

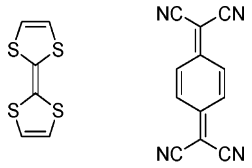

TTF, **1** TCNQ

By now, over 10 thousand papers reporting the synthesis, properties, and application of TTF derivatives, its complexes, and ion radical salts have appeared. The huge amount of research activity in the 1970s and 1980s has been directed toward achieving metallic conductivity and superconductivity in TTF derivatives, although no industrially important TTF-based materials have ever been created. However, the field of TTF chemistry is very much alive, and new functional TTF derivatives, making use of the electron-donor and charge-transfer complexing abilities of TTF, are being synthesized as materials for different applications, which include electrochemical switches, sensors, surface modification agents, and so forth. Several reviews outlining these new applications have been published in recent years.[8−11]

Although dibenzoTTF (**2**)[12] was synthesized in the 1920s and dimethyl- and diphenyl-[13] derivatives were reported in the 1960s, the broad interest in sulfur donors arose in the early 1970s with the synthesis of the unsubstituted TTF by Coffen,[14] Hünig,[15] and Wudl.[16] Coffen prepared it as part of a study of tetrathioethylenes, Hünig prepared it as part of an ongoing study of disproportionation of radical ions, and Wudl prepared it as a possible cathode of an all-organic battery. The later group was the first to show the rich science resulting from the redox properties of this molecule, which can form a stable radical cation and dication at rather low redox potentials. The good donor properties of TTF are partly due to aromatization energy gain when going from the dithiolylidene moiety in the neutral molecule to dithiolium aromatic rings in the oxidized states (Scheme 1). Gas-phase vertical ionization potential values in the range 6.4−7.0 eV have been reported for TTF (**1**).[17,18] The electrochemical redox potentials of TTF (**1**) ($E°_{1ox} = 0.34$ V, $E°_{2ox} = 0.78$ V vs Ag/AgCl in MeCN) are sensitive to substituents on the dithiole rings, and most substituents including the most

Scheme 1. Redox Transformation of TTF 1

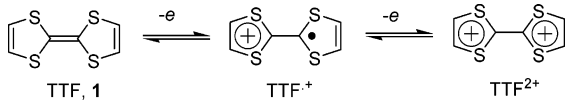

frequently used alkylthio groups act as electron acceptors. The only exception is due to alkyl groups, which decrease the oxidation potential by ∼15−30 mV per introduced methyl group.

The majority of TTF's applications are determined by the donor abilities of this molecule, which are the result of the high-lying HOMO. The LUMO energy in such compounds is, generally, also rather high, as good donors are usually poor acceptors. It is difficult but not impossible to combine the high HOMO and low LUMO in the same molecule, and the outcome of such a "marriage" can arise in fascinating electronic properties, such as, for example, in low-band-gap polymers. The design and properties of TTF-based materials combining the concepts of low oxidation potential and reduced HOMO−LUMO gap will be the subject of this section.

2.1. General Synthetic Approaches to Functionalized TTF Derivatives

Since the first synthesis of the TTF skeleton in compound **2**, a number of different synthetic methods with yields up to ∼90% have been elaborated (Scheme 2). As these have been exhaustively reviewed by

Scheme 2. Synthetic Methods for Construction of the TTF Skeleton (Reproduced with Permission from Ref 19a. Copyright 1987 Taylor & Francis Group.)

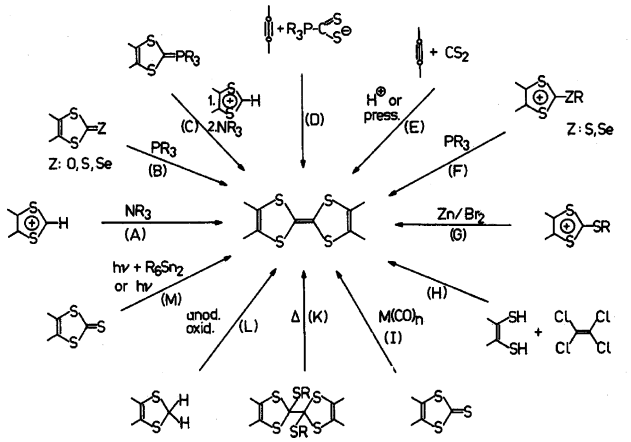

Fanghaenel and co-workers,[19] only a short overview is given here. The three most popular synthetic paths to the TTF nucleus are indicated in Scheme 2 by arrows A, B, and C (see also reviews by Gorgues et al., by Yamada et al., and by Fabre in this thematic issue of *Chemical Reviews*). The base- or phoshite-promoted coupling of dithiolium salts or dithiole-2-chalcones (methods A and B, respectively) are usually the most straightforward paths to symmetrical TTF derivatives. The asymmetric TTFs are easily accessible by method C, which includes a base-promoted coupling of a Witting reagent (usually generated by reaction of another dithiolium salt with phosphine). An important modification of this method was the

Scheme 3. Synthetic Routes to the Two Most Important TTF Precursors: (a) 1,3-Dithiole-2-thione and (b) the 1,3-Dithiolium Salt (Reproduced with Permission from Ref 19a. Copyright 1987 Taylor & Francis Group.)

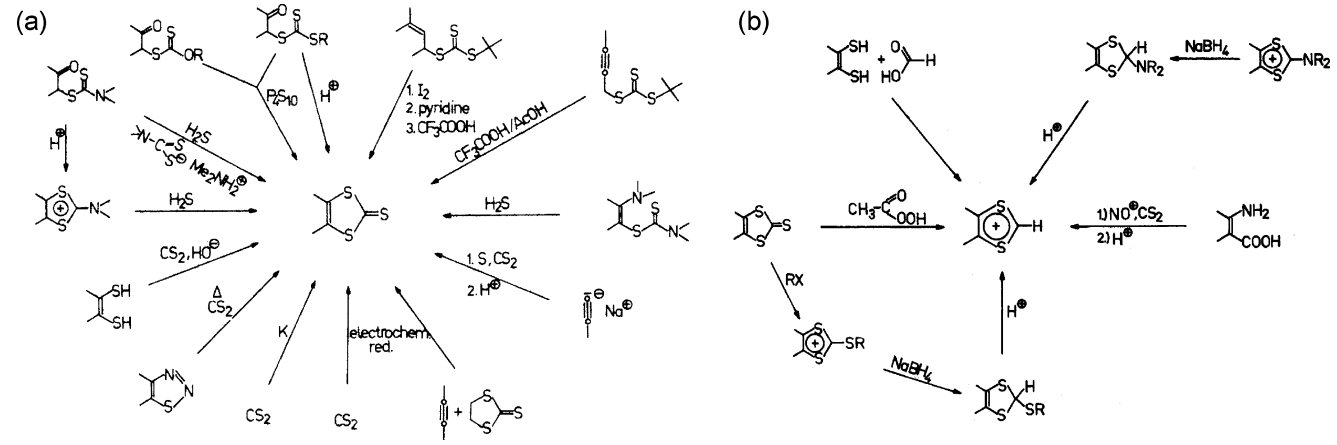

use of a phosphite derivative (Wittig−Horner reagent), which allowed to substantially increase the reaction yield. The starting 1,3-dithiole-2-thione and 1,3-dithiolium salts can be generated in a number of ways, as illustrated in Scheme 3.

The synthetic strategy toward functionalized TTF derivatives can, a priori, be based either on (a) construction of the TTF skeleton from functionalized precursors or on (b) functionalization of the preformed (nonfunctionalized) TTF compound. In the early days, the majority of synthetic efforts were based on strategy a, which gave birth to numerous components for organic metals and later afforded π-extended TTF derivatives (see section 2.2). On the other hand, the diversity of complex TTF derivatives described in this paper would have been highly unlikely without elaboration of some reliable reactions allowing the realization of strategy b. The most fertile among these were the approaches based on deprotection of S-(β-cyanoethyl)thioTTF, followed by alkylation of the resulting thiolate (Scheme 4a)[20] and

Scheme 4. Functionalization of TTF via (a) the Protecting (β-Cyanoethyl) Group Route, (b) the Lithiation Route, (c) the Diels−Alder Cyclization Route, and (d) the PyrroloTTF Route

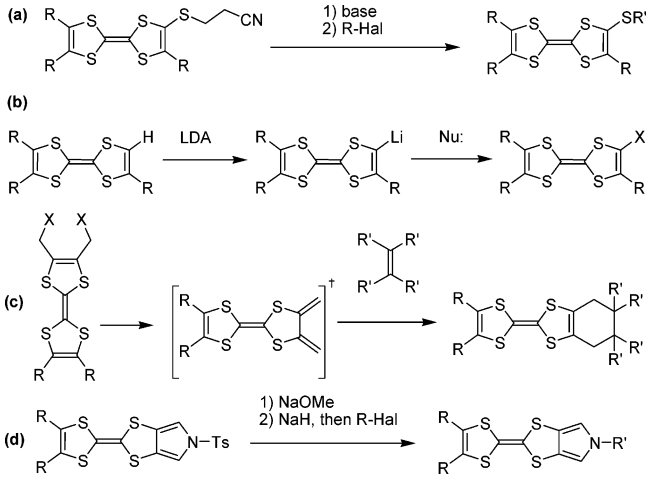

lithiation of the TTF molecule followed by reaction with a number of electrophilic agents, affording aldehydes, alcohols, carboxylic acids, and so forth (Scheme 4b), which are convenient synthons for further functionalization.[21] Among the other functionalization methods, we would like to mention two approaches which deliver symmetrical monofunctionalized TTF derivatives. The first is the Diels−Alder reaction of dimethylene[2H]TTF [generated in situ from bis(bromomethyl)TTF or 3-sulfolenoTTF] with different dienophiles (Scheme 4c), which was used in the synthesis of several annulated TTF−quinones (e.g., compounds **29**−**31** in section 2.3.1) and TTF−fullerene conjugates (e.g., compounds **106** and **114**−**116** in section 2.5.2). The second route, which was particularly effective in supramolecular chemistry,[9] is based on *N*-alkylation of mono-/bis-pyrroloTTF compounds.[22]

2.2. π-Extended TTFs and TTF−Acenes

The search for molecular metals in the 1970s and 1980s has given birth to the idea of extending the π-conjugated system of the TTF in order to decrease the intra- and intermolecular Coulombic repulsion between the charges on the molecules in the solid state (and thus improve the intermolecular interaction). The first π-extended TTF, dibenzo derivative **2**, was synthesized half a century before the parent molecule,[12] but its electron-donor properties were acknowledged much later (Chart 1). The annulated benzene rings have an electron-withdrawing influence, increasing the oxidation potential by ~250 mV with respect to the parent TTF (Table 1).[23] Several homologues of **2**, such as bisnaphthoTTF **3**[24] and bisphenanthroTTF **4**,[25] are known, and numerous benzene-fused oligomers[26,27] and a polymer[28] of type **5** were synthesized. For the oligomers **5**, multiredox behavior was documented (four and six reversible oxidation waves for $n = 1$ and 2, respectively[26b]), and reduction of the optical gap to 2.3 eV was shown for similar pyridazine-fused bis-TTF.[26a] However, even for the polymer **5**, no electrochemical amphotericity or significant (to less than 2 eV) reduction of the band gap was observed.[28]

Several heterocycle-annulated TTFs, such as bisfuranoTTF **6a**,[29] bis-pyrroloTTF **6b**,[30,31,22] bis-thiopheneTTF **6c**,[32] and bis-selenopheneTTF **6d**,[33] have been prepared (Chart 1). The tetramethylated de-

Table 1. Cyclic Voltammetry and Optical Absorption Data of Some π-Extended TTFs

compd	RE//solvent[a]	E°_{1ox}, V	E°_{2ox}, V	$E^\circ_{1ox} - E^\circ_{2ox}$, V	$h\nu$,[b] eV	ref
TTF, **1**	Ag/AgCl//PhCN	0.34	0.71	0.37		23
2	Ag/AgCl//PhCN	0.60	0.98	0.38		23
4	SCE//ODCB	0.52	0.98		3.2	25
6a	SCE//MeCN	0.72(p.a.)	1.03(p.a.)	0.31		29
6b	Ag/AgCl//MeCN	0.38	0.72	0.34		30
6c	SCE//DMF	0.78	0.96			34
7a	Ag/AgCl//MeCN	0.23(2e)		0		35b
8a	Ag/AgCl//MeCN	0.20	0.36	0.16		35b
8b	Ag/AgCl//DCM	0.48	0.71	0.23	2.89	36
10	SCE/MeCN	0.42(2e)		0	2.39	38b
11	Ag/AgCl//DCM−MeCN (1:1)	0.35	0.76, 1.09, 1.25	0.41		39
18a	SCE//MeCN	−0.11	−0.04	0.15	2.51	47
18b	not known	0.06[c]	0.33			48
19a	SCE//MeCN	0.00(2e)		0		47
19b	Ag/AgCl//MeCN	0.03(2e)[d]		0		49
19c	SCE//MeCN	0.18(2e)		0		47
20	SCE//MeCN	0.24(2e)		0		47
21a	SCE//DCM	0.44(2e)[e]		0	2.99	64
21b	Ag/AgCl//MeCN	0.55(2e, p.a.)		0		62
21c	Ag/AgCl//MeCN	0.48/0.35[f]		0		53
21d	Ag/AgCl//MeCN	0.43/0.07[f]		0		51
22	Ag/AgCl//DCM	0.28(2e, p.a.)	1.64, 2.2(p.c.)	0		54
23a	SCE//DCM	0.39(2e)[e]	1.47p	0	2.97	64
23b	SCE//DCM	0.55(2e)[e]	1.47p	0	2.94	64
23c	SCE//DCM	0.52(2e)[e]	1.45p	0	2.86	64
23d	Ag/AgCl//MeCN	0.41/0.09 (2e)		0		57
24a	SCE//DCM	0.50(2e)[e]	1.48p	0	3.07	64
24b	SCE//DCM	0.63(2e)[e]	1.41p	0	3.05	64
24c	SCE//DCM	0.65(2e)[e]	1.41p	0	2.95	64
25a	SCE//DCM	0.49(2e)[e]	1.31p		2.71	64
25b	SCE//DCM	0.59(2e)[e]			2.70	64
25c	SCE//DCM	0.59(2e)[e]			2.75	64
26a	Ag/AgCl//MeCN	0.48/0.01[f]				57
26b	Ag/AgCl//MeCN	0.45/0.11[f]				57

[a] RE = reference electrode. [b] The longest wavelength absorption maxima. [c] Determined as $E_{1/2}$ by differential pulse polarography of **18b**$^{2+}$. [d] Determined as the cathodic peak of the reduction of **19b**$^{2+}$. [e] Determined as the half-wave potential. [f] Quasi-reversible two-electron process; anodic and cathodic peak potentials are given.

Chart 1. Structures of Annulated TTFs

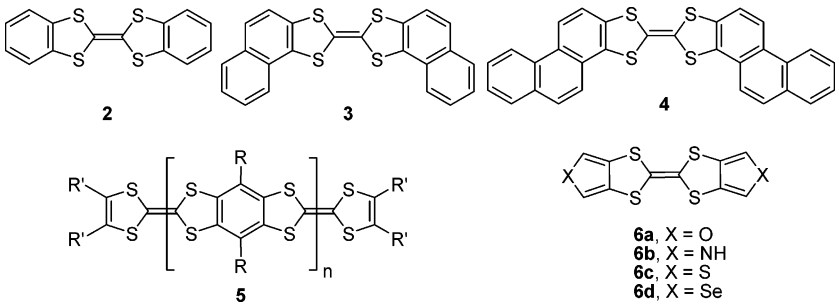

rivative of bis-pyrroloTTF **6b** was the only fused TTF derivative showing lower (by 10−30 mV[30,31]) oxidation potential than the parent TTF **1**. Very recently the first field-effect transistor from a TTF derivative (**6c**) has been demonstrated.[34] In the solid state, **6c** forms closed-packed stacks with an interplane distance of 3.56 Å, and the molecule itself is completely planar, which is in contrast to the case of the parent, neutral TTF, where twisted and boat-type conformations have been observed (Figure 1). Single crystals of **6c** show excellent hole mobility, often above 0.1 cm^2/V·s, with the highest value of 1.4 cm^2/V·s. A relatively high oxidation potential of this compound (E°_{1ox} = 0.78 V, E°_{2ox} = 0.96 V vs SCE, Table 1) is responsible for its stability (for months in air) and, probably, explains the reported high on/off ratio of the FET devices (above 7 × 10^5).[34]

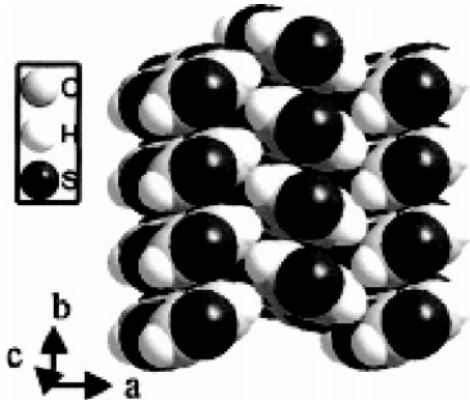

Figure 1. Crystal packing of TTF **6c**. (Reproduced with permission from ref 34. Copyright 2004 American Chemical Society.)

Chart 2. Structures of Some TTF Vinylogues

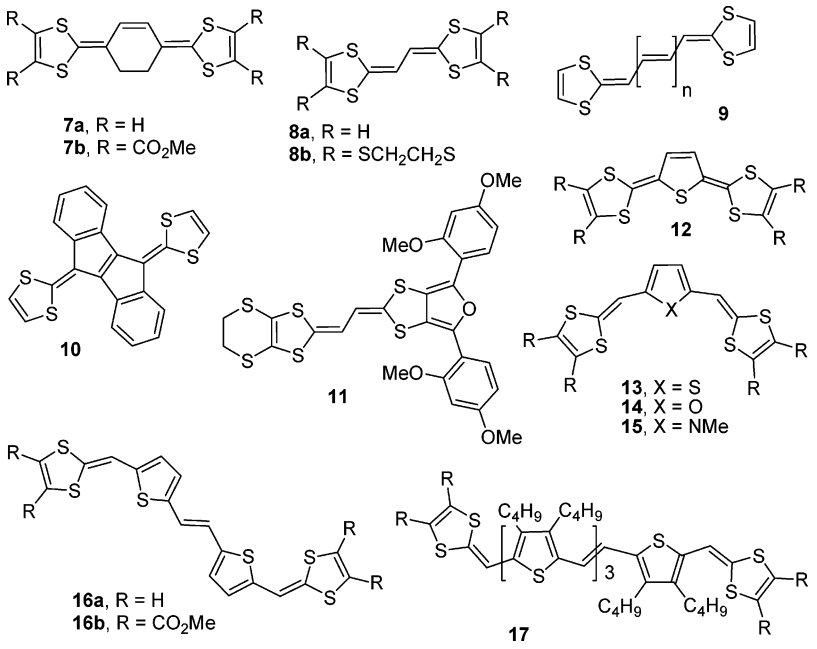

After the first vinylogue of TTF (**7**) was prepared in 1979 by Cava et al.,[35] a vast number of π-extended TTFs, where the dithiol rings were separated by up to nine conjugated vinylene units (e.g., compounds **8**,[35b,36] **9**,[37] **10**,[38] and **11**[39]) and/or thiophene and other heterocyclic moieties (e.g., compounds **12**,[40] **13**−**15**,[41] **16**,[42] and **17**[43]), were synthesized (Chart 2). Recently, a series of derivatives of **8** with a macrocyclic structure have been synthesized.[44] Predictably, extension of the conjugated system decreases the HOMO−LUMO gap, and the longest compound of this series, **17**, shows a gap on the level of 2 eV (1.8 eV, based on the absorption red-edge).[43] Despite a reduced gap, electrochemical reduction was not observed. On the other hand, the extension of π-conjugation does enrich their electrochemistry. The conjugated **17** can reversibly donate up to four electrons (in one two-electron process and two one-electron processes). The recently reported, less extended, compound **11** shows four reversible single-electron oxidation waves (Figure 2). For more information on linear π-extended TTFs, the reader can consult a detailed review by Roncali.[37]

A large and important series of π-extended TTFs was created by combining the TTF and acene electronic systems in a quinoid-type structure (Chart 3).[45] The parent molecule of this series (**18a**), having a single benzenoid ring separating two dithiole moieties, was reported in 1989 by Yamashita et al.,[46] although the diphenyl[47] and dibenzo (**18b**)[48] derivatives had been known before. The donor **18a** is the strongest reducing agent among all TTF derivatives (Table 1), and its red color (compared to yellow-orange for TTF) suggests a reduced HOMO−LUMO gap. Interestingly, this is the only compound in the series of TTF−acenes which oxidizes in two separate single-electron waves. Extending the acene linker to naphthalene and higher should result in steric hindrance between the sulfur atoms and hydrogen atoms of the acene moiety, which may drastically affect the electrochemistry and can render these as two-electron-

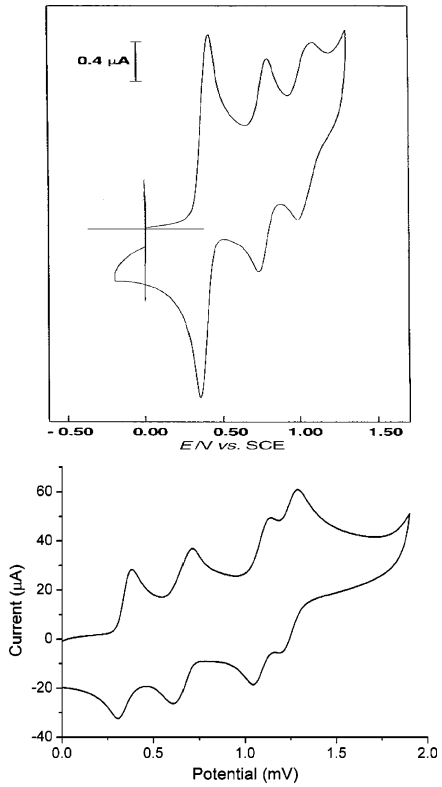

Figure 2. Cyclic voltammetry of linear π-extended TTFs **17** (top) and **11** (bottom, potential in V vs Ag/AgCl). (Reproduced with permission from refs 43 and 39. Copyright 1995 and 2004, respectively, Elsevier Science Ltd.)

donor (see below) molecules. The first TTF−naphthalene **19b** was synthesized by Bryce and Moore as dication salts,[49] and the neutral molecule **19a** was reported soon after.[46] The higher homologue, anthracene-TTF **20**, showed electrochemical behavior resembling that of TTF−naphthalene **19**.[47] A single two-electron oxidation was observed at +0.24 V, which is 60 mV higher than that of **19c**, although this could be due to different kinetics of

Chart 3. Structures of TTF–Acenes

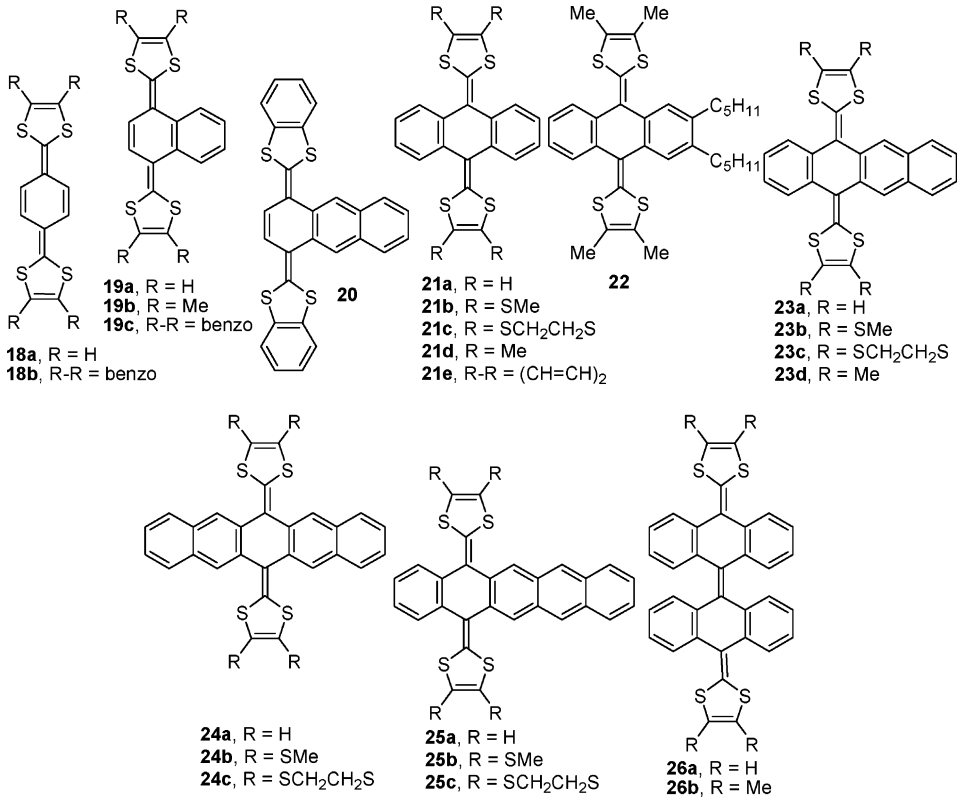

these electrochemically quasireversible processes (Table 1).

When the dithiole moieties are attached to the central benzene rings of an anthracene linker, strong steric repulsions, due to the *peri* hydrogen atoms of adjacent benzene rings in 9,10-bis(1,3-dithiol-2-ylidene)-9,10-dihidroanthracene (TTFAQ), enforce a "saddle-type" conformation in the neutral molecule (Scheme 5). The first TTFAQ **21e** was reported in

Scheme 5. Two-Electron Oxidation of TTFAQ

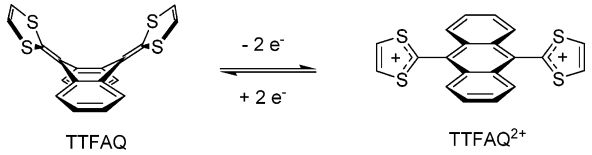

1978 by Akiba et al.,[50] although the in-depth studies of the electronic properties of these compounds were initiated in the 1980s by Bryce et al. The later group synthesized the strongest electron donor in the TTFAQ series, tetramethylated **21d** (in neutral[51] and dication[49] forms) and was the first to report the peculiar redox behavior of TTFAQ compounds.[51] Many other derivatives of TTFAQ, with substituents on dithiole rings (e.g., unsubstituted **21a**,[46] tetramethylthio-TTFAQ **21b**,[52] bis(ethylenedithio)TTFAQ **21c**[53]) and the anthracene core (e.g., **22**[54]), were synthesized, and over 240 different[55] TTFAQs were reported to date.

In contrast to the parent TTF, TTFAQ derivatives oxidize in a single two-electron process (Scheme 5). The rereduction of the dication occurs at significantly lower (by 200 mV and more, depending on the molecule and the conditions[56]) potential, which suggests dramatic structural changes between neutral and oxidized molecules. Furthermore, these changes are slow enough to be observed on the time scale of cyclic voltammetry experiments. Thus, decreasing the temperature from +20 to −70 °C shifts the position of the $TTFAQ^{2+} \rightarrow TTFAQ^{0}$ cathodic peak from ~ -0.07 V to ~ -0.4 V (Figure 3),[54] and a similar

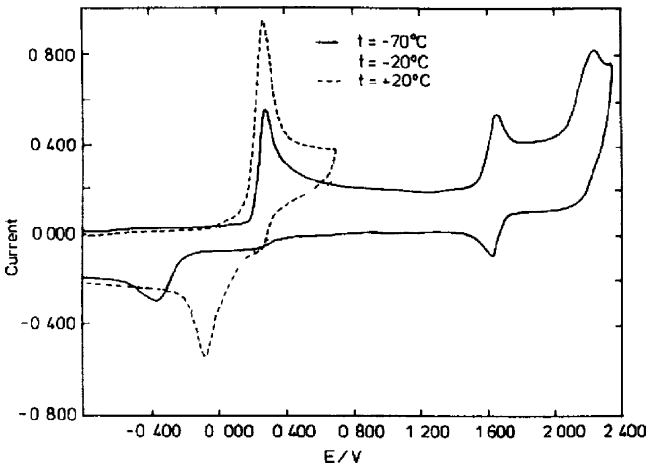

Figure 3. Cyclic voltammetry of TTFAQ **22**. The three oxidation waves at −70 °C correspond to formation of $TTFAQ^{2+}$ (irreversible two-electron oxidation at $E_{p.a.}$ = 0.28V vs Ag/AgCl), $TTFAQ^{3+}$ (reversible, $E° = 1.64$ V), and $TTFAQ^{4+}$ (irreversible, $E_{p.a.} = 2.2$ V). (Reproduced with permission from ref 54. Copyright 1991 Elsevier Science Ltd.)

effect can be achieved by increasing the scan rate. Introducing additional steric hindrance by replacing the sulfur atoms with more bulky selenium atoms also slows down the rearrangement process, as manifested by increased anodic/cathodic peak separation for mono- and diselenaTTFAQs.[57]

These interpretations were proved by X-ray crystallography of neutral and oxidized dicationic TTFAQ **21d** (Figure 4).[58] Whereas the steric hindrance in the

Figure 4. Crystal structure of neutral TTFAQ **21d** (top) and its dication **21d**$^{2+}$ (bottom).[58] The drawings are produced from the data stored at the Cambridge Crystallographic Data Center (CCDC).

neutral TTFAQ results in puckering the molecule, which adopts a saddle-shaped conformation, a decrease of the bond order between the anthracene and dithiole nucleus in the dication allows a 90° rotation of the substituents, so that the anthracene fragment becomes planar and the molecule fully aromatic. The aromatic anthracene in the TTFAQ dication (for **22**) can be further oxidized in two one-electron waves, giving the radical trication (reversibly) and tetracation (irreversibly) (Figure 3).[54] On the other hand, the distorted structure of the neutral molecule compromises the decrease of the HOMO−LUMO gap, which can be expected from the extension of the conjugated system. Consequently, TTFAQ and its homologues do not show amphoteric redox behavior, and the optical gap reduction is also minimal.

The strong aromaticity gain during the loss of the second electron results in an interesting electrochemical phenomenon—inverted potentials in a two-electron process (similar to that observed in 9,10-bis(dimethylamino)anthracene[59]). That is, the oxidation potential of the TTFAQ radical cation is *lower* than that of the neutral molecule.[60] Consequently, the transient radical cation is not thermodynamically stable and not observable in routine ESR experiments.

The inverted potentials also influence the behavior of the molecule in its charge-transfer complexation. Thus, whereas the parent TTF, with a similar oxidation potential, forms a complex with TCNQ with only partial (~60%) charge transfer, full two-electron transfer has been observed for the TCNQ complexes of TTFAQ. The first crystallographically characterized complex, $(TCNQ)_4$(**21a**), had a D/A ratio of 1:4(TTFAQ is in a dication state, whereas TCNQ bears a −0.5 charge, as $TCNQ^{(-)}TCNQ^{(0)}$).[58] Yet, 1:2 complexes of other substituted TTFAQs with TCNQ[61] and nitrofluorene (acceptor of similar electron affinity)[60] have been characterized later. The tendency of TTFAQ to form fully ionic charge-transfer salts can be rationalized by the fact that, unlike the case in TTF complexes, the resonance between the completely neutral and fully ionic forms is not possible due to different geometries of TTFAQ^0 and TTFAQ^{2+}, which makes partial charge transfer thermodynamically unfavorable.

The radical cation of TTFAQ can be synthesized by UV photolysis (as demonstrated for **21b**[62]) or γ-radiolysis (as demonstrated for **21a**−**c**, **23**, and **24**[63]). It was characterized as a metastable species which readily disproportionates to yield the TTFAQ dication and neutral species, with a half-life time from $\sim10^{-4}$ s (ref 62) to $\sim10^{-3}$ s,[63] determined from the spectral decay. The UV−vis spectra of **21b**$^{\bullet+}$ are typical for TTF radical cation, showing an absorption band at ~650 nm with weak vibronic structure. Time-resolved resonance Raman (τR^3) spectroscopy suggests that the geometry of TTFAQ radical cation is closer to the quinoid-type structure of the neutral molecule, rather than to the aromatic dication state. The latter adequately explains the inverted oxidation potentials and also is in agreement with the theoretical calculations at the semiempirical (PM3), ab initio (HF/6-31G(d)), and DFT (B3-P86/6-31G(d)) levels.[64]

A series of higher TTF−acenes **23**−**25** was reported by Martín et al. in 1998,[64] although the first tetracene-TTFs **23a**,**d** were synthesized by Moore and Bryce in 1991, together with a more complex bisanthro-TTF **26** (Chart 3).[57] Basically, the structural feature in these resembles that observed in TTFAQ **21**, and a quasi-reversible two-electron oxidation wave was observed. Unexpectedly, the oxidation potential of tetracene derivative **23** is lower than that of pentacene derivatives **24** and **25** by 100 mV (but higher than that of TTFAQ **21**), although this is likely a reflection of the quasi-reversible nature of the oxidation (with influence of kinetic factors) and adsorption phenomena for the less soluble pentacene derivatives. All higher TTFAQ derivatives also exhibited a second single-electron oxidation wave resulting in radical trications. Again, electrochemical amphotericity was not observed for these TTF−acenes, and the lowest electronic transition corresponded to a HOMO−LUMO gap of 2.68 eV (for pentacene derivative **25c**).

To conclude, although the extended conjugation approach was very successful to generate a low HOMO−LUMO gap in polymers and several molecular materials (e.g., long oligoporphyrins[65]), it has, so far, not proved feasible for TTF derivatives.

2.3. Conjugated TTF−Acceptor Systems

One of the original reasons for synthesis of TTF D−A systems was a search for novel charge-transfer materials with predefined D/A stoichiometries, for example, molecular conductors,[66] although the fundamental interest in such systems and the possible applications are beyond this review. In this and the following subsection we describe another concept of the HOMO/LUMO gap control based on a donor−acceptor (D−A) molecule with spatially separated HOMO and LUMO orbitals.

2.3.1. Fused TTF−A Compounds

The first compound having an electron-acceptor moiety conjugated with TTF, TTF−benzoquinone **27**,

Table 2. Cyclic Voltammetry and Optical Absorbance Data for Fused TTF−A Compounds

compd	RE//solvent	$E°_{1ox}$, V	$E°_{2ox}$, V	$E°_{1red}$, V	$E°_{2red}$, V	E_g, eV	$h\nu_{ICT}$, eV	ref
27	NHE//toln−MeCN (9:1)	0.5ir		−0.32	−0.90ir	~0.8		27
27	Ag/AgCl//ODCB−MeCN (19:1)	0.96	1.35	−0.56	−0.61; 1.2	1.52		67
28a	SCE//DCM	0.60	1.02	−0.27		0.87	1.41[a]	68
31	Ag/AgCl//DCM	0.64(2e)		−0.95		~1.6		70
32	Ag/AgCl//DCM−MeCN (9:1)	0.74	0.11	−0.21	−1.20	0.95	1.39	67
33	Ag/AgCl//DCM−MeCN (9:1)	0.99	1.36	−0.20	−0.28	1.19	1.53	67
34	Ag/AgCl//EtCN	0.65	0.80, 1.25	−0.51		1.16		71
35	SCE//PhCN	0.73	0.98	−0.52		1.25	1.63	72

[a] Measured in DCM for **28b**; $h\nu_{ICT}$ in the solid state is 1.19 eV.

was synthesized by oxidation of the corresponding bis(hydroquinone) in 1993 by Watson et al. (Chart 4).[27] Its electrochemical behavior was characterized by a reversible reduction at −0.32 V (vs NHE), although the second reduction and the oxidation waves were irreversible. The difference between the first reduction and oxidation waves suggests a fairly low HOMO−LUMO gap of ~0.8 eV (Table 2) which, however, was questioned by more recent studies.[67] The carefully controlled cyclic voltammetry of **27** in an ODCB−MeCN solvent mixture (for increased solubility) revealed two reversible oxidation waves and three reversible reduction waves. These redox potentials suggest an essentially higher gap of 1.52 eV. A few years later, Frenzel and Müllen reported donor−acceptor triads **28**, containing two TTF moieties and one benzoquinone (BQ) moiety.[68] The redox behavior of this triad was quite clear: two reversible two-electron oxidations of TTF fragments and one-electron reduction of BQ, providing an electrochemical gap E_g as low as 0.87 eV (the second reduction was not observed due to the narrow electrochemical window of the solvent used) (Table 2). The near-IR absorption spectrum of **28** displayed an intramolecular charge-transfer band of moderate intensity with a maximum at ~800−900 nm (positive solvatochromism). A weak paramagnetic signal at g = 2.0075 (in solution), corresponding to $TTF^{\bullet+}$ was observed for **28** but was attributed to impurities (the signal diminished with purification).

Later, Hudhomme et al. synthesized TTF−BQ diads **29** and **30**, with donor and acceptor separated by a benzene ring, but their electrochemistry was not reported.[69] A related diad **31**, having a π-extended donor moiety, TTFAQ, reported the same year by Bryce et al., displayed a moderate amphotericity with a gap $E_g \sim 1.6$ eV, but no charge-transfer interaction in the diad was observed.[70] Very recently, Hudhomme et al. reported a new TTF−BQ diad **32** and a BQ-TTF−BQ triad **33**.[67] The compounds showed pronounced amphotericity in cyclic voltammetry (Table 3) that accounted for a HOMO−LUMO gap of 0.95 eV (for **32**). A very weak and broad intramolecular CT band ($\epsilon \sim 425$ M^{-1} cm^{-1} for **32**) was observed in these compounds, and similar to the case of TTF−BQ **28**, the corresponding optical gap (1.39 eV for **32**) is larger than the electrochemical gap (Table 2). However, in contrast to the case of compound **28**, the CT absorption of **32** and **33** demonstrated a pronounced negative solvatochromism; that is, the λ_{max} of **32** decreases from 892 to 762 nm on going from a low polarity (CS_2) to high polarity (DMSO) medium. Interestingly, despite direct fusion of the acceptor and donor fragments, the HOMO and LUMO orbitals are essentially localized on the TTF and BQ fragments, respectively (Figure 5).

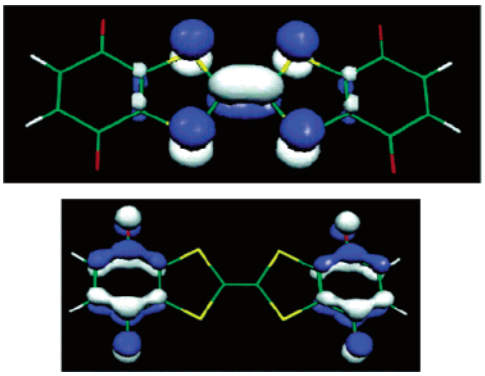

Figure 5. HOMO and LUMO orbitals of the triad **33**, as calculated at the B3LYP/6-31G* level. (Reproduced with permission from ref 67. Copyright 2004 American Chemical Society.)

An interesting TTF-related donor acceptor molecule **34** (Chart 4) was obtained by introducing dithiole moieties into cyclohexanetrione.[71] The compound can be easily prepared by reaction of 1,3,5-benzenetriol (phloroglucinol) (which can be represented as the enol tautomer of cyclohexanetrione) with 2-methylthio-1,3-dithiolium iodide in the presence of pyridine. Due to the presence of three donor dithiol moieties, **34** can donate three electrons in subsequent electrochemical stages, although only the first two processes are reversible. A reversible one-electron reduction was also observed, and the difference between the first oxidation and the first reduction potentials renders the HOMO−LUMO gap to be 1.16 eV. However, no absorption in the vis-NIR spectrum, which could be attributed to a HOMO−LUMO transition, was reported for this orange compound. The thioindigo moiety, which possesses similar electron affinity to that of BQ, was attached to TTF by Khodorkovsky et al.[72] The resulting diad **35** possesses an electrochemical gap of 1.25 eV. In addition, a long-wavelength absorption band at 760 nm can be tentatively attributed to a charge-transfer electronic transition, although the electronic transition energy $h\nu_{ICT}$ (1.63 eV) is somewhat higher than the E_g.

Several other TTFs fused with electron-deficient heterocycles, such as 2,4-dioxo(1H,3H)pyrimidine (e.g., **36**[73]) or 1,2,5-thiadiazole[66c] (fused to the dithiole nucleus in TTF as in **37** or to the acene nucleus in π-extended TTFs), are known, but the electrochemical amphotericity was not established.

Chart 4. Structures of TTF-Fused Acceptor Molecules

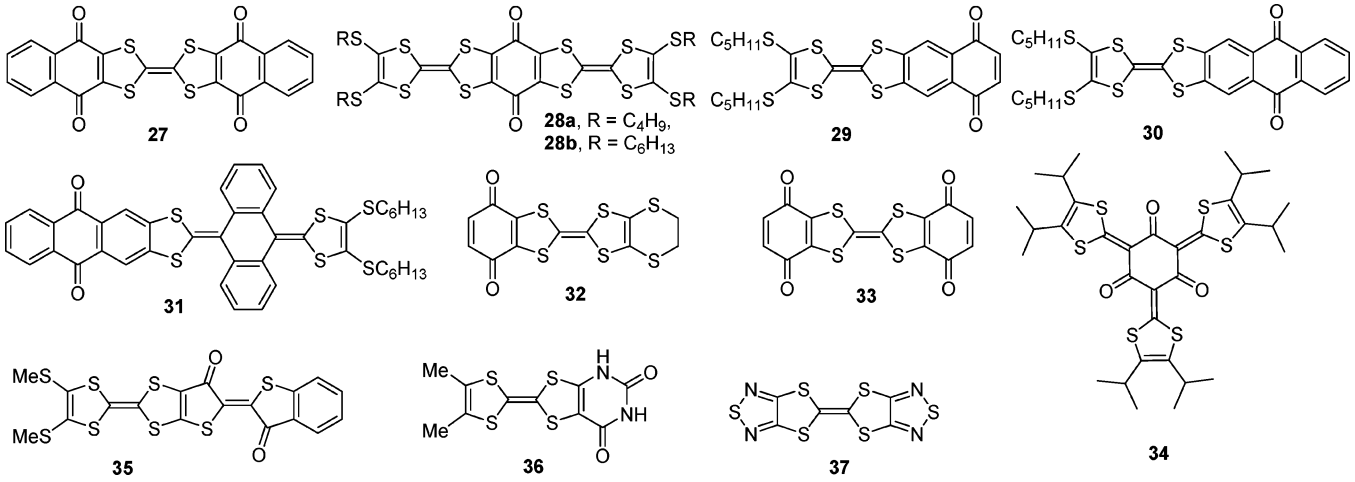

Chart 5. Structures of TTF−π-A Molecules

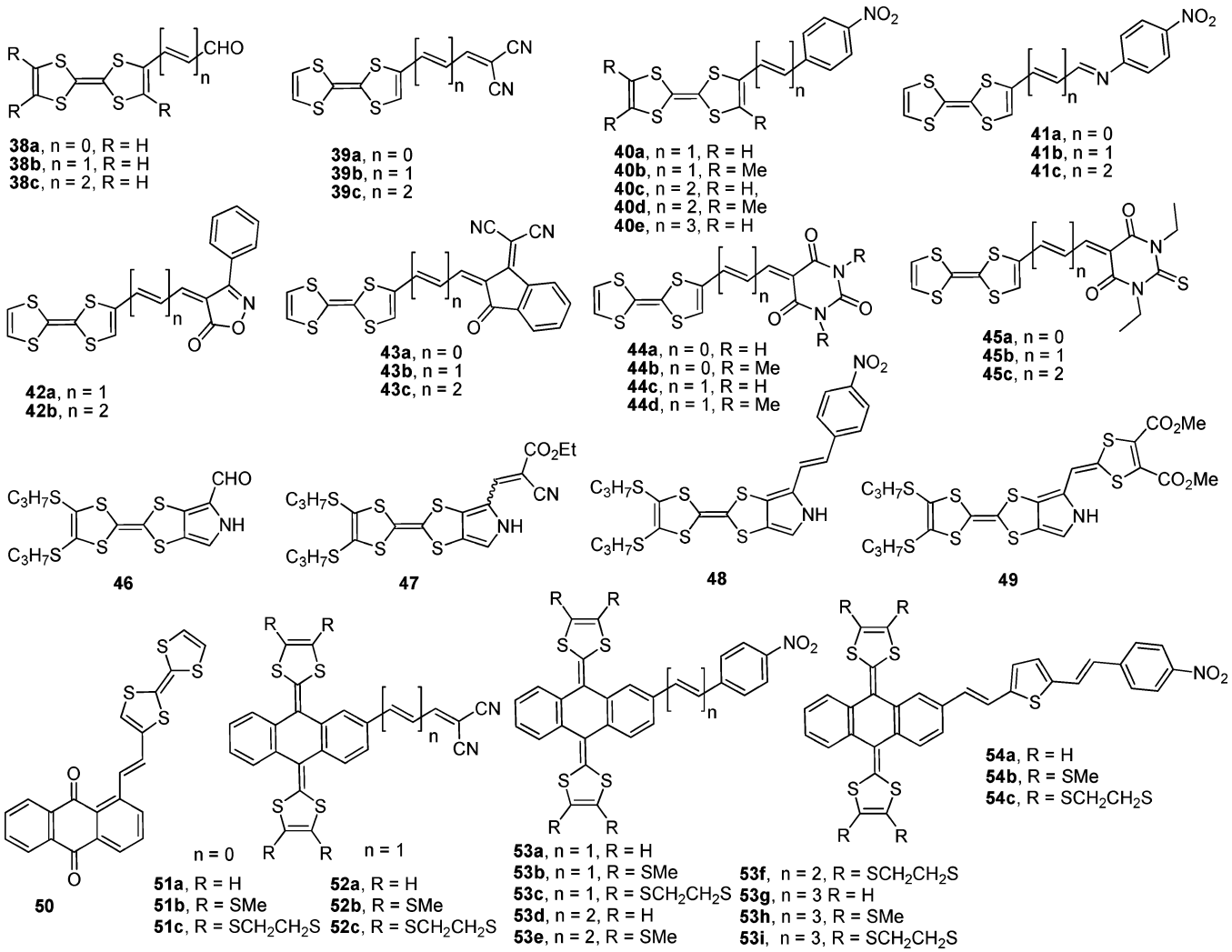

2.3.2. TTF–π-Acceptor Captodative ("Push-Pull") Compounds

There was considerable interest in TTF−π-A compounds with a long π-linker as nonlinear optical (NLO) materials for second-harmonic generation (SHG) applications due to good electron-donor properties and polarizability of the TTF unit. The first determination of SHG efficiency (EFISH-determined hyperpolarizability parameters $\mu\beta_0$) of TTF−π-A molecules was reported in 1997 for the simplest derivative, TTF−carbaldehyde **38b** (Chart 5).[74] The moderate acceptor properties of the aldehyde group can be easily enhanced by conversion into dicyanomethylene derivatives **39** (**a**,**b**;[74] **a**−**c**[75]). Later, transformations of TTF−aldehydes into nitrophenyl (**40**[76]) and cyanophenyl,[76] nitrophenylimine (**41**[76]), oxazolone (**42**[75]), 3-dicyanomethyleneindan-1-one (**43**[75,77]), barbituric acid (**44**[78]), and thiobarbituric acid (**45**[69,75])

Table 3. Cyclic Voltammetry, Optical Absorbance, and Hyperpolarizability Data for TTF−π-A Compounds

compd	RE//solvent	$E°_{1ox}$, V	$E°_{2ox}$, V	$E°_{1red}$, V	$E°_{2red}$,V	E_g, eV	$h\upsilon_{ICT}$, eV	$10^{-48}\mu\beta_0$, esu	ref
38a	SCE//DCM	0.60	1.03				2.61	33 (ref 76)	74
38b	SCE//DCM	0.59	1.00				2.48	85; 46 (ref 76)	74
38c							2.38 (ref 75)	80	76
39a	SCE//DCM	0.63	0.87	−0.89i		∼1.5	1.99		75
39a	SCE//DCM	0.69	0.97	−0.89i		∼1.6	1.99		74
39b	SCE//DCM	0.54	0.84	−0.87i		∼1.4	2.00	234	75
39b	SCE//DCM	0.59	0.92	−0.88i		∼1.5	2.00		74
39c	SCE//DCM	0.50	0.83	−0.87i		∼1.4	2.04	320	75
40a	Ag/AgCl//MeCN	0.45	0.77				2.48	150	76
40b	Ag/AgCl//MeCN	0.37	0.74				2.40	240	76
40c	Ag/AgCl//MeCN	0.42	0.78				2.48	180	76
40e	Ag/AgCl//MeCN	0.41	0.75				2.45	210	76
41a							2.38	62	76
41b							2.41		76
41c							2.47		76
42a	SCE//DCM	0.53	0.86	−0.88i		∼1.4	1.88	295	75
42b	SCE//DCM	0.49	0.83	−0.91i		∼1.4	1.97	611	75
43a	SCE//DCM	0.46	0.75	−0.92i		1.42	1.55		75
43b	SCE//DCM	0.47	0.75	−0.96i		∼1.4	1.71	259	75
43c	SCE//DCM	0.45	0.75	−0.97i		∼1.4	1.80	570	75
44a	Ag/AgCl//DMF	0.55	0.80	−0.76i		∼1.3	1.93	39	78
44b	Ag/AgCl//DCM	0.58	0.92	−0.78i		∼1.3	1.91	67	78
44c	Ag/AgCl//DMF	0.61	0.82	−0.67i		∼1.2	2.08	104	78
44d	Ag/AgCl//DCM	0.59	0.97	−0.70i		∼1.2	2.04	154	78
45a	SCE//DCM	0.60	0.97	−0.63i		∼1.2	1.73	180	75
45b	SCE//DCM	0.60	1.00	−0.57i		∼1.1	1.85	347	75
45c	SCE//DCM	0.56	0.90	−0.52i		∼1.0	1.91	455	75
46	Fc/Fc^+//MeCN	0.14	0.43	−2.18		2.32	3.18		79
47	Fc/Fc^+//MeCN	0.15	0.43	−1.65		1.80	2.66		79
48	Fc/Fc^+//MeCN	0.08	0.40	−1.43	−1.61	1.51	2.95		79
49	Fc/Fc^+//MeCN	0.26i	0.54i	−1.76		2.02	1.72		79
50							2.34		80
51a	SCE//DCM[a]	0.51(2e)		−1.10		∼1.6	2.07	138	81
51b	SCE//DCM[a]	0.58(2e)		−0.97		∼1.6	2.23	154	81
51c	SCE//DCM[a]	0.62(2e)		−1.04		∼1.6	2.17	172	81
52a	SCE//DCM[a]	0.48(2e)		−0.99		∼1.5	2.23	272	81
52b	SCE//DCM[a]	0.58(2e)		−0.97		∼1.6	2.26	334	81
52c	SCE//DCM[a]	0.60(2e)		−0.95		∼1.5	2.19	325	81
53a	SCE//DCM	0.51/0.13[b]		−1.01i	−1.49	∼1.5		140	82
53b	SCE//DCM	0.62/0.43[b]		−1.00i	−1.44	∼1.6		163	82
53c	SCE//DCM	0.64/0.38[b]		−1.02i	−1.47	∼1.6		155	82
53d	SCE//DCM	0.45/0.20[b]		−1.01i	−1.37	∼1.4		180	82
53e	SCE//DCM	0.62/0.43[b]		−1.00i	−1.42	∼1.6		277	82
53f	SCE//DCM	0.65/0.40[b]		−0.97i	−1.43	∼1.6		191	82
53g	SCE//DCM	0.47/0.19[b]		−0.97i	−1.37	∼1.4		247	82
53h	SCE//DCM	0.65/0.37[b]		−0.93i	−1.41	∼1.5		270	82
53i	SCE//DCM	0.66/0.35[b]		−0.94i	−1.39	∼1.5		250	82
54a	SCE//DCM	0.48/−0.07[b]		−1.06i	−1.47	∼1.5			82
54b	SCE//DCM	0.60/0.21[b]		−1.05i	−1.45	∼1.6			82
54c	SCE//DCM	0.57/0.16[b]		−1.07i	−1.46	∼1.6			82

[a] Anodic (for oxidation) and cathodic (for reduction) peak potentials are given for these waves. [b] Two electron quasi-reversible waves; the anodic/cathodic peak potentials are given. *i* = the peak potential of the irreversible wave.

derivatives with larger hyperpolarizability were reported. Generally, increasing the electron-withdrawing properties of the acceptor part reduces both the electrochemical and optical gaps and provides higher hyperpolarizability $\mu\beta_0$ (Table 3). The lowest E_g (∼1.0 eV) for TTF−π-A systems was realized with the thiobarbituric acceptor group, and these compounds (**45**) also showed good hyperpolarizabilities ((180−455) × 10^{-48} esu), although the highest $\mu\beta_0$ ((259−611) × 10^{-48} esu) values have been obtained with oxazolone and dicyanomethyleneindanone groups (compounds **43**) (Table 3). On the other hand, as evident from Table 3, there is no direct correlation between the electrochemical (E_g) and optical ($h\upsilon_{ICT}$) gaps, which hinders determination of HOMO−LUMO gaps for these molecules. This is partially (but not entirely) attributable to the irreversible nature of the electrochemical reduction, where the peak potential does not correspond to the thermodynamic redox potential. Also, the HOMO−LUMO nature of the longest wavelength transition has not been established in these compounds, and the low intensity of these bands (as for highly conjugated molecules, $\epsilon \sim 10^3\ M^{-1}\ cm^{-1}$) reported in many cases puts reasonable doubt on these assignments. In many (cf., series **39a**−**c** or **43a**−**c**) but not all cases, the elongation of the π-linker between the donor and acceptor results in small but consistent *hypso*chromic shifts of the long-wavelength absorption, although the electrochemical gap is reduced (Table 3). Regardless of this behavior, the hyperpolarizability of all TTF−π-A compounds increases with elongation of the π-linker.

A similar approach toward NLO chromophores, based on the carbaldehyde **46**, was recently demonstrated.[79] Compounds **45**−**49** contain a stronger

TTF−pyrrole donor moiety and, in contrast to compounds **38**−**41**, can be reversibly reduced to radical anions (and even a dianion for **48**), which allows for more precise determination of the HOMO−LUMO gap (Table 3). The lowest E_g was found for nitrophenyl derivative **48** (Chart 5). Again, the optical gaps seem to disagree with the electrochemical data, but the assignment of these low intensity bands (1600−2500 M^{-1} cm^{-1}) for the HOMO−LUMO transition is questionable. No SHG properties have been reported for these diads, although third-harmonic generation studies showed a moderate second-order hyperpolarizability γ of 1.5×10^{-33} esu.

Diad **50**, bearing a weak-electron-acceptor anthraquinone fragment, was synthesized as an intermediate for TTF−TTFAQ diads.[80] An extremely weak (log $\epsilon = 0.72$) intramolecular CT band at 530 nm (2.34 eV) was observed for this compound, but its electrochemical and NLO properties have not been addressed.

The donor moiety, TTFAQ, has been used in D−π-A diads, first in **51** and **52**[81] and later in **53** and **54**.[82] The $\mu\beta_0$ values of the TTFAQ NLO chromophores [$(138-334) \times 10^{-48}$ esu, Table 3] are comparable to and even somewhat higher than those of TTF−π-A diads with the same π-linker and acceptor groups. Furthermore, relatively high thermal stability revealed by TTFAQ compounds (e.g., **54**) makes them more attractive for practical applications.

Nevertheless, no high-performing NLO materials based on TTF have, so far, been created despite all the syntheses shown above. The hyperpolarizabilities are not high [$\mu\beta_0 \sim (100-600) \times 10^{-48}$ esu] as compared to those of the best organic molecular NLO chromphores (an order of magnitude higher values have been obtained with dialkylamino and 1,3-dithiol-2-ylidene donor moieties[83]), and the stability of the TTF moiety toward photodegradation is not particularly good.

2.3.3. TTF–Metal Complexes

A very low HOMO−LUMO gap can be achieved in transition metal complexes of TTF ligands. This field has attracted significant research efforts in the past decade, especially after the first demonstration of metallic conductivity (down to 0.6 K, $\sigma_{rt} = 400$ S/cm) in a single-component molecular metal, the neutral nickel-TTF complex **55** (Chart 6).[84] Since this topic is reviewed in detail in this thematic issue of *Chemical Reviews* by A. Kobayashi et al., we will give only a brief overview of the field in connection with the low HOMO−LUMO gap aspect.

Metal−dithiolene complexes with promising conductive properties (including superconductors) and low HOMO−LUMO gaps have been known for a long time.[85] The first use of 3,4-dithioTTF as an extended dithiolene ligand to bind transition metals was reported in 1979 by Engler et al.[86] This type of complexes can exist in the neutral form and several anionic forms. Many of these with alkyl, alkylthio, and alkoxy[87] substituents on the TTF ligands and different metals, such as nickel, copper, zinc, cobalt, palladium, platinum, mercury, gold, and cadmium, are known.[88−93] Also, the TTF complex family has been expanded to include the metalocene moiety (titanium complex **56**[94]), non-sulfur binding ligands (pyridine derivative **57**[95]), tris(TTF) hexacoordinated vanadium complex **58**,[96] mono(TTF)-bypyridyl complexes **59**,[97] and multi-metal-bridged compounds **60**.[93]

Recently, on the basis of the study of electronic absorption spectra in the IR region, neutral **55a-Pd**, **55b-Ni**, **55c-Ni**, and **55g-Ni** complexes and the metallic nickel−TTF complexes **55b-Ni** and **55c-Ni** were claimed to be the lowest HOMO−LUMO gap molecular compounds (Chart 6).[98] The maxima of

Chart 6. Structures of TTF−Metal Complexes

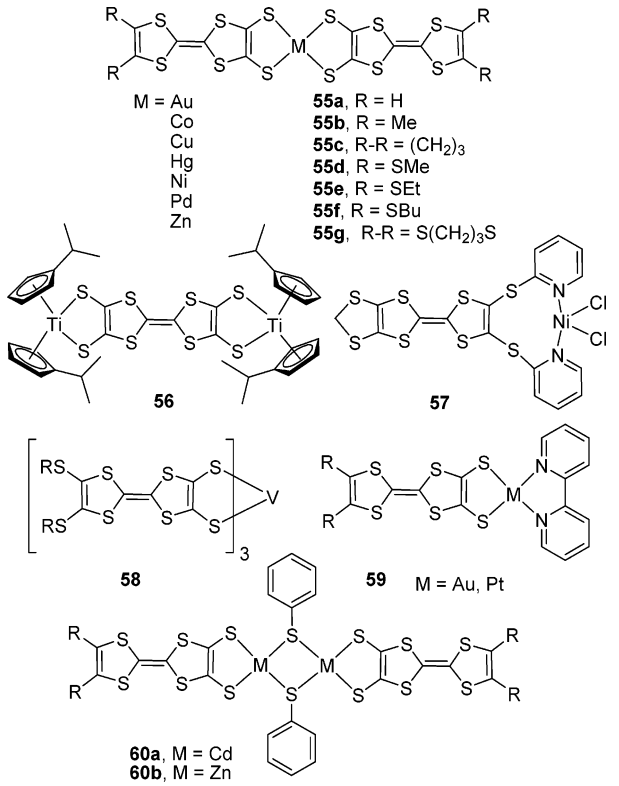

the electronic absorption of dialkyl-TTF complexes **55b-Ni** and **55c-Ni** (0.27 eV) are shifted bathochromically, as the HOMO energy is compromised by placing electron-withdrawing alkylthio substituents on the TTF ligands (compound **55g-Ni**, 0.58 eV), although the authors explained this by a change in the crystal band structure. Admitting that the maximum of the electronic transition is not a direct measure of the HOMO−LUMO gap, particularly in the solid state, the authors performed band structure calculations. The observed IR spectra maxima were reproduced assuming a HOMO−LUMO gap of 0.14 $\pm$ 0.06 eV for nickel complexes and 0.12 $\pm$ 0.08 eV for the palladium complexes.[98] However, it is difficult to assess the accuracy of the extended-Huckel calculations, especially considering the large error ($\pm$0.08 eV for the 0.12 eV result). In fact, in a majority of related materials (such as charge-transfer complexes), the energy of the electronic transition in the solid state was significantly lower than that in solution. Unfortunately, the low solubility of the complexes does not allow solution spectral studies, nor could reliable electrochemical data be obtained. Some indication of the low HOMO−LUMO gap

Table 4. Electrochemical and Optical Absorption Data for TTF−Metal Complexes

compd	RE//solvent	E_1, V	E_2, V	E_3, V	E_4, V	E_g (neutral), eV	$h\nu_{ICT}$, eV	ref
(**55e-Hg**)$^{2-}$	??//DCM	−0.04	−0.07	0.76(2e)	1.09	0.83		88
(**55g-Ni**)−	SCE//MeCN	−0.45	−0.15	1.20		0.30	0.58ss	99
(**55g-Cu**)$^{2-}$	SCE//MeCN	−0.73(2e?)	−0.08	1.15		0.65		99
56	Fc/Fc//MeCN	−1.28(2e)	0.26	0.48		1.54	1.61	94
57	Ag/AgCl//DCM	−0.70	0.63	0.95		1.33		95
60a	SCE//??	−0.17	0.78	0.89		0.95		93

possessed by the neutral complexes can also be seen in the solution electrochemical properties of the anionic complexes, which are oxidized in situ to form the neutral species. The anionic Me_4N[**55g-Ni**] undergoes three redox waves, and the difference between the redox peak potentials (0.3 V) can be tentatively assumed to correspond to the HOMO−LUMO gap of the neutral complex (Table 4).[99] The electrochemical gap of the majority of complexes is higher (Table 4). A similar behavior, but with a larger electrochemical gap, was demonstrated by the copper complex $(Me_4N)_2$[**55g-Cu**] (0.65 V)[99] and the mercury complex $(Me_4N)_2$[**55e-Hg**] (0.81 V).[88] The irreversibility (chemical and electrochemical) of the oxidation of most of these complexes and the adsorption phenomena (due to poor solubility of the neutral species) seriously affected the applicability of the redox potentials to substantiate the HOMO−LUMO gap in these materials. On the other hand, when the complex (in)stability does not affect the electrochemistry, as demonstrated for bis-titanium neutral TTF complex **56**, a very good match between the electrochemical and optical gap (1.54 and 1.61 eV, respectively, Table 4) could be observed.[94]

It should be noted that these complexes cannot be simplified to a donor−acceptor model with TTF−dithiolene ligands acting as a donor and the formally tetracationic metal center acting as an acceptor. In accord with a strong ESR signal observed in neutral complexes,[91,96] Hartree−Fock calculations predict the triplet state of the complex to be more stable than the singlet state, although it is slightly less stable by DFT.[100] The *g*-value (2.005−2.009) of the latter suggests exclusive localization of the unpaired electron on the TTF moieties. Therefore, an extremely low HOMO−LUMO gap is achieved in these open-shell systems due to singly occupied orbitals. The very low gap of the ion radical species is not rare, although the charge-compensation in the TTF−metal complexes has allowed the realization of this concept in a single-component metallic system (i.e., without external counterion "dopant").

2.4. Nonconjugated TTF–A Systems

The challenge of covalently linking an electron acceptor to a TTF unit in a nonconjugated D−σ-A diad was first set up by Aviram and Ratner in their famous theoretical proposal of unimolecular rectification in 1974.[101] They proposed that a single molecule, such as TTF−σ-TCNQ (Figure 6), placed between two equal electrodes, can preferentially pass current in the acceptor → donor direction.[102] Although most of the following experimental studies have used diads with only moderate electron-donor and electron-acceptor components, the original calculations assumed a HOMO−LUMO gap (more precisely, IP − EA) of 0.3 eV.[101] On the other hand, recent high-level DFT calculations failed to reproduce the rectification behavior in diads containing amino and nitro groups as donor and acceptor moieties, respectively, and the authors argued that much lower HOMO−LUMO gap molecules are needed to generate rectification.[103] As will be shown below, the reliable synthesis of such molecules has become possible only recently and their implementations in different areas of organic electronics remain to be explored.

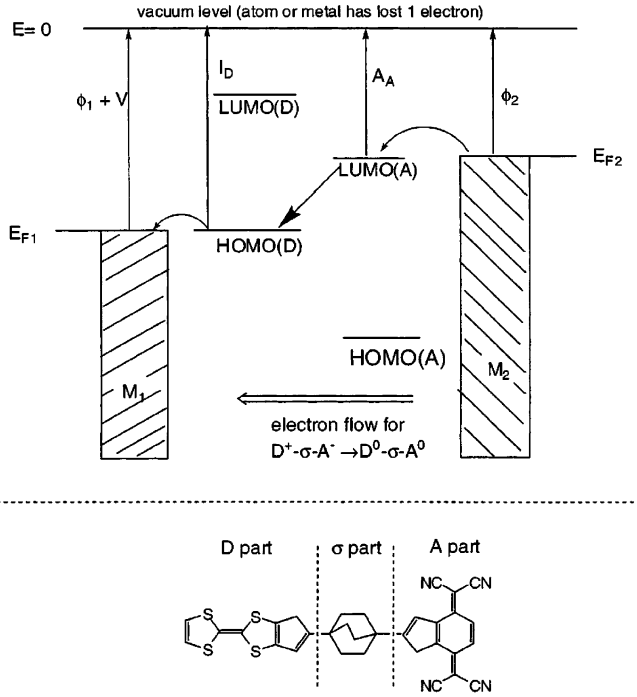

Figure 6. Chemical structure of the Aviram-Ratner molecular rectifier TTF−σ-TCNQ and the proposed mechanism of current rectification. (Reproduced with permission from ref 102. Copyright 2004 American Chemical Society.)

2.4.1. TTF–σ-A Compounds with Weak Acceptor Moieties

The first well-characterized TTF−σ-A compounds were compounds **61a**−**c**, prepared by Robert et al.[66a,104] in the search of single-component molecular conductors, but the very weak electron affinity of the A part of the molecules could not give rise to unusual properties in such diads. No charge-transfer interac-

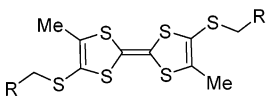

61a, R = C_6F_5
61b, R = C_6H_4-pNO_2
61c, R = $CH_2C_6H_4$-pNO_2

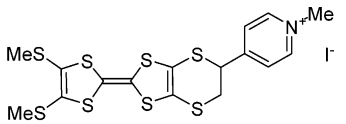

62

Table 5. Cyclic Voltammetry and Optical Absorption Data for TTF−σ-A Diads

compd	RE//solvent	$E°_{1ox}$, V	$E°_{2ox}$, V	$E°_{1red}$, V	$E°_{2red}$, V	E_g, eV	$h\nu_{ICT}$, eV	ref
63	SCE//MeCN	0.52	0.77	−0.39	−0.83	0.91	1.99	106
64	SCE//MeCN	0.53	0.78	−0.39	−0.84	0.92		106
65	SCE//MeCN	0.53	0.78	−0.38	−0.85	0.91	1.78	106
66a	SCE//MeCN	0.58	0.82	−0.36	−0.85	0.94	1.84	106
66b	SCE//MeCN	0.54	0.78	−0.37	−0.85	0.91	1.98	106
66c	SCE//MeCN	0.51	0.76	−0.40	−0.86	0.91	1.91	106
67	SCE//MeCN	0.45	0.76	−0.36	−0.84	0.81	1.94	106
68	Ag/AgCl//MeCN	0.64	0.94				1.92	107
69	Ag/AgCl//MeCN−DCM (10:1)	0.79	1.01				2.30	108
70							1.58	108
72	Ag/AgCl//DCM	0.54	0.89				2.10	114
73	Ag/AgCl//DCM	0.51	0.86					114
74a	Ag/AgCl//DCM	0.51	0.85					114
74b	Ag/AgCl//DCM	0.51	0.84					114
75	Ag/AgCl//DCM	0.50	0.81	−0.94	−1.35	1.44		115
76	Ag/AgCl//DCM	0.53	0.82	−0.93	−1.34	1.46		115
77	Ag/AgCl//$CHCl_3$	0.48	0.86	−0.67	−0.85	1.15		116
78	Ag/AgCl//$CHCl_3$	0.47	0.83	−0.67	−0.85	1.14		116
79a	Ag/AgCl//DMF	0.51	0.83	−0.74	−1.08	1.25		117
80a	Ag/AgCl//DMF	0.67	0.85					118
80b	Ag/AgCl//DMF	0.69	0.87					118
80c	Ag/AgCl//DMF	0.62(p.a.)	0.73					118
81	Ag/Ag^+//DCM	0.23	0.57	−0.98	−1.36	1.21		121
81b	Fc/Fc^+//DCM	0.04	0.405	−1.385	−1.65	1.43		122
81c	Ag/AgCl//DCM	0.63	1.10	−1.3		1.93		124
81d	Ag/AgCl//DCM	0.58	0.96	−1.3		1.88		124
82a	SCE//MeCN	0.44	0.79	−0.36(2e)		0.80		130
82b	SCE//MeCN	0.36	0.71	−0.36(2e)		0.72		130
83	SCE//MeCN	0.38	0.376	−0.24(2e)		0.62		130
84	SCE//MeCN	0.37	0.75	−0.28(2e)		0.65		130
85	Ag/AgCl//MeCN	0.53(2e)	0.90(2e)	−0.80(2e)		1.23	2.84	129
86a	SCE//DCM	0.495/0.20 (2e)		−0.39/−0.25 (2e)		∼0.8		131
86b	SCE//DCM	0.585/0.27 (2e)		−0.37/−0.255 (2e)		∼0.9		131
86c	SCE//DCM	0.625/0.25 (2e)		−0.425/−0.24 (2e)		∼1.0		131
87a	SCE//DCM	0.595	0.86	−0.394		0.99		132b
87b	SCE//DCM	0.596	0.872	−0.424		1.02		132b
88a	Ag/AgCl//MeCN−DCM (2:1)	0.55	0.825	−0.525	−1.20	1.08	1.81	133
89							2.92	134
90a	SCE//DCM	0.50	0.84	−0.59		1.09		135
90b	SCE//DCM	0.51	0.85	−0.60		1.11		135
91a	SCE//DCM	0.70	1.27	−0.55		1.25		135
91b	SCE//DCM	0.69	1.23	−0.56		1.25		135
92	Fc/Fc^+//MeCN	−0.09	0.37	−0.26	−0.77	0.17	0.75	137

tion (even in the solid state) was found, and the electron-acceptor properties of the molecules were not demonstrated. However, the increase of the oxidation potential in **61** was attributed to interaction of electron-deficient aryl groups with the TTF radical cation. A positively charged pyridinium group was used as an electron-acceptor unit in diad **62** (used in preparation of Langmuir−Blodgett films).[105] Again, no evidence of intramolecular donor−acceptor interaction or electrochemical amphotericity was presented. An isolated charged pyridinium group would be a very strong acceptor, but in reality its LUMO is highly stabilized by interaction with the counterion, which is very sensitive to the medium.

A significantly stronger acceptor moiety, which can give stable reduced states, is represented by the widely used viologen (4,4′-bipyridinium) unit. The first TTF−viologen donor−acceptor compounds **63**−**67** were reported jointly by Cava, Becher, and co-workers in 1997 (Chart 7).[106] A reasonably strong electron affinity of the bipyridinium moiety ($E_{1red} \sim -0.4$ V vs SCE) generated a distinct amphoteric multiredox electrochemical behavior in these molecules (Table 5), with an electrochemical gap between the first oxidation and the first reduction lower than 1 eV. The $\pi-\pi$ charge-transfer interaction between the TTF and bipyridinium moieties manifested itself in a charge-transfer absorption band at 1.9−2 eV, although there is a significant discrepancy between the $h\nu_{ICT}$ and the electrochemical gap. One explanation for this discrepancy could be the change of solvation factors associated with reduction of the charged acceptor moiety (in contrast to the neutral molecules, for which the similarity between optical, electrochemical, and DFT-calculated HOMO−LUMO gaps is often empirically established). Also, the $\pi-\pi$ donor−acceptor interaction disturbs the energy levels, causing the HOMO−LUMO gap of the complex (reflected by $h\nu_{ICT}$) to be higher than that in the uncomplexed state. Studies in a series of cyclophanes **66** demonstrated an increase in the electrochemical gap and the intensity of the ICT bands when the donor and acceptor parts were brought together by a shorter bridge. The related TTF−bisviologen cyclophane **68**[107] and TTF−(2,2′-bipyridinium) cyclophane **69**[108] demonstrated similar charge-transfer properties, although electrochemical amphotericity was not reported in these cases.

A further increase of the electron-acceptor (and charge-transfer complexing) ability is achieved with the bis-viologen cyclophane moiety in compounds **70a**,**b** (Chart 7).[109] An interesting peculiarity of

Chart 7. TTF−Viologen and Related Compounds

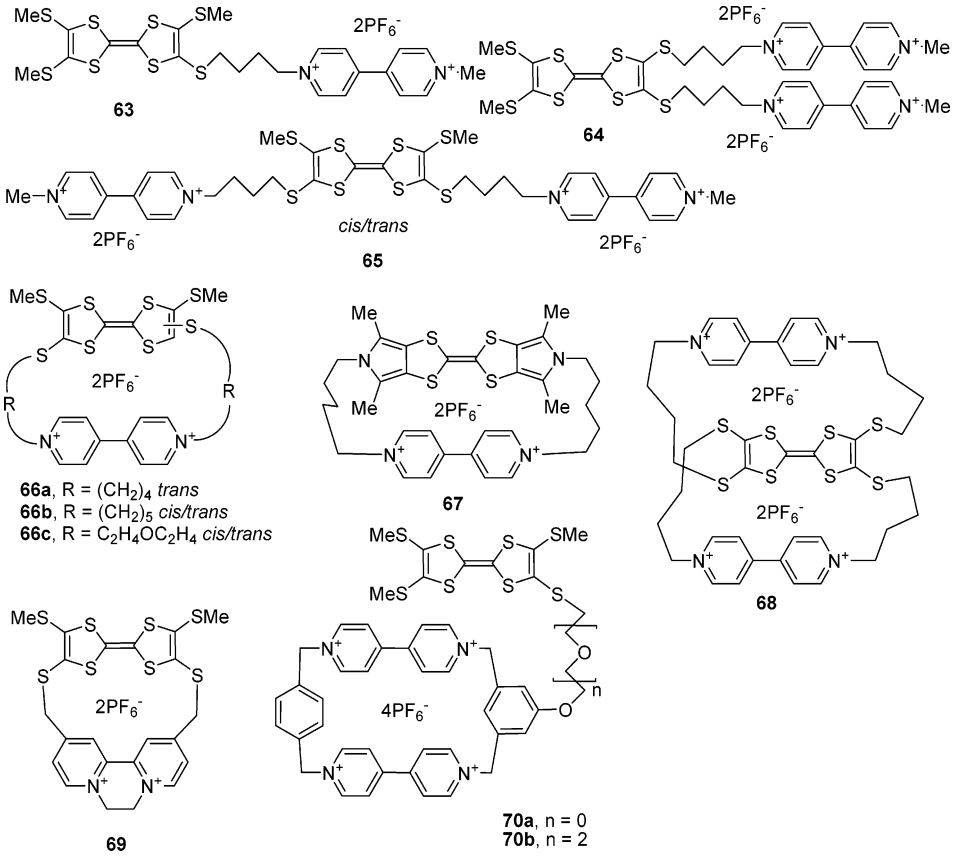

compound **70b** is very slow intramolecular complexation, which is observed as a developing ICT band at 785 nm over a few hours, as the TTF moiety is "sucked" inside the acceptor cyclophane cavity. Similar types of TTF D−A systems have been claimed, engendering skepticism and controversy, to be molecular switches in the solid state.[110] Some more examples of TTF−(viologen cyclophane) molecules, including the noncovalent rotaxane and catenane systems, can be found in a review by Becher et al.[111]

A similar donor−acceptor molecule **71** (Chart 8) consisting of the bis-TTF cyclophane donor "cavity" and covalently linked by the flexible bridge pyromellitic diimide (PI) was reported by the same group.[112] Although no electrochemical data have been reported, the known reduction potential of *N,N*-dialkylpyromellitic diimide (−0.95 V, −1.53 V vs SCE[113]) suggests **71** could be a moderate to weak acceptor. Few other TTF−PI cyclophanes (**72**, **73**) and linear analogues (**74**) have been reported, but the donor−acceptor interaction in these was rather weak and no amphotericity of redox properties was reported.[114] Extending the π-system in the acceptor going to naphthalene diimide and perylene diimide units reduces the LUMO energy, as demonstrated by enhanced electrochemical amphoterism in compounds **75**, **76**[115] and **77**, **78**[116] (Table 5).

Phthalocyanine as an acceptor moiety for TTF−σ-A conjugates was first used by Bryce et al. Compounds **79a**[117] and **79b**[118] (Chart 9) contained eight TTF units on the periphery of the phthalocyanine macrocycle, which resulted in amphoteric redox behavior: two oxidation waves of TTF and two reduction waves of phthalocyanine were observed, and an E_g value of 1.25 eV could be deduced from the redox potentials. Some other TTF−phthalocyanine diads with liquid-crystalline properties were synthesized.[119] Somewhat stronger electron-acceptor ability is expected from the phthalocyanine moiety in compounds **80**, which include zinc and copper complexes **80b** and **80c**.[120] Unfortunately, only the oxidation of these D−A conjugates has been studied. Later, silicon phthalocyanines, containing two TTF units connected through the silicon atom (e.g., **81a**), were studied as candidates for fluorescent switching devices.[121] The electrochemistry of **81a** was very similar to that of other TTF−phthalocyanine conjugates, and no redox switching of the fluorescence could be achieved. The phthalocyanine excited states were quenched by both neutral TTF (acting as donor) and TTF radical cation (acting as acceptor). However, redox switching of the fluorescence was recently reported by Becher et al. in the TTF−porphyrin diad **81b**.[122] Whereas the porphyrin fluorescence is effectively quenched (98%) in the neutral state of **81b**, its oxidation with $FeCl_3$ effectively restored the emission; that is, the TTF radical cation does not quench the excited state of the porphyrin (Figure 7). A similar electrochemical fluorescent switch was also demonstrated for bis-anthracene−TTF triads.[123] Compound **81b** revealed a clear four-stage amphoteric redox behavior with a HOMO−LUMO gap of ~1.4 eV. The apparent difference in fluorescence behavior of **81a** and **81b** cannot be explained by different energy levels of porphyrin versus phthalocyanine, since the electron-transfer quenching from the excited-

Chart 8. TTF−PI Diads and Triads

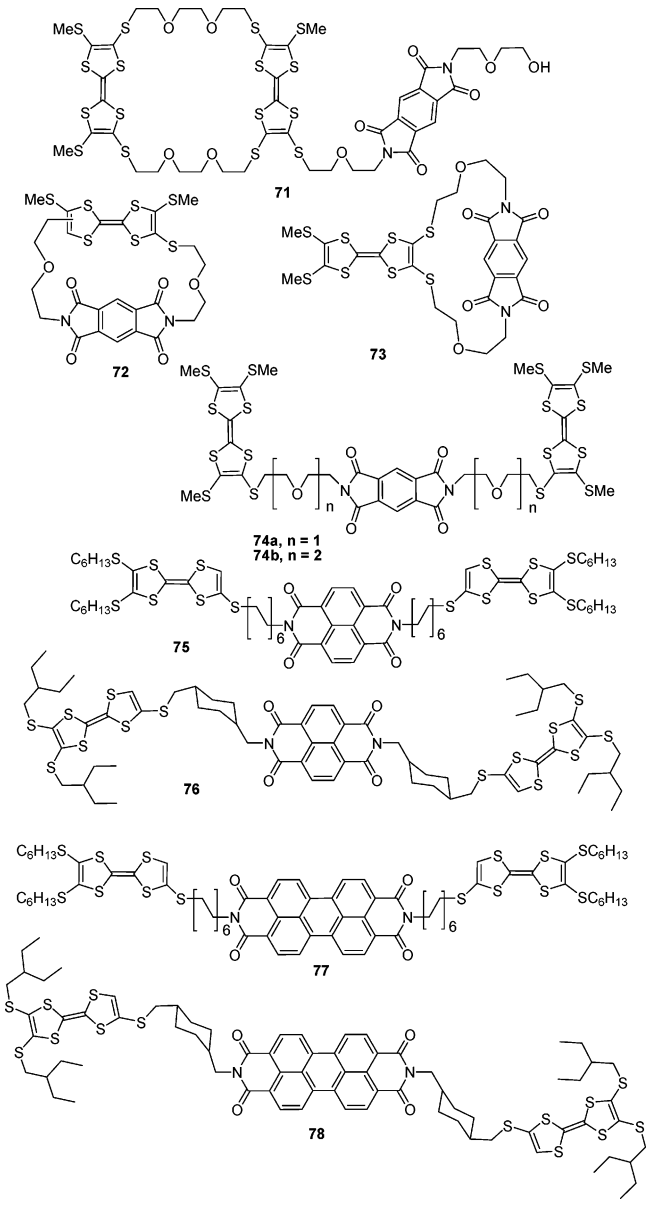

state porphyrin onto TTF radical cation (transfer from the LUMO of the excited acceptor onto the HOMO of $TTF^{\bullet+}$) for **81b** should be more efficient (compare the reduction potentials of **81** and **81b**, Table 5, considering that $Fc/Fc^+ = Ag/Ag^+ + 0.2$ V). On the basis of the fact that no intramolecular CT transition has been observed in **81b** in the ground state, one can speculate about the symmetry-forbidden nature of such a transition, precluding the quenching in the radical cation state.

The related TTF−porphyrin compounds with four fused TTF moieties (**81c** and **81d**) were synthesized, although their purification was a challenging task.[124] The electrochemical amphotericity was also established for these compounds, but the electrochemical gap was higher than that in phthalocyanine derivatives by ~0.5 eV (Table 5).

2.4.2. TTF–σ-TCNQ Systems

As demonstrated in Table 5, the electrochemical gap of all TTF−σ-A conjugates considered so far (compounds **61**−**81**) is ≥0.9 eV. The electron-donor ability of TTF is already close to the air-stability level, so a stronger acceptor unit (e.g., TCNQ[125]) should be used to achieve a lower HOMO−LUMO gap. After the first postulation of TTF−σ-TCNQ as an important synthetic target, many researchers have attempted the synthesis of such diads. However, it was soon realized that covalent linkage of such strong electron-donor and electron-acceptor units is very difficult.[126] The formation of insoluble charge-transfer complexes, electron-transfer processes, and subsequent side reactions of the radical ion species compete with covalent linking reactions. The first documented attempt to covalently link TTF and TCNQ appeared just two years after the Aviram and Ratner proposal. Hertler at Dupont laboratories has reported copolymerization of bifunctional TTF and TCNQ moieties, but no characterization of the black insoluble product (except elemental analysis) was presented (Scheme 6a).[127] Later, Panetta et al. used the same coupling method (as well as acid chloride−alcohol esterification) to obtain a TTF−TCNQ diad, but each reaction gave mixtures of, at least, two products whose structures were not thoroughly established (Scheme 6b).[128] Although a peak corresponding to the molecular ion can be observed in the mass spectrum, the elemental analysis was not sufficiently within accepted limits and the ambiguous electrochemical behavior (absence of characteristic TCNQ reduction waves) makes the postulated TTF−σ-TCNQ structure doubtful. No further studies of this reaction or product characterization have been reported.

The problem of charge-transfer complexation preceding the covalent coupling can be eliminated by employing the dibenzoTCNQ moiety (tetracyanoanthraquinodimethane, TCNAQ). Steric interactions in the TCNAQ result in "puckering" of the molecule, reducing the tendency to form a charge-transfer complex. Indeed, TTF−TCNAQ diads **82a**[129] and **82**−**84**[130] and triad **85**[129] can be readily synthesized by direct coupling of TTF acid chloride or fluoride with TCNAQ-containing hydroxy-functionality under nucleophilic catalysis. Very weak donor−acceptor interaction has been found in these diads in solution. A low-intensity ICT band is observed at 450 nm, although the bond length analysis of the crystal structure of **82b** shows no evidence of charge transfer. However, the distortion of the π-electron system in TCNAQ also dramatically reduces its electron-acceptor ability.[125] The electrochemical gap in the first TTF−TCNAQ diad **82a** (0.80 eV) was lately tuned by introducing electron-donating/withdrawing substituents (compounds **82b**, **83**, and **84**) to 0.62 eV, but it became obvious that ultimate amphotericity, similar to what was expected from a TTF−TCNQ diad, cannot be achieved in these systems.[130] Nevertheless, these compounds were the first well-characterized molecules containing both TTF and TCNQ structural fragments.

An interesting recent extension of this approach was demonstrated by Martín et al., who coupled anthraceno-TTF and anthraceno-TCNQ (TCNAQ) moieties in triad **86** (Chart 10).[131] Both donor and

Chart 9. TTF−Phthalocyanine and TTF−Porphyrine Compounds

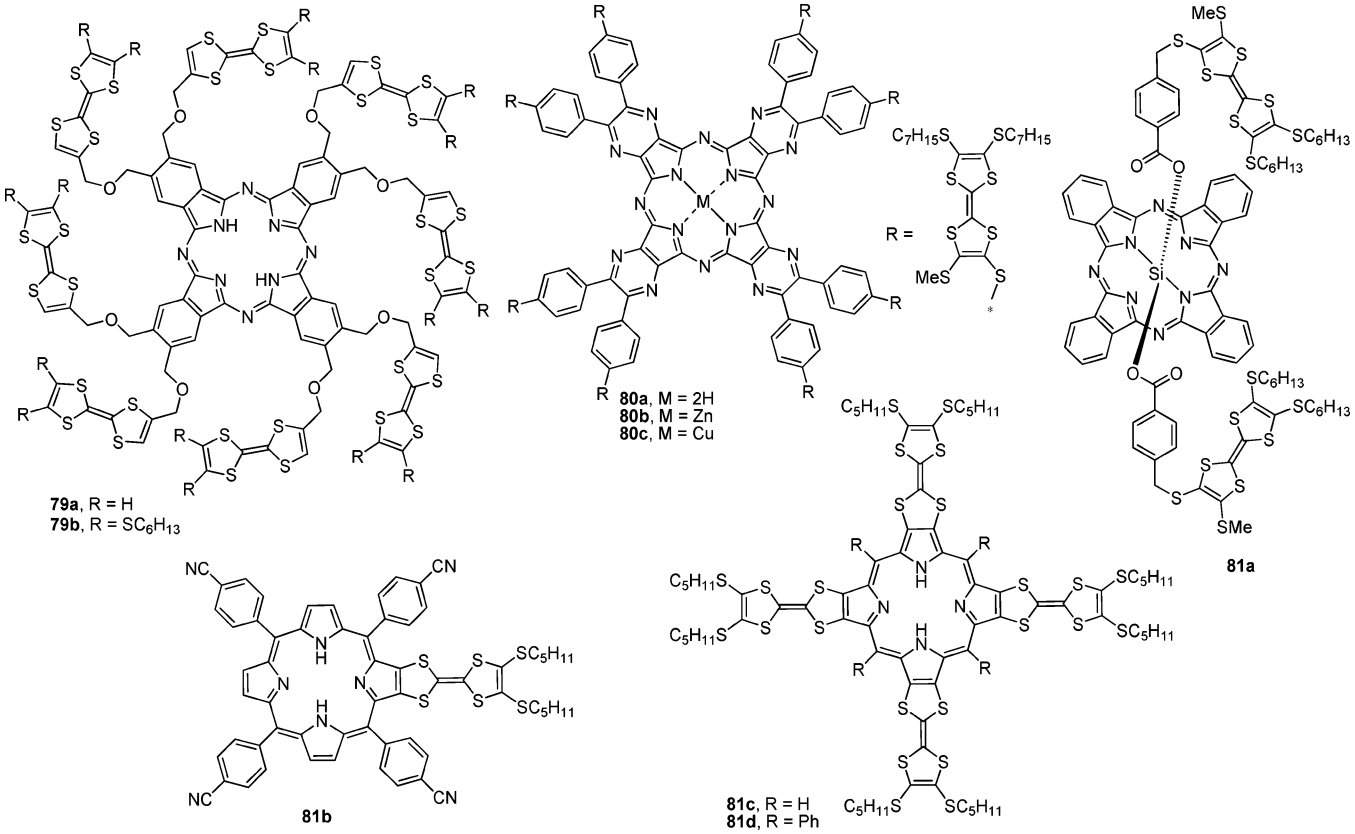

Chart 10. TTF−TCNAQ Diads and Triads

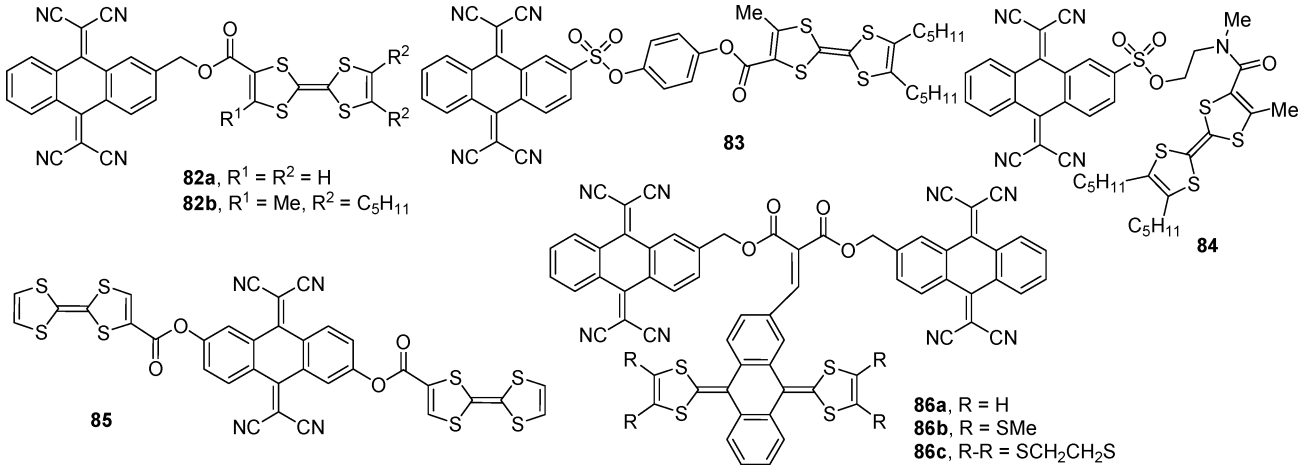

acceptor units in this molecule are quasi-reversible two-electron redox centers, where electron transfer is controlled by slow structural rearrangements. Lowering the temperature increases the separation between the anodic and cathodic peaks. Consequently, scanning the potential at −78 °C from the positive potential region (TTF^{2+}−TCNAQ) into negative potentials results in partial merging of the reduction of $TTFAQ^{2+}$ and TCNAQ, where the transient existence of the $TTFAQ^{2+}$−$TCNAQ^{2-}$ can be assumed (Figure 8).

To overcome a problem of covalently linking a strong electron donor and electron acceptor, TTF−benzoquinone compounds were designed as intermediates for the ultimate conversion into TTF−TCNQ molecules. After the first report by Watson et al.

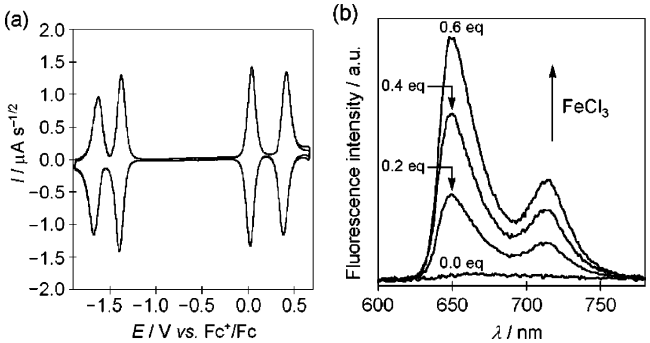

Figure 7. (a) Deconvoluted cyclic voltammogram of **81b**. (b) Restoration of the porphyrin fluorescence in **81b** upon oxidation of the TTF moiety. (Reproduced with permission from ref 122. Copyright 2003 Royal Society of Chemistry.)

Scheme 6. First Attempts at Covalently Linking the TTF and TCNQ Moieties in a Polymer[127] (a) and a Diad[128] (b) Structure

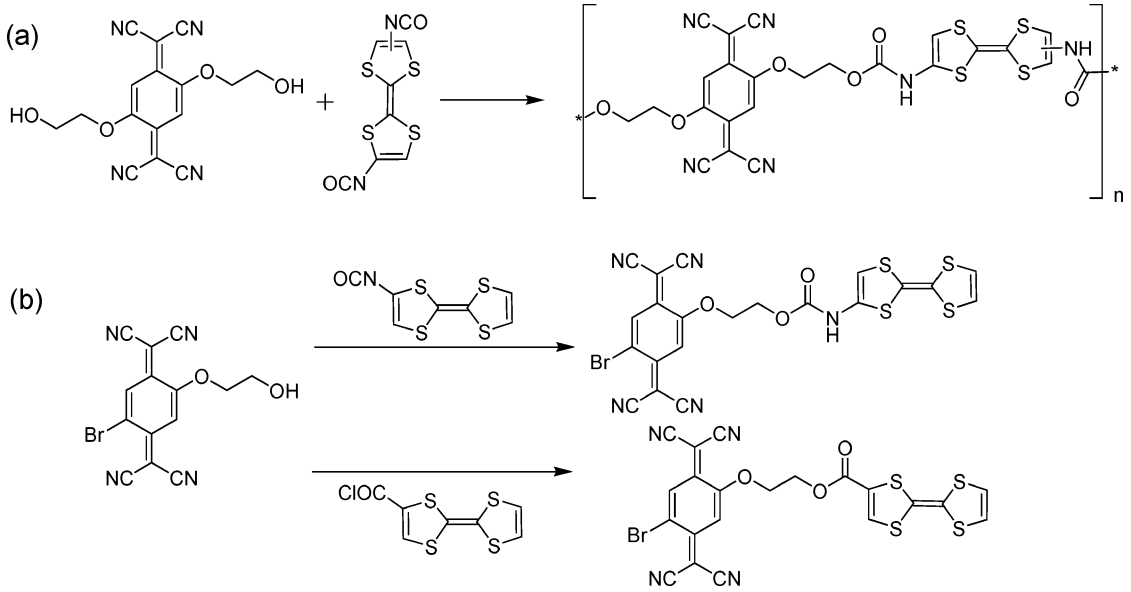

(compound **27**),[27] many other conjugated (**28**−**33**) and nonconjugated (**87**,[132] **88**,[133] **89**,[134] **90**, and **91**[135]) TTF−BQ compounds were synthesized. Being a moderate electron acceptor, BQ can be coupled with TTF in a relatively straightforward way, and the resulting conjugates possess a HOMO−LUMO gap of ~1 eV (Tables 2 and 5). Moderate semiconductivity was reported for some of these (e.g., **89**: $\sigma_{rt} = 2 \times 10^{-5}$ S/cm). To deliver a highly electrochemically amphoteric compound, the electron affinity of the acceptor group should be increased. However, all attempts to convert the BQ functionality to a TCNQ or dicyanoquinodiimine (DCNQI) moiety by treating with malononitrile or bis(trimethylsilyl)carbodiimide failed due to incompatibility of the TTF unit with the strongly acidic conditions ($TiCl_4$) of these reactions (Chart 11).[67,136]

Nevertheless, as was recently demonstrated, the TTF−σ-TCNQ diad can be synthesized by direct coupling of carefully chosen synthons. When the highly reactive TCNQ-containing acid chloride and TTF-containing lithium alcoholate were chosen, while performing the reaction at very low temperature (−100 °C), the byproduct charge-transfer complexation/electron-transfer processes can be suppressed, affording the target diad **92** in analytically pure form (elemental analysis, NMR, HPLC) in an acceptable yield of 27% (after chromatographic purification, Scheme 7).[137] Remarkably, despite exceptionally high electrochemical amphotericity, the diad **92** appeared to be a rather stable compound. Two reversible reductions of the TCNQ moiety and two reversible oxidations of TTF are very characteristic, and the difference between the first oxidation and the first reduction suggests the HOMO−LUMO gap of only 0.17 eV, which is the lowest reported value for closed-shell organic compounds (Figure 9). A low HOMO−LUMO gap allows thermal excitation electron transfer from the TTF onto the TCNQ fragment. Indeed, the solution ESR spectrum clearly shows two signals corresponding to TTF radical cation ($g = 2.0080$) and TCNQ radical anion ($g = 2.0045$), the intensities of which increase at elevated temperatures (Figure 10). Owing to its flexible σ-bridge, the molecule may exist in an "extended" conformation, with little interaction between the TTF and TCNQ moieties, and a "head-to-tail folded" conformation, with $\pi-\pi$ interaction between two moieties. The donor−acceptor interaction in the latter results in the appearance of a strong ICT band at $h\nu_{ICT}(max) = 0.75$ eV (1630 nm) and increases the HOMO−LUMO gap in the "folded" versus "extended" conformations, which is confirmed by DFT calculations at the B3LYP/6-311G(2d) level.[137] Due to the presence of two hydrophobic chains on TTF, **92** forms high-quality LB films, where the molecule adapts an "extended" conformation, with the TCNQ fragment laying flat on the surface and the TTF sticking out. This structure prevents donor−acceptor inter- or intramolecular interactions and renders the films bulk insulators, but the possible molecular rectification in these requires further studies.

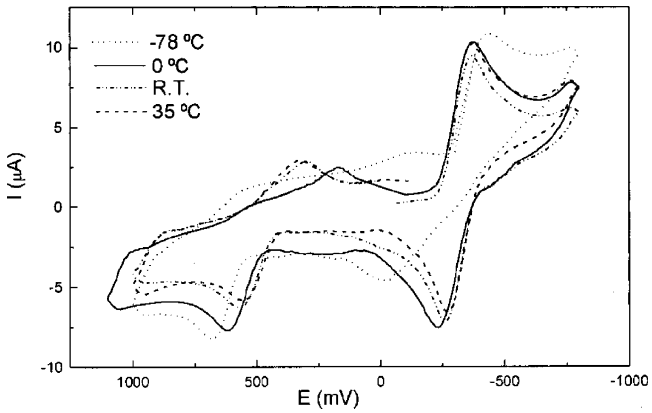

Figure 8. Cyclic voltammogram of TTFAQ−TCNAQ **86** at different temperatures. (Reproduced with permission from ref 131. Copyright 2001 Elsevier Science Ltd.)

2.4.3. TTF–Nitrofluorene Systems

A few years before the synthesis of the TTF−σ-TCNQ diad **92**, an alternative approach to low HOMO−LUMO gap TTF−A diads was demonstrated.

Chart 11. TTF−σ-Benzoquinone Diads

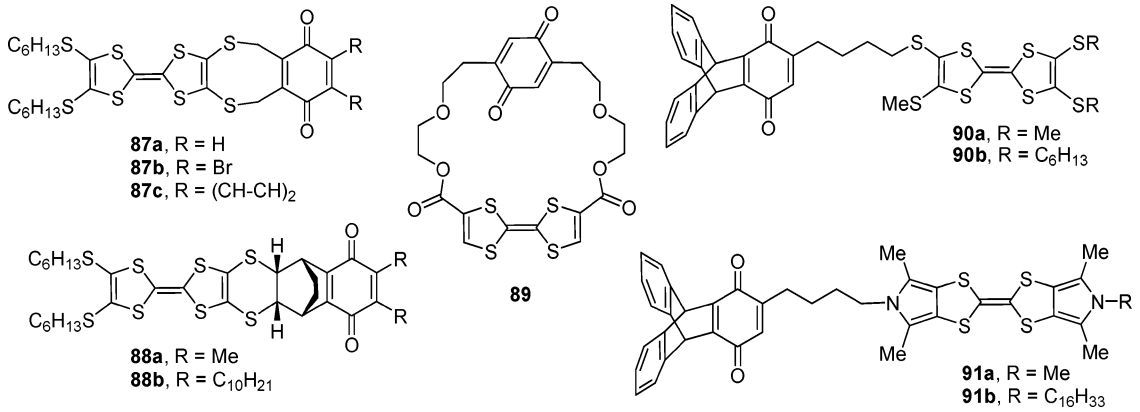

Scheme 7. Synthesis of the First Pure TTF−σ-TCNQ Diad 92

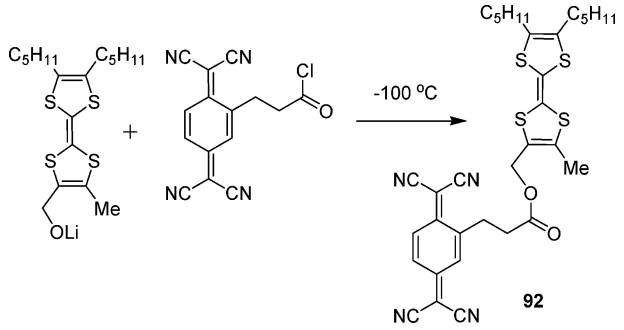

While the conversion of TTF−benzoquinone diads in the TTF−TCNQ derivatives failed due to highly acidic reaction conditions, it is known that condensation of polynitrofluoren-9-ones with malononitrile takes place under milder conditions[138] and the resulting dicyanomethylene derivatives have similar electron affinity to that of TCNQ. TTF−fluorene-9-one diads **93**−**98**(**a**) can be conveniently prepared (on a gram scale) by esterification of a TTF−alcohol moiety or amidation of TTF−amine moieties with readily synthesized nitrofluorenone acid chloride(s).[139] As determined by cyclic voltammetry, the TTF−fluorenone diads are already amphoteric compounds, displaying five reversible redox waves (two oxidations due to TTF and three reductions due to fluorenone), with a HOMO−LUMO gap as low as 0.5−0.6 eV (Figure 11, Table 6). The electron affinity of the fluorenone moiety can be essentially enhanced by simple treatment with malononitrile in DMF solution at room temperature (Scheme 8). The reduction waves of the resulting 9-dicyanomethylene derivatives **94**−**98**(**b**) are shifted into positive potentials by ∼300 mV (for E_{1red}), which shrinks the HOMO−LUMO gap to ∼0.3 eV. Similar to TTF−σ-TCNQ diad **92**, compounds **93**−**95** can also adopt an "extended" and "head-to-tail" self-complexed conformation, whose HOMO−LUMO gaps can be ascertained by electrochemistry and optical spectroscopy, respectively. On the other hand, the short σ-bridge in the diads **96** precludes formation of the "head-to-tail" conformation, and the ICT band, seen at $h\nu_{ICT} \sim 1$ eV for **94b** and **95b** (Table 6), is not observed in dilute solutions of **96** (although the intermolecular CT band appears in concentrated solutions and in the solid state).[139b] The stability of the redox states of **92**, **94b**, and **95b**, each with different characteristic absorption, makes these compounds attractive multichannel electro-

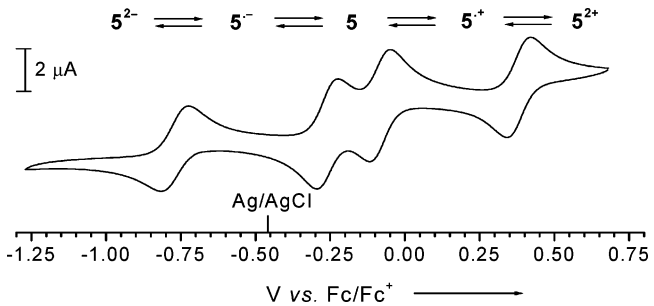

Figure 9. Cyclic voltammetry of **92** in MeCN at 100 m V/s. **5** stands for compound **92**. (Reproduced with permission from ref 137. Copyright 2003 WILEY−VCH Verlag GmbH.)

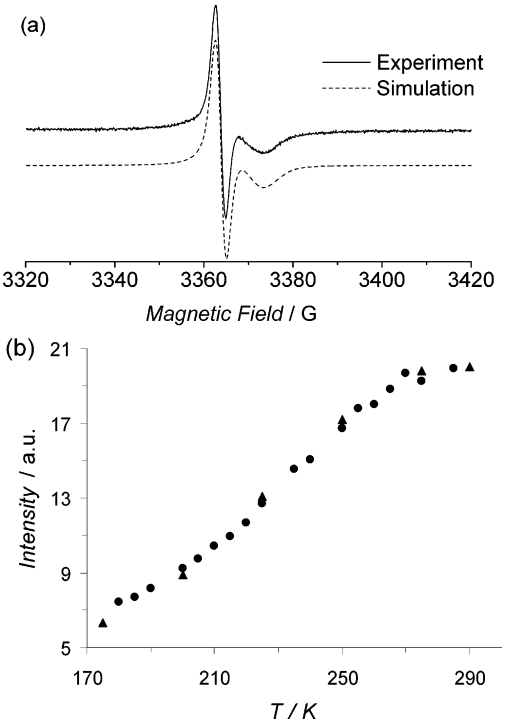

Figure 10. (a) X-band ESR signal of **92** in dicloromethane solution. The dashed line is a simulation assuming two signals with *g*-values of 2.0045 and 2.080, in 1:1 ratio. (b) Temperature dependence of the EPR signal of **92** in CH_2Cl_2 solution (circles and triangles represent two independent experiments). (Reproduced with permission from ref 137. Copyright 2003 WILEY−VCH Verlag GmbH.)

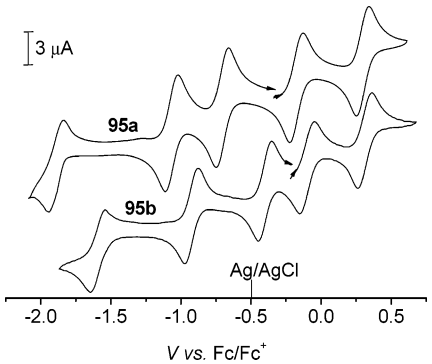

Figure 11. Cyclic voltammograms of TTF−fluorene diads **95a** and **95b**. (Reproduced with permission from ref 139b. Copyright 2002 WILEY−VCH Verlag GmbH.)

chromic materials: the change between up to five different colors in the visible and near-IR regions can be achieved by applying different voltages (from −1.5 to +1.0 V) to a single-component system (Figure 12). Remarkably, a red (dianion), green (radical cation), or blue (radical anion) color can be generated by switching the redox state of **92**.[137]

Analogous TTFAQ−fluorene diads **97** and triads **98** were synthesized later.[60] The oxidation potential of TTFAQ is very similar to that of TTF; therefore, the electrochemical gap of **97** is similar to that of the corresponding compounds **93**−**96** (Table 6). The small gap between the oxidation and reduction and the quasi-reversibility of the TTFAQ oxidation result in a remarkable consequence. As mentioned earlier, the oxidation TTFAQ → $TTFAQ^{2+}$ and its reverse (reduction) are a kinetically controlled process due to associated structural changes. Sweeping the potential from ∼ −0.1 V vs Fc/Fc^+ (corresponding to neutral **97b**) into the negative direction results in subsequent formation of radical anion, radical dianion, and radical trianion species (located on the fluorenone moiety), and the reverse (reoxidation) processes occur on the back sweep (Figure 13). When the potential exceeds ∼ +0.1 V, the TTFAQ fragment oxidizes to dication **97b**$^{2+}$. Repeating the scanning in the negative

Table 6. Cyclic Voltammetry and Optical Absorption Data for TTF−*σ*-Fluorene Compounds

compd	RE//solvent	$E°_{1ox}$, V	$E°_{2ox}$, V	$E°_{1red}$, V	$E°_{2red}$, V	$E°_{3red}$, V	E_g, eV	$h\nu_{ICT}$, eV	ref
93	Fc/Fc^+//DCM	−0.07	0.40	−0.66	−1.01		0.59	1.19	139
94a	Fc/Fc^+//DCM	−0.13	0.37	−0.68	−1.04	−1.86	0.55	1.25	139
94b	Fc/Fc^+//DCM	−0.09	0.35	−0.39	−0.90	−1.57	0.30	1.01	139
95a	Fc/Fc^+//DCM	−0.17	0.31	−0.69	−1.06	−1.84	0.52	1.27	139
95b	Fc/Fc^+//DCM	−0.10	0.32	−0.38	−0.90	−1.56	0.28	0.98	139
96a	Fc/Fc^+//DCM	−0.11	0.40	−0.72	−1.00	−1.81	0.61		139
96b	Fc/Fc^+//DCM	−0.10	0.41	−0.39	−0.93	−1.62	0.29		139
97a	Fc/Fc^+//DCM	−0.07/−0.30(2e)		−0.65	−1.02	−1.85	∼0.7		60
97b	Fc/Fc^+//DCM	−0.07/−0.33[a](e)		−0.35[a]	−0.94	−1.53	∼0.4		60
98a	Fc/Fc^+//DCM	−0.11/−0.43		−1.05	−1.24		∼1.1		60
98b	Fc/Fc^+//DCM	−0.11/−0.43		−0.61	−1.15	−1.77	∼0.7		60

[a] This peak could be determined only approximately, due to overlap with another redox peak.

Scheme 8. TTF−Fluorenone Donor−Acceptor Diads[a]

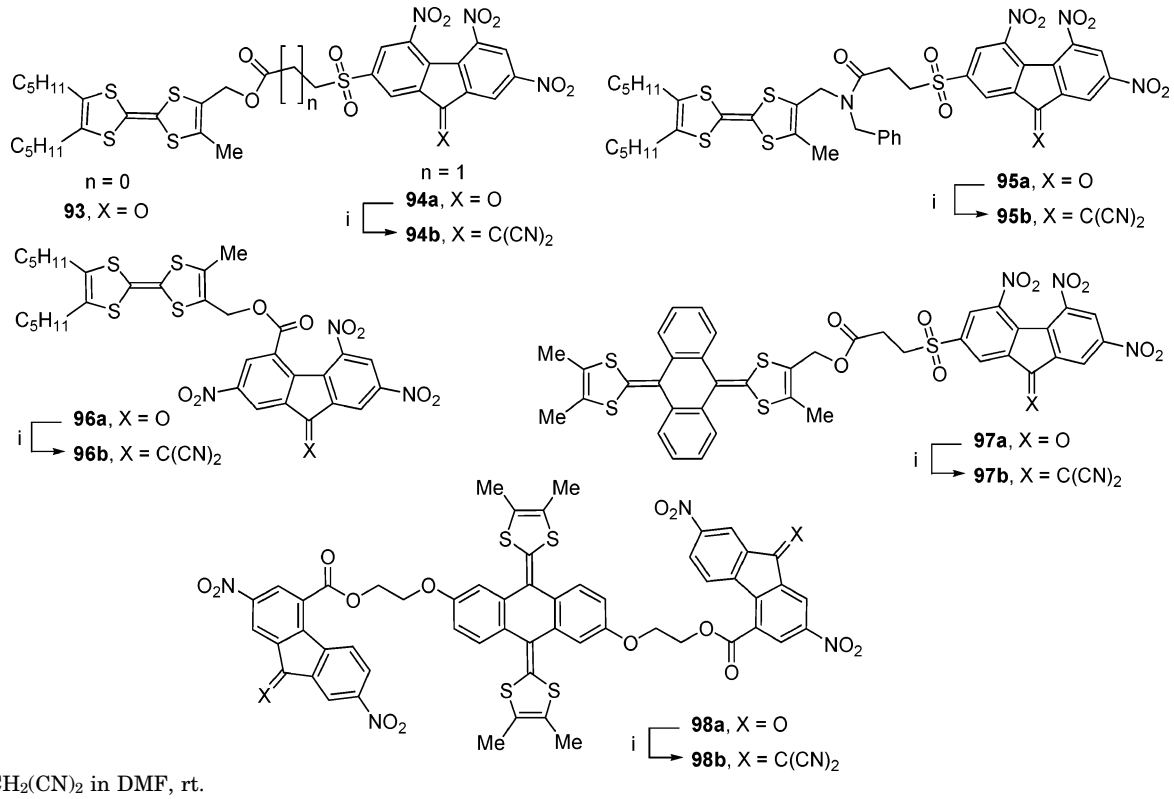

[a] (i) $CH_2(CN)_2$ in DMF, rt.

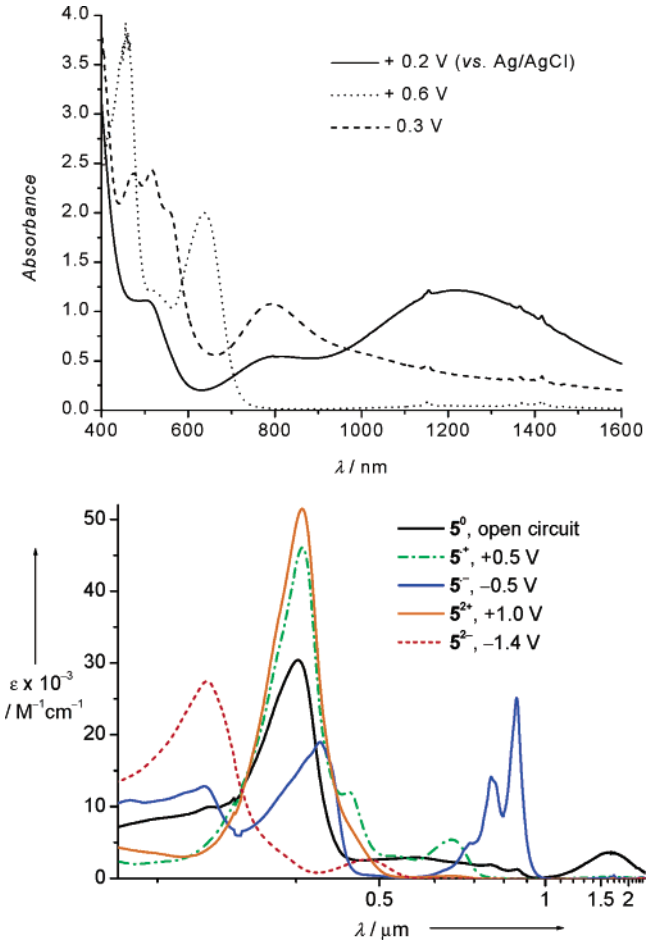

Figure 12. Solution spectroelectrochemistry of diads **94b** (top; solid, dotted, and dashed lines correspond to **94b**^{0}, **94b**$^{\bullet+}$, and **94b**$^{\bullet-}$, respectively) and **92** (bottom; potentials vs Ag wire; "**5**" stands for compounds **92**). (Reproduced with permission from refs 139a and 137, respectively. Copyright 2001 American Chemical Society and 2003 WILEY−VCH Verlag GmbH, respectively.)

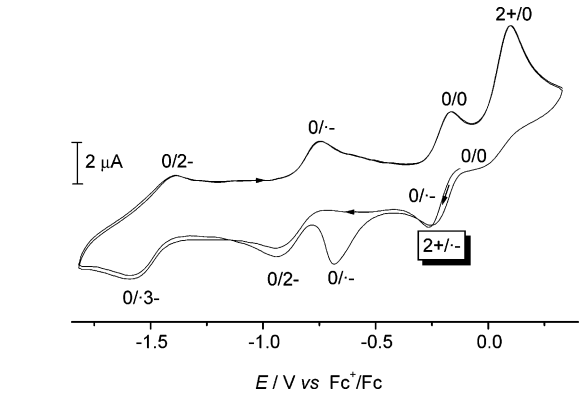

Figure 13. Cyclic voltammogram of **97b** in DCM at −15 °C. (Reproduced with permission from ref 60. Copyright 2003 American Chemical Society.)

direction is very different: at a relatively fast scan rate and/or lowered temperature, the reduction peak (due to formation of fluorene radical anion) *precedes* the rereduction of TTFAQ dication to the neutral species. Consequently, an unusual kinetically stable (fraction of a second to seconds, depending on the temperature) charge-separated state of **97b** $D^{2+}-\sigma-A^{\bullet-}$ is formed.[60] This is a very rare example of preferential electron transfer to a thermodynamically less favorable but kinetically more accessible site.[140] The conclusion is in agreement with an in-situ spectroelectrochemical experiment, where the characteristic UV−vis absorbances of both TTFAQ dication and fluorene radical anion coexist at a certain potential.

2.5. Fullerene as an Acceptor for Donor−Acceptor Diads

2.5.1. Electronic Properties of Fullerene

In the field of π-functional redox active molecular materials, a place of distinction definitely belongs to buckminsterfullerene (**100**, C_{60}), discovered in 1985 by Kroto, Smalley, and co-workers.[141]

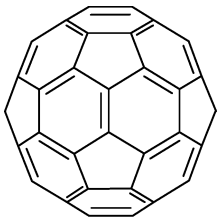

100 (C_{60})

Very soon after the discovery of this fascinating molecular structure, fullerene and its charge-transfer salts were demonstrated to be promising electronic materials. Metallic conductivity and superconductivity were found in several fullerene anionic complexes.[142] Special photophysical properties of buckminsterfullerene, including high absorption throughout the visible spectral region and the ability of rapid photoinduced charge separation, put the fullerene and its derivatives among the most important organic materials for photovoltaics applications and, particularly, plastic solar cells.[143,144]

The special electronic properties of buckminsterfullerene are directly connected with its low HOMO−LUMO gap, which is the result of its extended conjugated π-electronic structure based on an unusual hybridization resulting from an unconventional pyramidalization.[145] The long-wavelength absorption of C_{60} is expressed by a complex band with the most intense peak at λ_{max} = 540 nm, followed by lower intensity, presumably vibronic, bands with λ_{max} = 568, 591, 598, and 621 nm (Figure 14).[146] In accord with the low optical HOMO−LUMO gap (2.34 eV based on the most intense peak), both oxidation and reduction were observed for C_{60}, and the difference between $E°_{1ox}$ (1.27 V vs Fc/Fc$^+$) and $E°_{1red}$ (−1.06 V vs Fc/Fc$^+$) agrees well with the optical gap.[147] Generally, fullerene is a unique molecule with regard to the richness of its redox chemistry. Although two to three reversible reductions (and no oxidation) were described in early reports,[148] at lower temperatures and in mixed solvents, C_{60} shows six reversible single-electron reduction waves (Figure 15).[149] Using a low-nucleophilicity electrolyte (Bu_4NAsF_6), three (partially) reversible single-electron oxidation waves have been recently observed, although reduced states are more stable than oxidized states.[147] In interaction

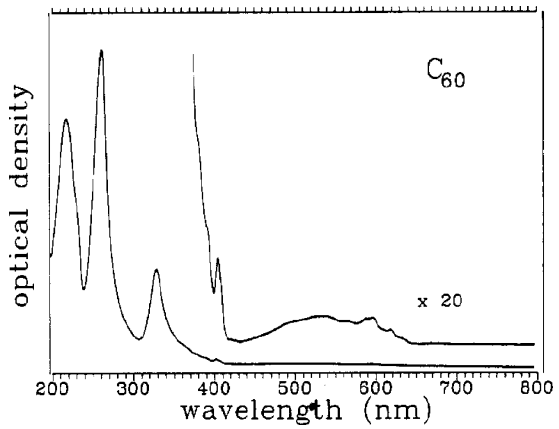

Figure 14. UV−vis spectra of fullerene **100** in hexane solution. (Reproduced with permission from ref 146. Copyright 1990 American Chemical Society.)

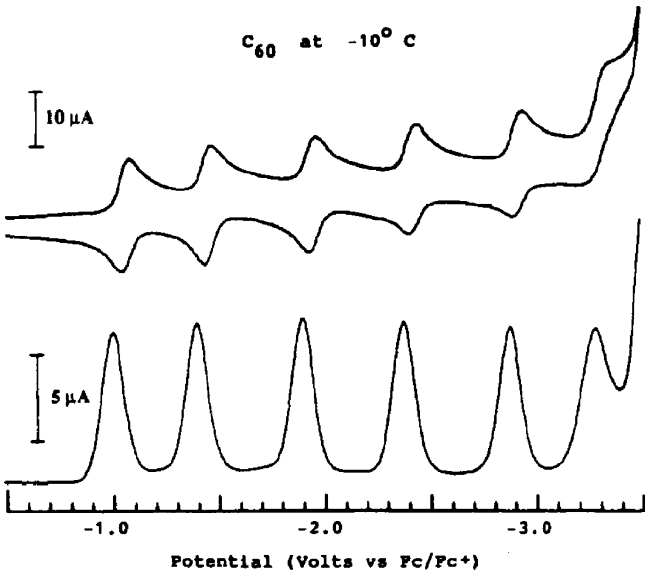

Figure 15. Cyclic voltammogram (top) and differential pulse voltammogram (bottom) of fullerene **100** in MeCN/toluene. (Reproduced with permission from ref 149. Copyright 1992 American Chemical Society.)

with other compounds, fullerene acts as a moderate strength electron acceptor. It forms weak charge-transfer complexes with many typical electron donors, including TTF derivatives.[150] With stronger electron donors, such as alkali metals, radical anion salts are formed; several of these become superconducting in the range 1−40 K.[142] On the basis of gas-phase measurements, the IP and EA values 7.6 and 2.7 eV, respectively, were found for C_{60}.[18]

2.5.2. Fullerene−TTF Conjugates

Bearing unique electrochemical and photophysical properties, fullerene was expected to and was found to be the most desirable moiety for construction of covalent donor−acceptor diads. The synthesis of the desired molecules became possible in the mid-1990s with the development of several synthetic approaches toward covalent functionalization of fullerene.[151] Many different donor moieties have been, so far, connected to C_{60}, and an electrochemical gap as low as 1 eV has been achieved for a fullerene−ferrocene diad.[150]

The first TTF−fullerene diads were prepared almost simultaneously by Prato et al. (compound **101a**[152]) and Martín et al. (compounds **101a**−**d**[153]) by [3 + 2] cycloaddition of an azomethine ylide intermediate (formed between *N*-alkylated β-alanine and a TTF-containing aldehyde) to the fullerene [6,6] double bond. Later, some more TTF−fullerene diads (**101e** and **102**,[154] **103a**,**b**[155]) were synthesized following the same approach. These compounds were, indeed, unique in the richness of their electrochemical behavior. The cyclic voltammetry clearly showed two reversible oxidation waves due to TTF and up to five reversible (or quasi-reversible) reduction waves due to fullerene, giving rise to eight possible redox states (2+; •1+; 0; •1−; 2−; •3−; 4−; •5−).[152] Moderately strong acceptor properties of the fullerene lead to an electrochemical HOMO−LUMO gap in these compounds in the range ∼1−1.2 eV (Table 7). This gap is quite independent of the linker between TTF and C_{60}, suggesting little interaction between them (cf. **103a** and **103b**). Replacement of electron-withdrawing alkylthio substituents on the TTF nucleus with hydrogen atoms reduces the HOMO−LUMO gap by ∼0.1 eV. On the other hand, with a few exceptions (e.g., fluorinated C_{60}, see below), any substituents in the fullerene moiety would decrease the electron-acceptor properties of the latter. In fact, its reduction potential had already decreased by 50−100 mV by saturation of a double bond, which prevents the achievement of a HOMO−LUMO gap $\ll$ 1 eV in such (nonfluorinated) diads. Therefore, only weak charge transfer occurs in TTF−fullerene diads in the ground state. However, photoexcitation of the fullerene moiety [λ_{abs} = 699 nm (1.77 eV), λ_{emis} = 719 nm (1.75 eV)] results in thermodynamically favorable electron transfer from TTF onto fullerene, which is observed as quenching of the fullerene fluorescence and the appearance of the characteristic absorption features of $TTF^{\bullet+}$ and $C_{60}^{\bullet-}$.[154] As expected, the rate of electron transfer decreases rapidly with elongation of the linker between the donor and the acceptor (cf. $k_{et} = 9.1 \times 10^9$ s^{-1} for **102**, 1.6×10^9 s^{-1} for **101c**, and 7.7×10^8 s^{-1} for **101e**).[154]

A diverse family of TTF−fullerene compounds has been synthesized in the last 5−6 years. The triazolinofullerene−TTF diad **104**, published by Guldi et al. by reaction of TTF−alkyl azide with C_{60}, has somewhat improved electron-acceptor properties (cf. **101** and **104**, Table 7)[156] and would have one of the lowest HOMO−LUMO gaps in the series, if electron-donating alkyl groups were to replace the reported alkylthio substituents in TTF.

The syntheses of compounds **105a**,**b** are based on a principally different approach, which includes reaction of C_{60}^{2-} with 1,3-dibromo-2-propanone, followed by reduction and esterification with a TTF-containing acid.[157] In contrast to the cases of compounds **103a**,**b**, elongation of the linker between donor and acceptor (from 1 to 10 methylene groups) resulted in a small but observable diminution of the HOMO−LUMO gap (from 1.25 to 1.21 eV, Table 7).

The Diels−Alder cyclization of fullerene with 4,5-dimethylideneTTF (generated in situ) gave rise to the largest series of TTF−fullerene compounds (**106**).

Table 7. Electrochemical Data for TTF−Fullerene Compounds

compd	RE//solvent	E_{1ox}, V	E_{2ox}, V	E_{1red}, V	E_{2red}, V	E_{3red}, V	$E_{4red(5red)}$, V	E_g, eV	ref
C_{60}	Fc/Fc^+//DCM	1.27	1.71[a]	−1.06	−1.46	−1.89			147
C_{60}	Ag/Ag^+//DCM			−0.84	−1.28				183
$C_{60}F_{46}$	Ag/Ag^+//DCM			0.51	0.01ir				183
$C_{60}H_{48}$	Ag/Ag^+//DCM			0.53	0.18				183
$C_{70}F_{54}$	Ag/Ag^+//DCM			0.76	0.32	−0.15			183
101a	Fc/Fc^+//toln−MeCN (3:1) (−45 °C)	−0.12	+0.24	−1.03	−1.43	−1.99	−2.41 (−3.09)	0.91	152
101a	SCE//toln−MeCN (4:1)	0.41	0.76	−0.67	−1.04	−1.53	−2.05	1.08	153
101b	SCE//toln−MeCN (4:1)	0.50	0.78	−0.71	−1.05	−1.56	−2.10	1.21	153
101c	SCE//toln−MeCN (4:1)	0.43	0.76	−0.67	−1.08	−1.58	−2.19	1.10	153
101d	SCE//toln−MeCN (4:1)	0.54	0.78	−0.71	−1.19	−1.61	−2.20	1.25	153
101e	SCE//toln−MeCN (4:1)	0.48	0.83	−0.66	−1.04	−1.58	−2.19	1.14	154
102	SCE//toln−MeCN (4:1)	0.51	0.87	−0.65	−1.08	−1.65	−2.12	1.16	154
103a	SCE//DCM	0.50	0.86	−0.72	−1.11			1.22	155
103b	SCE//DCM	0.51	0.85	−0.70	−1.08			1.21	155
104	SCE//toln−MeCN (4:1)	0.57	0.70	−0.57	−0.97	−1.52	−2.00	1.14	156
105a	Fc/Fc^+//toln−MeCN(3:1)	0.19	0.41	−1.06	−1.47			1.25	157
105b	Fc/Fc^+//toln−MeCN(3:1)	0.16	0.38	−1.05	−1.47			1.21	157
106a	Fc/Fc^+//DCM	−0.04	0.46	−1.08	−1.47	−1.98	−2.49	1.04	159
	Fc/Fc^+//ODCB	−0.08	0.43	−1.17	−1.53	−2.05		1.09	159
106b	Fc/Fc^+//DCM	−0.10	0.41	−1.08	−1.45	−1.96	−2.52	0.98	159
	Fc/Fc^+//ODCB	−0.15	0.41	−1.18	−1.55	−2.06		1.03	159
106c	Ag/AgCl//ODCB	0.64	1.08	−0.72	−1.11	−1.61		1.36	161
106c	SCE//ODCB	0.60	1.04	−0.76	−1.15	−1.65	−1.92	1.36	160a
106d	Fc/Fc^+//DCM	0.21	0.69	−1.04	−1.43	−1.96	−2.57	1.25	159
	Fc/Fc^+//ODCB	0.13	0.65	−1.21	−1.63	−1.99		1.34	159
106d	Fc/Fc^+//DCM	0.18	0.65	−1.08	−1.46	−1.97		1.26	158
106e	Ag/AgCl//ODCB	0.65	1.09	−0.72	−1.09	−1.59		1.37	161
106f	Ag/AgCl//ODCB	0.64	1.14	−0.72	−1.08	−1.60		1.36	161
106g	Ag/AgCl//ODCB	0.65	1.15	−0.72	−1.17			1.37	161
106h	Ag/AgCl//ODCB	0.66	1.16	−0.71	−1.10	−1.60		1.37	161
106h	Ag/AgCl//ODCB	0.549	1.034	−0.623	−0.993	−1.493		1.17	162
106i	Ag/AgCl//ODCB	0.67	1.04	−0.71	−1.09	−1.61		1.38	161
106j	Ag/AgCl//ODCB	0.68	1.05	−0.71	−1.08	−1.60		1.39	161
106k	Ag/AgCl//ODCB	0.547	0.928	−0.628	−0.999	−1.495		1.18	162
106l	Ag/AgCl//ODCB	0.503	0.845	−0.631	−0.997	−1.523		1.13	162
107	SCE//ODCB	0.57	0.88	−0.70	−1.07	−1.60		1.27	163
108	Ag-wire//DCM	0.76	1.30	−0.10	−0.48	−0.85		0.86	164
109	SCE//toln−MeCN (4:1)	0.49	0.73	−0.62	−1.25	−1.65	−1.96	1.11	166
110	SCE//DCM	0.51	0.92	−0.75	−1.15	−1.67		1.11	167
111	SCE//DCM	0.51	0.92	−0.75	−1.15	−1.67		1.26	168
112a	Ag/AgCl//ODCB	0.62	1.02	−0.75	−1.12	−1.84		1.37	161
112b	Ag/AgCl//ODCB	0.70	1.16	−0.82	−1.20	−1.83		1.52	161
112c	Ag/AgCl//ODCB	0.65	1.09	−0.85	−1.22	−1.85		1.50	161
112d	Ag/AgCl//ODCB	0.69	1.07	−0.83	−1.22	−1.85		1.52	161
112e	Ag/AgCl//ODCB	0.68	1.03	−0.85	−1.24	−1.61		1.53	161
112f	Fc/Fc^+//DCM	0.17	0.64	−1.16	−1.52	−1.95	−2.41	1.33	159
	Fc/Fc^+//ODCB	0.13	0.58	−1.27	−1.64	−2.02		1.40	159
113a	Ag/AgCl//ODCB	0.63	1.05	−0.77	−1.06			1.40	161
113b	Ag/AgCl//ODCB	0.69	1.14	−0.98	−1.35			1.67	161
113c	Ag/AgCl//ODCB	0.72	1.10	−0.98	−1.35			1.70	161
113d	Ag/AgCl//ODCB	0.72	1.11	−0.96	−1.34			1.68	161
113e	Ag/AgCl//ODCB	0.73	1.08	−0.95	−1.38	−1.67		1.68	161
114	Ag/AgCl//ODCB	0.61	0.84	−1.16				1.77	161
115	Ag/AgCl//ODCB	0.56	1.09	−0.61	−1.00	−1.45	−2.08	1.17	161
116a	Ag/AgCl//ODCB	0.58	1.11	−0.78	−1.34	−1.65		1.36	161
116b	Ag/AgCl//ODCB	0.62	1.04	−0.88	−1.13	−1.65		1.50	161
116c	Ag/AgCl//ODCB	0.61	1.10	−0.81	−1.19			1.42	161
117	SCE//ODCB	0.54	0.88	−0.67	−1.03	−1.58		1.21	163
118	SCE//ODCB	0.51	0.83	−0.70	−1.05	−1.58		1.21	163
119a	SCE//toln−MeCN (4:1)	0.46(2e)		−0.66	−1.01	−1.67	−1.96	1.12	170
119b	SCE//toln−MeCN (4:1)	0.60(2e)		−0.67	−1.10	−1.67	−2.20	1.27	170
119c	SCE//toln−MeCN (4:1)	0.50(2e)		−0.64	−0.99	−1.67	−1.95	1.14	170
119d	SCE//toln−MeCN (4:1)	0.50(2e)		−0.65	−1.05	−1.62	−1.90	1.15	171
119e	SCE//toln−MeCN (4:1)	0.71(2e)		−0.70	−1.10	−1.70	−2.06	1.41	171
119f	SCE//toln−MeCN (4:1)	0.61(2e)		−0.66	−1.07	−1.64	−1.93	1.27	171
120	SCE//ODCB−MeCN (4:1)	0.39(2e)		−0.69	−1.07	−1.61	−2.01	1.08	172
121a	SCE//toln−MeCN (4:1)	0.55(2e)	0.75	−0.63	−1.07	−1.64	−2.14	1.18	166
121b	SCE//toln−MeCN (4:1)	0.70(3e)		−0.66	−1.06	−1.64		1.33	166
122	SCE//toln−MeCN (4:1)	0.75(2e)		−0.72	−1.17	−1.75	−2.30	1.47	173
123a	SCE//toln−MeCN (4:1)	0.48(2e)		−0.68	−1.12	−1.62	−2.00	1.16	174
123b	SCE//toln−MeCN (4:1)	0.59(2e)		−0.65	−1.07	−1.59	−1.95	1.14	174
124a	SCE//toln−MeCN (4:1)	0.45(2e)		−0.67	−0.99	−1.59	−1.95	1.12	174
124b	SCE//toln−MeCN (4:1)	0.55(2e)		−0.64	−0.98	−1.61	−1.95	1.19	174

Table 7 (Continued)

compd	RE//solvent	E_{1ox}, V	E_{2ox}, V	E_{1red}, V	E_{2red}, V	E_{3red}, V	$E_{4red(5red)}$, V	E_g, eV	ref
125a	not known	0.48(2e)		−0.57	−0.98	−1.55		1.05	175
125b	not known	0.61(2e)		−0.59	−1.01	−1.53		1.20	175
127a	SCE//toln−MeCN (4:1)	0.52(2e)		−0.68	−1.08	−1.66	−2.20	1.20	176
127b	SCE//toln−MeCN (4:1)	0.60(2e)		−0.65	−1.00	−1.72	−2.33	1.25	176
127c	SCE//toln−MeCN (4:1)	0.60(2e)		−0.66	−1.02	−1.64		1.26	176
128a	SCE//toln−MeCN (4:1)	0.50(2e)		−0.63	−0.99	−1.58		1.13	177
128b	SCE//toln−MeCN (4:1)	0.66(2e)		−0.65	−1.03	−1.55		1.31	177
128c	SCE//toln−MeCN (4:1)	0.67(2e)		−0.63	−1.02	−1.52		1.40	177
129b	SCE//toln−MeCN (4:1)	0.55(2e)		−0.78	−1.23	−1.80		1.33	177
130a	SCE//toln−MeCN (4:1)	0.45(2e)		−0.62	−0.98	−1.50		1.07	177
130b	SCE//toln−MeCN (4:1)	0.67(2e)		−0.64	−1.04	−1.54		1.31	177
130c	SCE//toln−MeCN (4:1)	0.63(2e)		−0.67	−1.00	−1.53		1.30	177
131b	SCE//toln−MeCN (4:1)	0.60(2e)		−0.67	−1.02	−1.52		1.27	177
132a	SCE//ODCB−MeCN (4:1)	0.41(4e)		−0.70	−1.08	−1.61	−2.01	1.11	172
132b	SCE//ODCB−MeCN (4:1)	0.43(4e)		−0.59	−1.07	−1.61	−1.99	1.02	172
134a	SCE//PhCN	0.48(2e)	1.02	−0.56	−0.97	−1.17		1.04	179
134b	SCE//PhCN	0.50(2e)	0.82	−0.56	−1.00			1.06	179
135	Me10Fc//$C_2H_4Cl_2$	0.53(2e)		−0.005				0.54	187

[a] A third oxidation wave at 2.14 V was observed at −55 °C.

Chart 12. TTF−Fullerene Diads

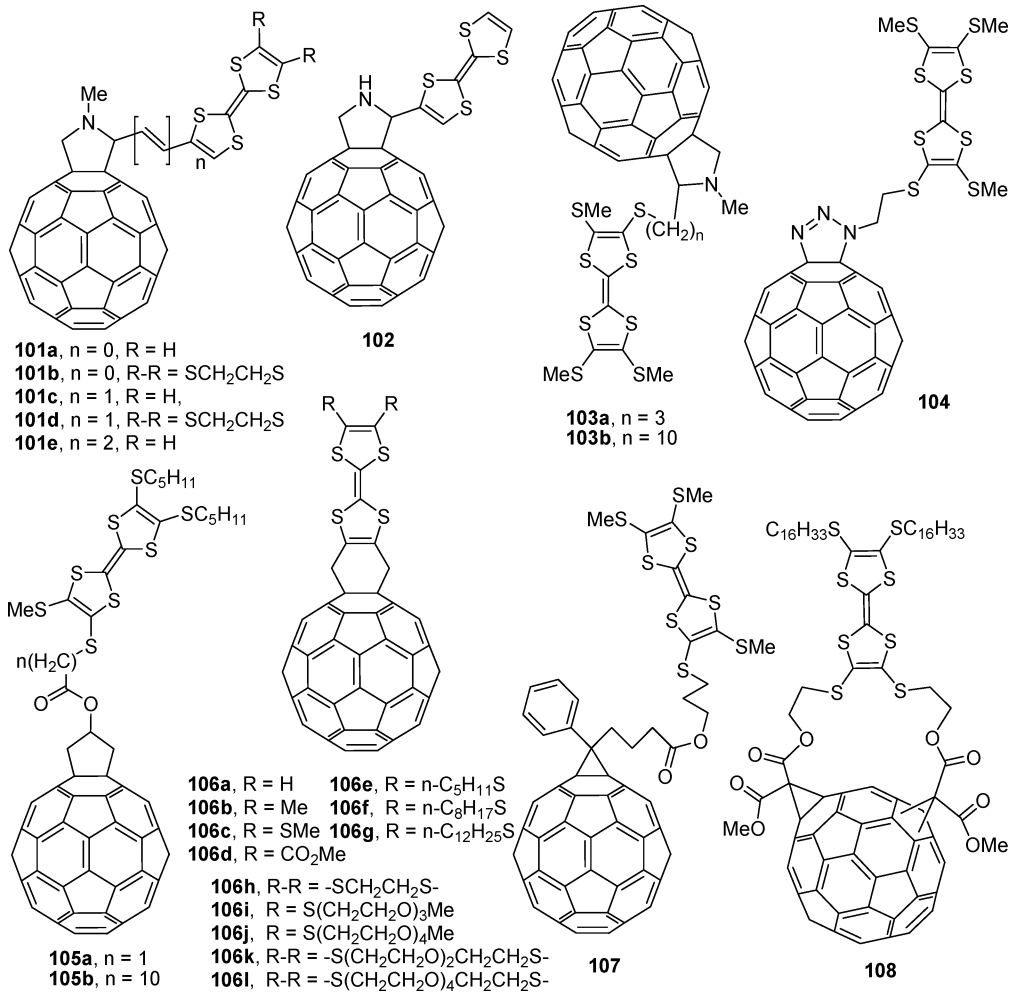

Introduced in 1997 by Rovira et al. for the synthesis of compound **106d**,[158] the reaction has been used recently for preparation of diads **106a**,**b**,**d**,[159] **106c**,[160] **106e**−**j**,[161] and **106h**,**k**,**l** (Chart 12).[162] The substitution effect in diads **106** is quite predictable: the only known electron-donating substituent (in TTF nucleus), the methyl group (**106b**, E_g = 1.03 eV), decreased the oxidation potential of the donor, shrinking the HOMO−LUMO gap, whereas the alkylthio (**106c**, E_g = 1.36 eV) and carbomethoxy (**106d**, E_g = 1.34 eV) substituents have an opposite effect. Worth mentioning is the discrepancy between the redox potentials for alkylthio-substituted diads **106**. The electrochemical gap (which is independent of the reference electrode) was reported to be 1.17 and 1.37 V (Table 7) for the same compound **106h**, studied under the same conditions (0.05 M Bu_4NPF_6 in ODCB). Both research groups were quite solid in their experimen-

tal approaches, and the only apparent difference was using Pt[161] or glassy carbon (GC)[162] working electrodes. This suggests that specific interaction of the carbon surface of the electrode with fullerenes or absorption phenomena can have an effect on the electrochemistry. With the GC electrode the fullerene reduction waves showed significantly higher currents than the TTF oxidation waves,[162] whereas equal currents were observed with a Pt electrode[161] (Figure 16). Generally, very different structures of the donor

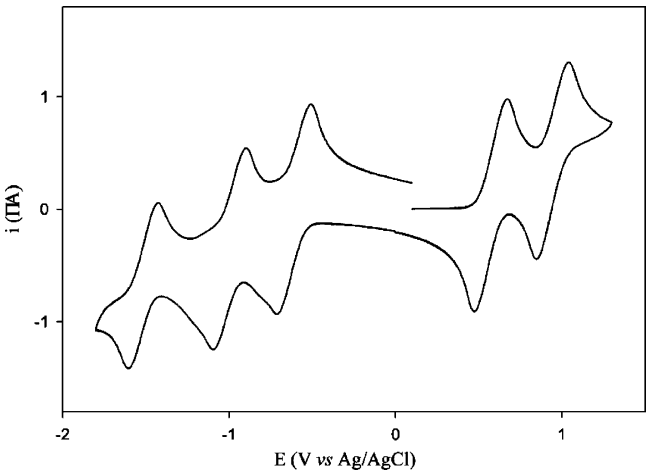

Figure 16. Cyclic voltammogram of TTF−C_{60} diad **106j**, recorded in ODCB. (Reproduced with permission from ref 161. Copyright 2002 Royal Society of Chemistry.)

(TTF) and acceptor (C_{60}) fragments and the associated difference in solvation effects result in high sensitivity of the electrochemical gap to the media. Thus, changing DCM to ODCB can increase the E_g by 50 mV (cf. compounds **106a**,**b**, Table 7).

A different, more strained cyclopropane "anchor" has been used to hook the TTF to the fullerene in diad **107**.[163] As expected, the latter showed a HOMO−LUMO gap of 1.27 eV, and the authors mention that only photoexcitation would allow the donor and acceptor fragments to interact efficiently. Somewhat surprising is the HOMO−LUMO gap of 0.86 eV, reported for compound **108**, particularly because bis-substitution in the fullerene moiety is expected to decrease its reduction potential and, thus, to enlarge the gap.[164] Comparing the reported first reduction potential of **108** of −0.1 V to those of other methanofullerenes (Table 7) and keeping in mind that no vigorous purification (e.g., chromatographic) was reported for **108**, and no proof of purity (e.g., elemental analysis) was presented, it is most logical to attribute this first observed reduction to impurities, very likely C_{60}, due to de-cyclopropanation.[165] In this case, the difference between the next reduction wave (−0.48 V) and the first oxidation wave (0.76 V) would give a more reasonable HOMO−LUMO gap of 1.24 V.

Different types of TTF−fullerene triads and higher ratio conjugates have been synthesized. Compound **109** contains another redox center (ferrocene), but the photophysical studies show that (photoinduced) electron transfer occurs solely from the TTF moiety.[166]

Two similar triads with fullerene/TTF ratio 1:2 (compound **110**[167]) and 2:1 (compound **111**[168]) have been synthesized by Martín et al. (Chart 13). Comparing the electrochemical data for triads (**12a**−**e**[161] and **12f**[159]), tetrads **113**,[161] and quintads **114**[161] to those for the corresponding diads **106** (Table 7), it is clear that multiple substitution of the fullerene core decreases its reduction potential and enlarges the HOMO−LUMO gap. The same conclusion can be reached comparing the triad **115** to **116a**−**c**.[161] Another interesting series of TTF−fullerenes are **107**, **117**, and **118**, which are electronically identical but have different numbers of fullerene units attached to the TTF core.[163] Although no particular application of these molecules has been demonstrated, they could be important for construction of multiterminal electronic devices.[102,169]

2.5.3. Fullerene–TTFAQ Conjugates

A two-electron donor TTFAQ has also been introduced into fullerene diads, mainly by Martín et al. Compounds **119a**−**c**, synthesized in 1997, were the first molecules of this type and had the TTFAQ and fullerene moiety connected via a pyrrolidine bridge.[170] Later, similar diads **119d**−**f**,[171] having an additional vinylene linker in the bridge, diad **120**,[172] with a phenylene−carboxymethyl bridge, and triad **121**,[166] with ferrocene as a second donor moiety, were synthesized by the same group. The electrochemical gap of ∼1.1−1.4 eV (Table 7) is certainly too high for non-photoexcited electron transfer, and one would expect no unpaired spin on these molecules. At the same time, Faraday balance measurements on **119a**−**c** in the solid state clearly show a magnetic moment of $\sim(2-5) \times 10^{-3}$ emu mol^{-1}, and the temperature dependence of the magnetic susceptibility is purely paramagnetic. The authors, however, do not give an explanation for the observed phenomenon, and it is not clear if it can be explained by a possible impurity influence. Also, the conductivity of **119a**, $\sigma_{rt} = 10^{-6}$ S cm^{-1}, though small, is relatively high for a single-component system but not as high as those observed by Kobayashi[84] (vide supra).

TTFAQ−fullerene Diels−Alder adduct **122** was synthesized in 25% yield by treating C_{60} with dimethylene−TTFAQ transient diene (generated from the corresponding bis(bromomethyl) derivative). A more rigid cyclohexane bridge fixes the relative position of TTFAQ and fullerene moieties, precluding through-space donor−acceptor interactions.[173]

Compounds **123** and **124** were synthesized by reaction of fullerene with a diazo derivative of TTFAQ (generated in situ from TTFAQ−carbaldehyde *N*-tosylhydrazone).[174] The initially obtained [5,6] fulleroids **123** can be easily transformed into thermodynamically more stable [6,6] methanofullerenes **124**. Despite the different connection types between TTFAQ and fullerene in these diads, the electrochemical properties, fluorescence, and electron-transfer parameters are almost the same. Triazole-bridged compounds **125a**,**b** can be easily synthesized by reaction of fullerene with TTFAQ−methyl azide.[175] Upon heating, the resulting diad underwent recyclization into a [5,6] azafulleroid diad **126** (with a trace amount of [6,6] isomer).

A reversible covalent linkage of the fullerene and TTFAQ moieties has been realized in diads **127a**−**c**.[176]

Chart 13. TTF−Fullerene Triads and Multiads

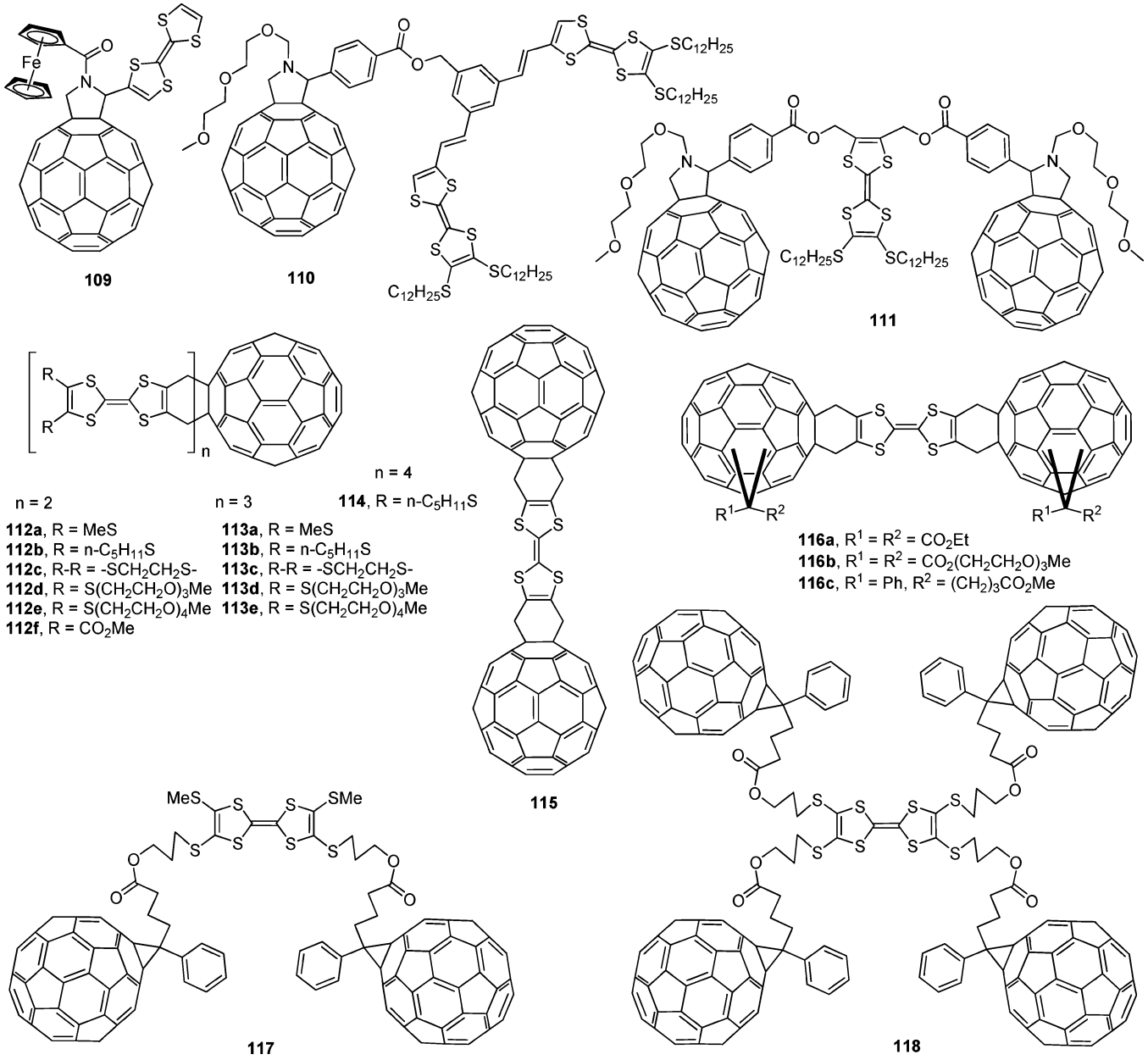

The reaction between C_{60} (**100**) and TTFAQ **25** in toluene at 60 °C results in Diels−Alder cycloaddition to afford the diad **127**, which can be reverted into starting materials by simply increasing the temperature to 80 °C. As the fluorescence of TTFAQ **25** is strongly quenched in the diad **127**, due to intramolecular electron transfer, the authors propose this diad as a temperature-activated molecular switch.

A series of fullerene−TTFAQ diads and triads **128**−**131** was recently synthesized in 8−32% yield via reaction of C60 with TTFAQ-containing malonic ester in the presence of 1,8-diazabicyclo[5.4.0]undec-7-ene (DBU) and CBr_4 (Chart 14).[177]

The C_{60}−TTFAQ−TTFAQ triad **132**[172] and C_{60}−porphyrin−TTF triads **133**[178] and **134**[179] were prepared to control short- and long-range electron-transfer processes (Chart 15). The initial photoexcitation of the porphyrin group in **133a** leads to effective (92%) and fast (0.2 ns) charge separation into a $(C_{60})^{\bullet-}$−porphyrin−$(TTF)^{\bullet+}$ state with lifetime 660 ns. The energy of this charge-separated state (~1 eV) agrees well with the electrochemical gap. Very long-lived charge-separated states can be photoinduced in triads **132**. Studying the decay of the absorbance of $C_{60}^{\bullet-}$ and $TTFAQ^{\bullet+}$ (1000 nm and 660−680 nm, respectively), lifetimes of 105−708 ns (depending on the solvent) were demonstrated for the $C_{60}^{\bullet-}$−$TTFAQ^{\bullet+}$−TTFAQ state, and further charge separation produces the species $C_{60}^{\bullet-}$−TTFAQ−$TTFAQ^{\bullet+}$ with lifetimes as long as 12−111 μs.[172]

2.5.4. Fluorinated Fullerenes as Ultimate Acceptors for Donor−Acceptor Diads

As we mentioned before, the functionalization of fullerene in most cases reduces its electron affinity due to disruption of the conjugated system. However, introducing strong electron-withdrawing groups may compensate the loss of conjugation. Thus, the reduction potentials of [1,2]dicyanofullerene[180] and dicyano-[6,6]methanofullerene[165] were reported to be 0.1−0.15

Chart 14. TTFAQ–Fullerene Compounds

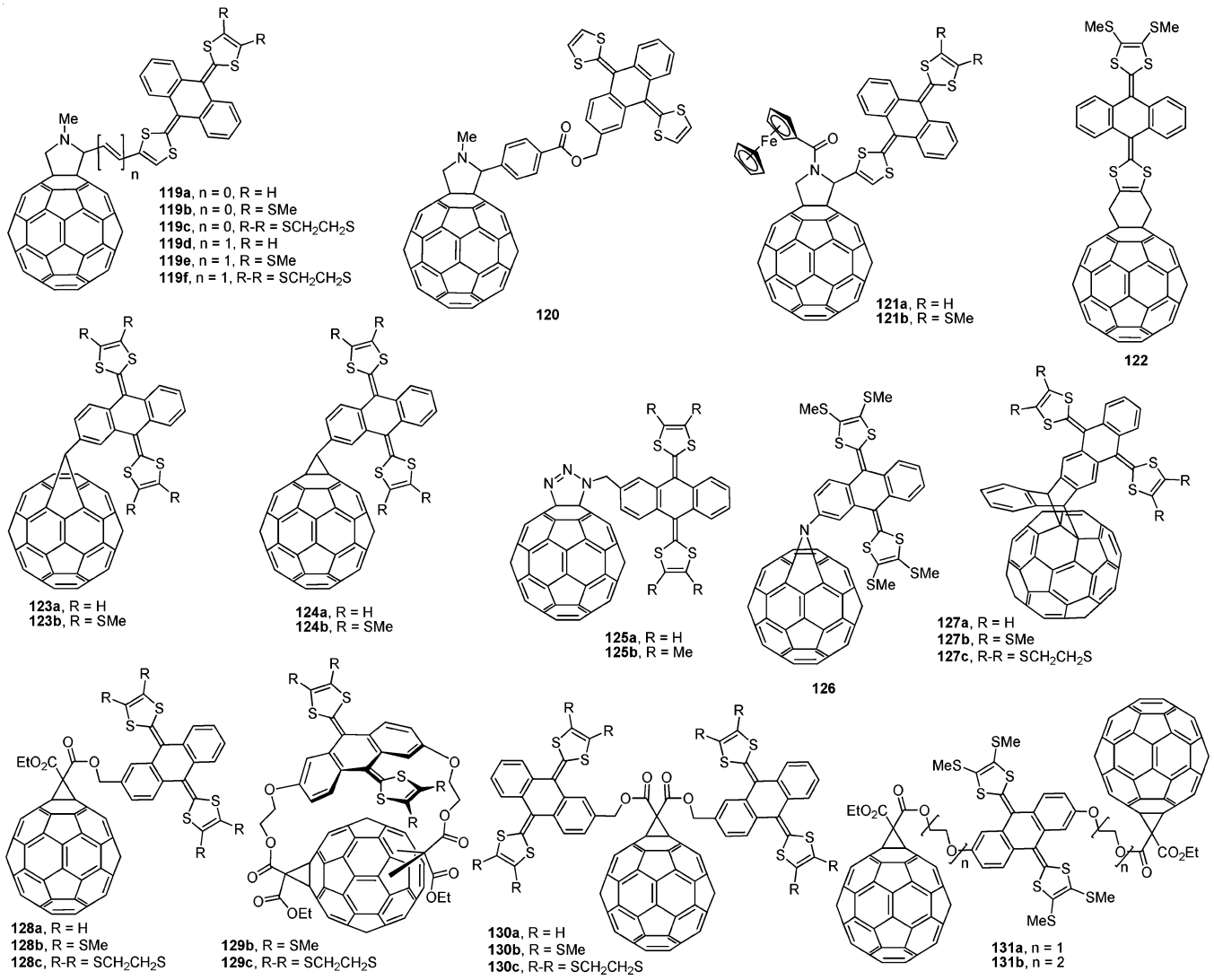

V more positive than that of parent fullerene **100** (although reversible reductions for these were observed only at low temperatures). The other exceptions to this rule are the halogenated fullerenes, of which only fluorinated species are stable,[181] while the brominated and chlorinated derivatives decompose readily in solution, especially in the presence of electron-donor molecules.[182] The electron affinity of the fluorofullerenes is increased by ~0.05 eV per each fluorine atom added (the increment decreases at high functionalization levels).[181] Highly fluorinated fullerenes were reported as exceptionally strong electron acceptors (stronger than TCNQ), although this behavior can hardly be attributed simply to the inductive electron-withdrawing effect of fluorine atoms (separated from the π-system by an sp^3 carbon). The electrochemical studies of $C_{60}F_{46}$,[183] $C_{60}F_{48}$,[184] and $C_{70}F_{54}$[183] revealed extremely high reduction potentials of 0.51 V (vs Ag/Ag^+; ~0.3 V vs SCE), −0.43 V (vs 9,10-diphenylanthracene; 0.79 V vs SCE[185]), and 0.76 V (vs Ag/Ag^+; ~0.5 V vs SCE), respectively. Studying the rate of electron-transfer reactions, the reduction potential of another fluorinated fullerene, $C_{60}F_{18}$, was deduced to be 0.04 V (vs SCE).[186]

Thus, attaching TTF units to fluorinated fullerenes could afford otherwise unavailable donor–acceptor compounds with a very low HOMO–LUMO gap. The first example of such a system, compound **135**, with a π-extended TTF unit (TTFAQ), was recently synthesized.[187]

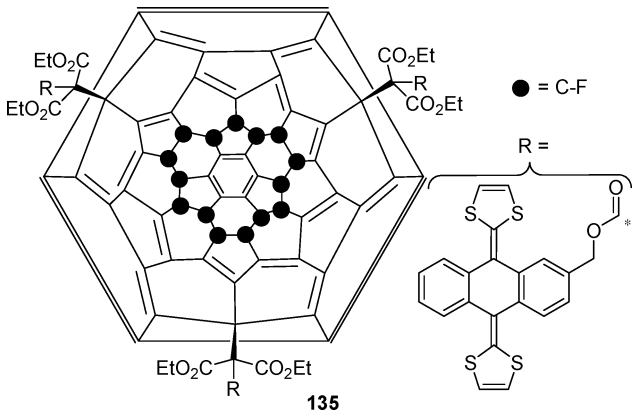

The cyclic voltammetry of **135** (Figure 17) demonstrates high electrochemical amphotericity with an E_g as low as ~0.5 eV (Table 7). The fullerene reduction is seen as a perfectly reversible single-electron wave. The oxidation of TTFAQ is quasi-reversible with a very large separation between the

Chart 15. TTF(TTFAQ)−Fullerene Triads with Long-Range Electron Transfer

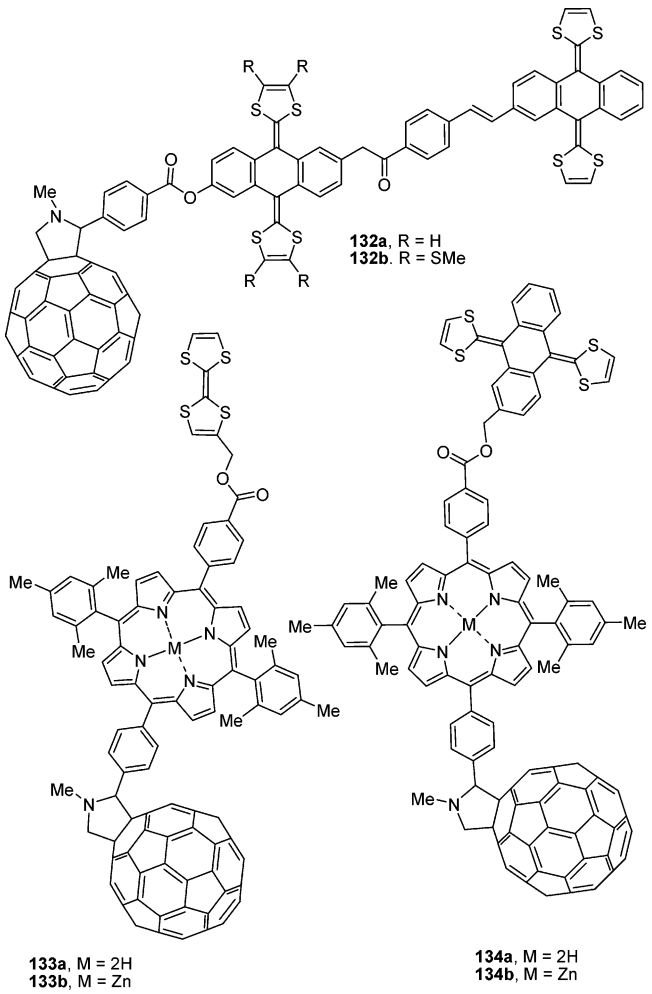

anodic and cathodic peaks. On the basis of the oxidation current, which was approximately three times higher than that of the fullerene reduction wave, the authors suggested a three-electron process, although it contradicts the well-established two-electron nature of TTFAQ oxidation. Having three TTFAQ moieties, **135** is expected to lose six electrons upon oxidation, although grossly inaccurate oxidation/reduction current ratios have been observed for other TTF−fullerene diads. This could be (at least partially) due to absorption phenomena (the unusually sharp cathodic peak of the TTFAQ/TTFAQ^{2+} wave is supportive of this assumption). On the other hand, no data confirming the structure of **135** with three TTFAQ substituents were presented in the paper.[187] The time-resolved fluorescence studies suggest the fluorescence quenching through formation of a charge-separated state [(TTFAQ$^{\bullet+}$)−σ-(fullerene$^{\bullet-}$)], whose low energy (as suggested by electrochemistry) results in a rather long lifetime of 870 ns.

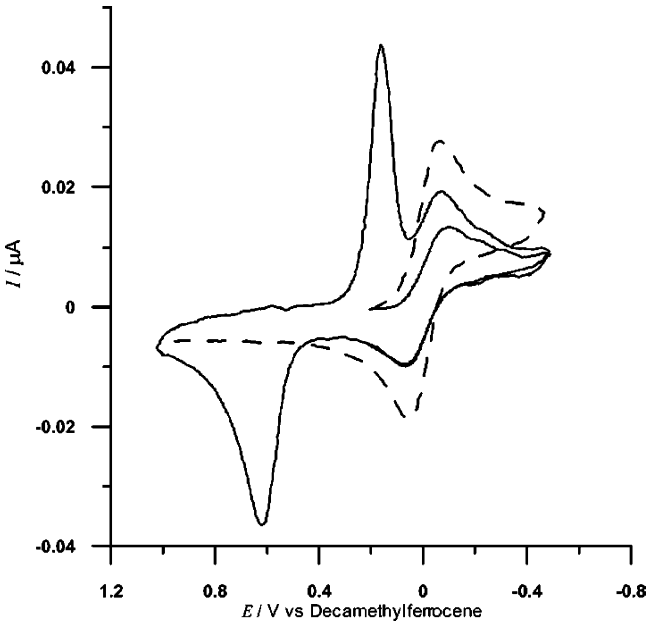

Figure 17. Cyclic voltammogram of the TTFAQ−C_{60} diad **135** (solid line) and of a related C_{60} derivative without a TTFAQ fragment (R = C_2H_5, broken line). (Reproduced with permission from ref 187. Copyright 2003 Royal Society of Chemistry.)

3. Acenes: Promising Organic Electronic Materials

3.1. Introduction

Polycyclic aromatic hydrocarbons (PAHs) are currently among the most widely studied organic π-functional materials.[188,189] Particular attention has been paid to linear PAHs composed of laterally fused benzene rings and called linear acenes or simply acenes, due to their importance as organic semiconducting materials (Chart 16). Tetracene and pentacene are among the most promising molecular conductors based on acenes and semiconductors for organic field-effect transistors (OFETs). The oligoacene units are a basic building unit of graphite[190] as well as carbon nanotubes,[191] and studying their electronic properties is important for understanding the structure and properties of the latter materials. To the best of our knowledge, the chemistry and applications of acenes have never been reviewed previously.[192,193] Recent reviews, however, exist on organic thin-film field-effect transistors (TFTs) which include discussions of pentacene applications.[194,195] Due to significant numbers of publications on acenes, especially in the past decade, no attempt was made to cover all published data, neither on acenes themselves nor on their applications as electronic materials, but rather the focus was set on controlling the HOMO−LUMO gap.

Benzene, the smallest member of the acene family, was discovered in 1825[196] and gives rise to a family of aromatic compounds that is one of the major fields of chemistry in general.[197] Oligoacenes are aromatic molecules;[197−199] however, the degree of aromaticity has been a subject of recent debate.[200] The lower homologues, from benzene to anthracene, can be extracted from coal, while higher homologues, such as pentacene or hexacene, can be obtained only by multistep synthesis. Benzene is the most stable aromatic hydrocarbon known; however, larger members of the acene family starting from heptacene appear to be so reactive that they can only be probed by theory. The synthetic accessibility of oligoacenes is limited to hexacene (**136.6**), and a thorough

Chart 16. Structures of Oligoacenes

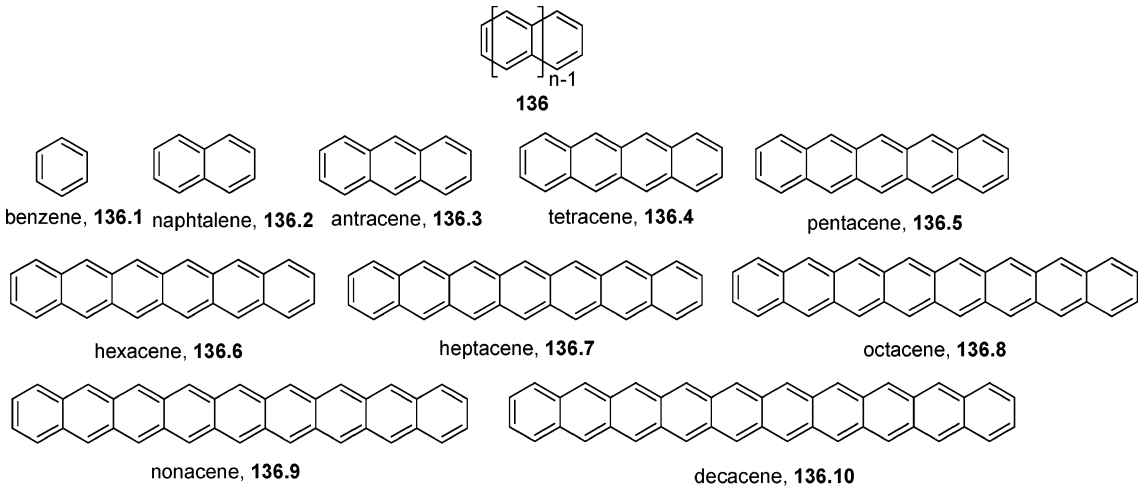

Scheme 9. Synthesis of Pentacene[212]

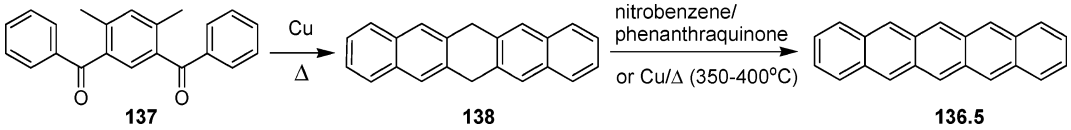

understanding of electronic properties hovers at pentacene (**136.5**).[201] Some reports suggesting the synthesis of higher homologues, especially heptacene, have been published, but its synthesis remains controversial (see section 3.2). The carcinogenic properties of PAHs in general and acenes in particular have been in the news for some time but are not the purview of this review.[202]

In 2000−2002 attention to acenes was at an all-time high due to several claims of superconductivity in anthracene, tetracene, and pentacene ($T_c = 4$, 2.7, and 2 K, respectively),[203] extremely high mobility in pentacene for both holes (up to 1200 $cm^2 V^{-1} s^{-1}$) and electrons (up to 320 $cm^2 V^{-1} s^{-1}$),[204] and tetracene-based organic solid-state injection lasers[205] and due to observation of a fractional quantum hall effect for tetracene and pentacene with hole and electron mobilities exceeding 10^4 $cm^2/V{\cdot}s$ at 2 K.[206] However, these claims were later retracted[207] as a result of an independent investigation conducted at the behest of Bell Laboratories, Lucent Technologies.[208,209]

3.2. Synthesis of Oligoacenes

The syntheses of a large number of polycyclic aromatic hydrocarbons were summarized previously,[188,189] and pentacene syntheses were briefly described.[210]

Although many excellent syntheses have been developed for angular condensed aromatic hydrocarbons,[211] no good general method has been worked out for the linear condensed ring system. This is due to the fact that most common ring closures tend to proceed in the angular position. Pentacene (**136.5**) was first synthesized by Clar and John[212] starting from *m*-xylophenone (Scheme 9). A vigorous Friedel−Crafts reaction yielded 40% of 4,6-dibenzoyl-1,3-dimethylbenzene (**137**). Heating with copper converted **137** into dihydropentacene (**138**) in an unstated yield. Dehydrogenation of **138** to **136.5** was accomplished by boiling the dihydro derivative in nitrobenzene with phenanthraquinone or by passing over copper at 350−400 °C.[212]

In more modern times, pentacene was easily prepared by reduction of pentacenequinone (**139**) by an aluminum−cyclohexanol mixture (Scheme 10).[213] Before the above short synthesis, it had been shown that pentacene could be synthesized from 1,2-dimethylenecyclohexane by a three-step procedure in an overall yield of 30%.[214]

Scheme 10. Reduction of Pentacenequinone

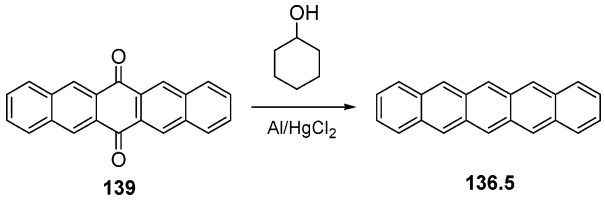

3.2.1. Acenes Longer than Pentacene

Marschalk and Clar were largely responsible for spearheading many of the larger polyacenes known today. The synthesis of hexacene was reported independently by both Marschalk[215] and Clar in 1939,[216] and since then, alternative methods[217,218] for its preparation have been developed. Both synthetic pathways took advantage of a key metal catalyzed dehydrogenation step (Scheme 11). Marschalk[215] heated dihydrohexacene **140** in trichlorobenzene, while Clar[216] sublimed hexacene directly from the

Scheme 11. Dehydrogenation of Dihydrohexacene[215,216]

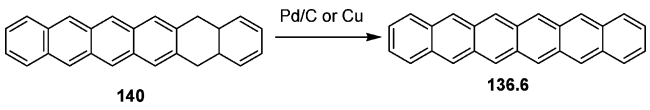

precursor using copper powder. The electronic spectra of hexacene were recorded by Angliker et al. with greater detail.[201]

Hexacene was also synthesized from octahydro-1,4-anthraquinone (prepared from 1,2-dimethylenecyclohexane and benzoquinone) and 2,3-dimethylenedecalin in four steps in an overall yield of 15% (Scheme 12).[217] Clar[219] was able to synthesize hexacene in an unreported yield by taking advantage of the fact that partially hydrogenated aromatic derivatives will give some of the linear product. A laborious four-step synthesis starting from 4-(2-carboxybenzoyl)phthalic anhydride and tetralin produced only a small amount of hexacene.

Scheme 12. Synthesis of Hexacene[217]

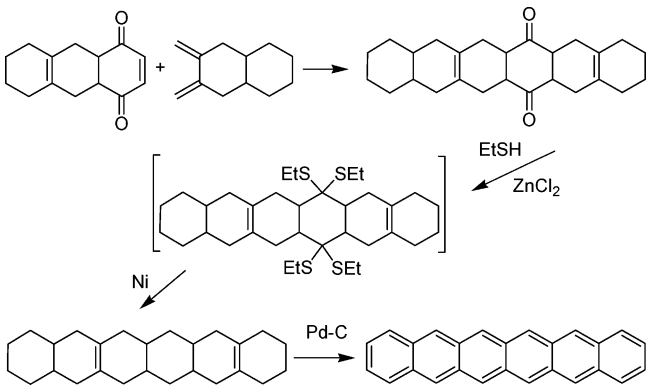

Heptacene is the next member in the polyacene family. Today, as it stands, the validity of heptacene remains highly controversial. It was described by Clar as a dark greenish-black solid that decomposed at about 400 °C.[220] There are two published claims of successful preparation of heptacene. Clar,[221,222] in 1942, claimed to have synthesized heptacene (**136.7**) in an unreported yield using a method similar[219] to the synthesis of hexacene. Clar's evidences for heptacene were substantiated by UV−vis spectroscopy (λ_{max} = 736, 657, 594, and 503 nm) and elemental analysis. Enlightened by Clar's approach, Marschalk attempted to repeat the work.[222] He noted that treating a pure sample of dihydroheptacene under the same conditions described by Clar failed to give heptacene as reported. Other approaches with dihydroheptacene derivatives were also attempted, but none has led to successful preparation of the hydrocarbon. However, when the entire synthesis was repeated using the exact method described by Clar, a "green solid" was observed. Marschalk concluded that in Clar's experiment the described "heptacene" material was not derived from dihydroheptacene but rather from some impurity that was carried over from previous reactions. Bailey and Liao[217] in 1955 claimed to have synthesized heptacene (**136.7**) in three steps from 2,3-dimethylenedecalin in an overall yield of 14% (Scheme 13).[217] The latter report noted the similarity in color with Clar's heptacene and provided an elemental analysis. Two years after Bailey and Liao reported the second and only other "successful" synthesis of heptacene, Clar dismissed his claim.[223] Clar was unable to isolate pure heptacene as described. Moreover, he stated that the material obtained after dehydrogenation was rapidly decomposing even in the solid state. It is now commonly agreed that heptacene cannot be isolated in the pure state.[223,224]

On the basis of theories (see below) ranging from very simple to very high-level, longer acenes are expected to exhibit a smaller HOMO−LUMO gap, which should make them potentially more interesting materials for molecular electronics. However, it is well documented that preparation of such extended benzenoid molecules is plagued by facile photooxidation, insolubility, and, most detrimental, dimerization and polymerization.[225] Thus far, the longest reliably described isolated system with only moderate stability is hexacene (**136.6**).[188,226]

[*n*]Cyclacenes (**141**, Chart 17) represent the basic cylindrical carbon units of "zigzag" (*n*,0) nanotubes.[227]

Chart 17. Structure of Cyclacene 141

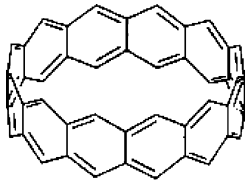

141

In line with the general high interest in carbon nanotubes, several theoretical studies were published on cyclacenes in the recent past.[242,228] However, despite several experimental attempts,[229,230] no member of the cyclacene series has been synthesized, very likely due to their expected difficult synthesis and high reactivity.

3.3. Theoretical Studies of Acenes

The intrinsic conductive property of graphite as well as the discovery of conductivity in doped *trans*-polyacetylene in the late 70s[231] has stimulated an ongoing investigation of the electronic properties of polyacenes (PAs). From a theoretical standpoint, in recent years, the electronic properties of large oligoacenes have been examined by a relatively large

Scheme 13. Synthesis of Heptacene[217]

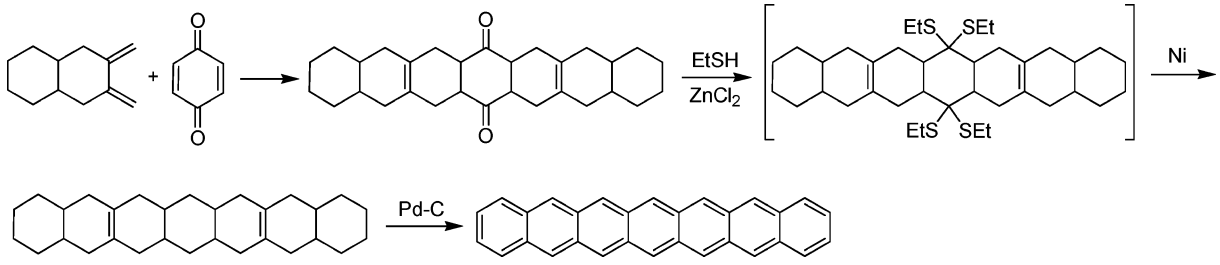

number of researchers. Thus, despite large strides in sophistication of theoretical treatments over the last 30 years, the electronic structure, stability, aromaticity, and, most importantly, band gap (or HOMO−LUMO gap) in oligoacenes and polyacenes are still subjects of controversy.[232] Large polyacenes were predicted to behave as one-dimensional organic conductors (zero band gap semiconductor akin to graphite).[232−235] It was proposed that PAs with an odd number of benzene rings might have singlet Hartree−Fock instabilities.[236] Quantitative MO theory was used to describe the electronic structure of polyacenes on the basis of the MO determination and energies of the monomer (naphthalene).[237] High-temperature superconductivity and ferromagnetism of polyacenes were theoretically proposed by Kivelson and Chapman in 1983.[238]

Early investigations focused on predicting which of the three structures of polyacenes—undistorted, cis-distorted, or trans-distorted—is energetically preferable (Chart 18). Predictions of stability favoring all

Chart 18. Structures of Polyacene

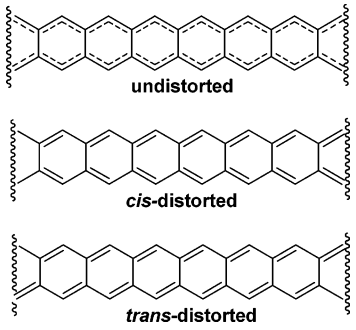

three can be found in the literature.[239] One of the reasons for this plethora of theoretical studies is prediction of a zero energy gap for polyacene by a simple tight-binding Hückel Hamiltonian.[240] Obviously, the electronic properties, band structure, and conducting properties of polyacene depend on the preferred structure. The question of Peierls instability in polyacenes has been discussed in the literature.[232,241−243] The character of the degeneracy at the Fermi level of polyacenes is fundamentally different from that of polyacetylene.[240,241] The undistorted PAs reveal a metallic band structure which does not undergo a Peierls distortion invoked by Yamabe and co-workers on the basis of the tight-binding self-consistent field molecular orbital (SCF-MO) method.[244] The extended Hückel method predicts that the undistorted structure should be less stable than the distorted one by ~6.0 kcal/mol.[245] Kertesz et al.[246] have carried out crystal-orbital semiempirical MNDO calculations to shed some light on the presence (or absence) of energetically favorable Peierls distortions in polyacenes and found the cis-distorted structure to be more stable than the undistorted one by 1.3 kcal/mol per unit cell, which, in turn, was predicted to be favored over the trans-distorted isomer by 0.4 kcal/mol per unit cell. Within the same Hamiltonian, using a finite-cluster approach with fictitious periodic boundary conditions and no extrapolation, Chandrasekhar and Das[247] reached similar conclusions, but with the respective energy differences of only 0.2 and 0.0 kcal/mol. Properties of both the undistorted and the Peierls-distorted polyacene polymers were studied with Padé approximants from the results of HF/6-311G** and MP2/6-311G** calculations on the respective finite clusters. At the Hartree−Fock level, the cis-distorted structure has the lowest energy per unit cell; however, at the correlated MP2 level, the undistorted structure is slightly favored.[248] The very small energy difference means that it is very probable that undistorted and Peierls-distorted regions may coexist due to local defects or local thermal excitations. Interestingly, in some more recent studies using modern levels of theory, projector quantum Monte Carlo (PQMC)[243] and density-matrix renormalization group (DMRG)[232] studies corroborated the cis-distorted structure. Ramasesha et al. suggested that the instability in polyacenes is conditional.[232,243] They found strong similarities between polyacene and polyacetylene and showed that electron correlations tend to enhance the Peierls instability in polyacene. Opposite to this view, Houk et al. concluded that the fully delocalized nonalternating nature of polyacenes differs from the bond alternation resulting from Peierls distortion in polyenes.[242] This is in line with previous conclusions by Kertesz and Hoffmann.[241] In recent investigations at the B3LYP/6-31G* level of theory, no sign of Peierls distortion was found.[242,249]

The polyacenes (as well as cyclacenes) were described by Houk et al. as consisting of two fully delocalized nonalternating ribbons joined by relatively long bonds.[242] Polyacenes were predicted to have smaller band gaps than the corresponding polyenes and triplet ground states for nine or more benzene rings. The structures, energies, and other properties of a series of oligoacenes were compared with those of the corresponding series of annulated oligoarenes of phenanthrene type (Chart 19). The

Chart 19. Examples of Annulated Oligoarenes of Phenanthrene Type

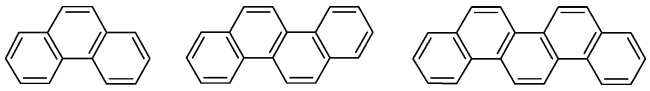

compounds in the latter series were consistently found to have a lower total energy than their isomers in the former series.[250]

Increasing the number of rings in PAs results in successive reduction of the band gap (reflected in the UV spectra), reduction of the ionization potential,[280] and an increase in proton[251] and electron affinities,[252] which is also reflected in decreased stability. These progressions in PAs' properties were usually explained by the sequential loss of benzenoid character (aromaticity) predicted by MO treatments[253] and by Clar's qualitative sextet concept.[188] Since only one ring in each acene can be assigned three double bonds without duplication, the number of nonsextet rings increases along the acene series.[254] Another view was presented recently by Schleyer et al.[200] Despite the increase in reactivity as a result of benzannulation (from benzene to heptacene), it was predicted that the acene resonance energy per π-electron remains nearly constant. The activation energies for Diels−

Alder reaction of acetylene with different acene rings were computed at the B3LYP/6-31G* level.[200,255] The activation energies of the individual acene rings correlated with the reaction energies (Figure 18).

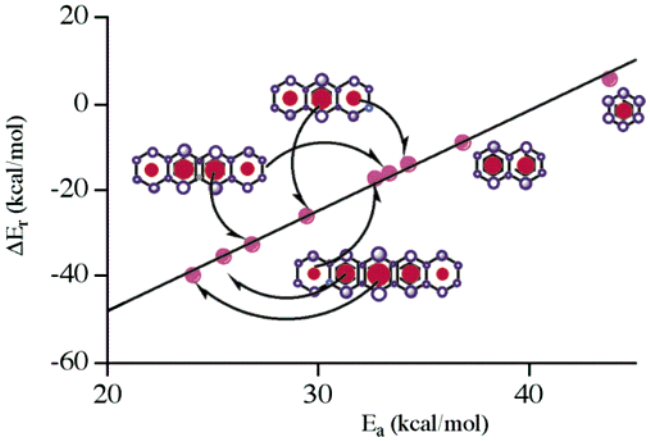

Figure 18. Correlation of the activation (E_a) versus the reaction (ΔE) energies (B3LYP/6-31G* + ZPE data) of acetylene addition to acene rings. The red dots are based on total NICS(0) values. The HOMO coefficients are indicated in blue. (Reproduced with permission from ref 200. Copyright 2001 American Chemical Society.)

Nucleus independent chemical shifts (NICS)[256] (which were used as a measure of aromaticity) indicate that the more reactive inner rings actually are more aromatic than the less reactive outer rings and even more aromatic than benzene itself. The aromaticity increases from the end to the center rings, as shown by NICS(total) and NICS(π).[200] At the same time, the HOMO coefficients (Figure 18) are consistent with the regioselectivity of Diels–Alder reactions that prefer the middle rings (despite their greater aromaticity) to an increasing extent.[200] Clearly, the definition of aromaticity based on NICS is counterintuitive because there is no correlation with experimentally determined reactivity.

Recently, the optical gaps in nonacene (**136.9**) and polyacene (**136**, $n = \infty$) were predicted to be very large, 2.59 and 2.46 eV, respectively, using density-matrix renormalization group calculations within a PPP Hamiltonian.[257] However, the gaps are even larger than the experimentally known optical gap in pentacene (2.1 eV), reducing confidence in these predictions. In another recent paper, a singlet–triplet gap of 0.446 eV and an effective conjugation length of 12 rings were predicted for polyacenes on the basis of valence-bond (VB) calculations.[258]

J. Aihara analyzed the kinetic stability of oligoacenes using some conventional indices defined by Hückel molecular orbital (HMO) theory.[259] He concluded that higher members of the oligoacene series are aromatic and explained their high reactivity using conventional indexes of kinetic stability, such as localization energy and a HOMO–LUMO energy separation. These molecules are presumed to be thermodynamically more stable but kinetically less stable than nonaromatic polyolefins.

Octacene was predicted to exhibit a triplet ground state on the basis of extrapolation from the singlet–triplet difference of benzene through hexacene,[260] but the actual triplet relative energy was not calculated or measured. It was also proposed that linear polyacenes would behave as two polyacetylene chains with a triplet ground state and a vanishing band gap.[242] Bendikov et al.[249] found that, at the RB3LYP/6-31G(d) level of theory, the wave function for the relatively small oligoacene hexacene (and all longer oligoacenes) becomes unstable. Reoptimization, using the unrestricted broken symmetry B3LYP method (UB3LYP), leads to a singlet state with large amounts of diradical character.[249] Open-shell ground-state singlet biradicals are rare but known, for example, tetramethyleneethane (TME) biradical.[261] In contrast to the common view that acenes are closed-shell systems or have triplet ground states, the ground states of oligoacenes are predicted to be singlets, as a result of their disjointed[262] biradical nature. At the B3LYP level of theory, the singlet–triplet gap for hexacene is 10.3 kcal/mol (triplet is above singlet) and the closed-shell RB3LYP solution is 0.8 kcal/mol above the open-shell singlet biradical state, while the spin contamination for the singlet state is small ($\langle S^2 \rangle = 0.26$). The singlet–triplet gap decreases from hexacene to heptacene and octacene; however, starting from octacene, it stays constant at about 5–6 kcal/mol. The relative energy of the triplet state for decacene is 5.7 kcal/mol higher than that of the open-shell singlet state; however, even the triplet state is 4.7 kcal/mol lower than the nonphysically significant RB3LYP solution. Triplet structures are always higher in energy than open-shell singlet structures, but the singlet–triplet gaps become smaller for pure DFT methods (BLYP, PW91, and BPW91).[249] Hence, these calculations predict that oligoacenes will maintain a ground state singlet even above octacene, although the triplet state is only several kilocalories per mole above the singlet state. According to the Su–Schrieffer–Heeger (SSH) model, the soliton's effective length in the π-conjugated oligoene system is about 14 carbon atoms.[263] This is in agreement with ref 249, predicting biradical character in oligoacenes; heptacene already possesses a long enough π-system (15 carbon atoms) to produce two oligoene solitons. Investigation of frontier molecular orbitals gives more insight into the nature of the open-shell ground state in oligoacenes. The two singly occupied orbitals of decacene are shown in Figure 19.[249] They are essentially localized on the two ribbons.

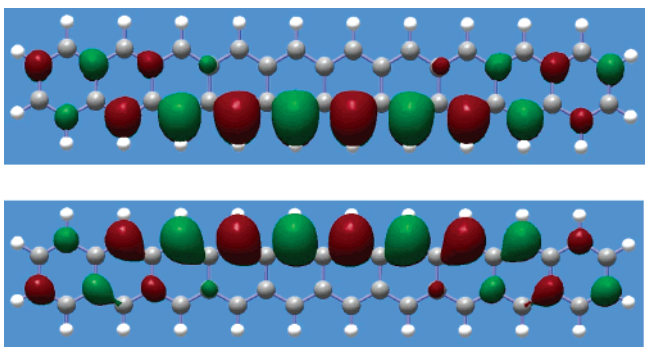

Figure 19. Singly occupied orbital of decacene (UB3LYP/6-31G(d)). (Reproduced with permission from ref 249. Copyright 2004 American Chemical Society.)

The frequency upshift of the Kekulé-type b_{2u} modes in the 1^1B_{2u} electronically excited state of several acenes and other PAHs is well documented[264−267] and will be explained here. For instance, the frequency of the skeletal mode **142** in the 1^1B_{2u} state of benzene (the ν_{14} mode, 1570 cm^{-1}) is 261 cm^{-1} higher than that of the same mode in the ground 1^1A_{1g} state.[264,265] In naphthalene,[264] the Kekulé-type mode in the 1^1B_{2u} state undergoes a frequency exaltation of 189 cm^{-1} relative to the ground state. In anthracene, one of the Kekulé-type modes was assigned and undergoes a shift to higher energy of 231 cm^{-1}.[267]

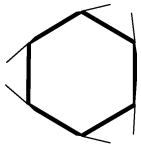

142

In 1996 Shaik, Zilberg, and Haas developed a concept which explains the properties of the first covalent excited state of benzene and linear acenes.[268,269] Figure 20 shows a schematic description of the

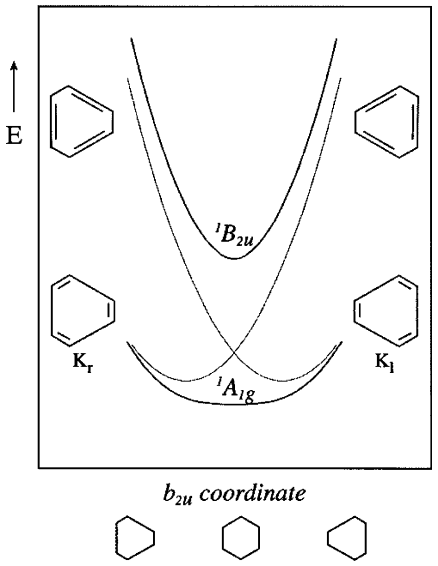

Figure 20. Avoided crossing of the Kekulé structures of benzene. (Reproduced with permission from ref 268. Copyright 1996 American Chemical Society.)

intended crossing of the potential energy curves of the two Kekulé structures (K_l and K_r) of benzene along the b_{2u} coordinate, alternating these structures, as well as of the state curves (shown in bold print) resulting from their avoided crossing. The steeper slope of the $^1B_{2u}$ potential curve, compared to the shallow slope of the $^1A_{1g}$ curve, is responsible for the discussed excited-state frequency anomaly. This is the physical reason for a larger force constant as well as for the frequency exaltation of the Kekulé-type b_{2u} mode in the excited state relative to the ground state. This theory was also expanded to polyacenes. In all the acene compounds, a frequency exaltation of at least one b_{2u} mode is expected in the lowest lying (the covalent) $^1B_{2u}$ state.[268,269]

3.4. Physical Properties of Acenes

The longest UV absorption of all acenes shows a characteristic vibronic structure in both solution and solid state. The solid-state UV spectrum of pentacene has a longest wavelength transition around 670 nm (1.85 eV) that is attributed to the band gap [Figure 21 (bottom)].[270,271] In solution[272] or in an

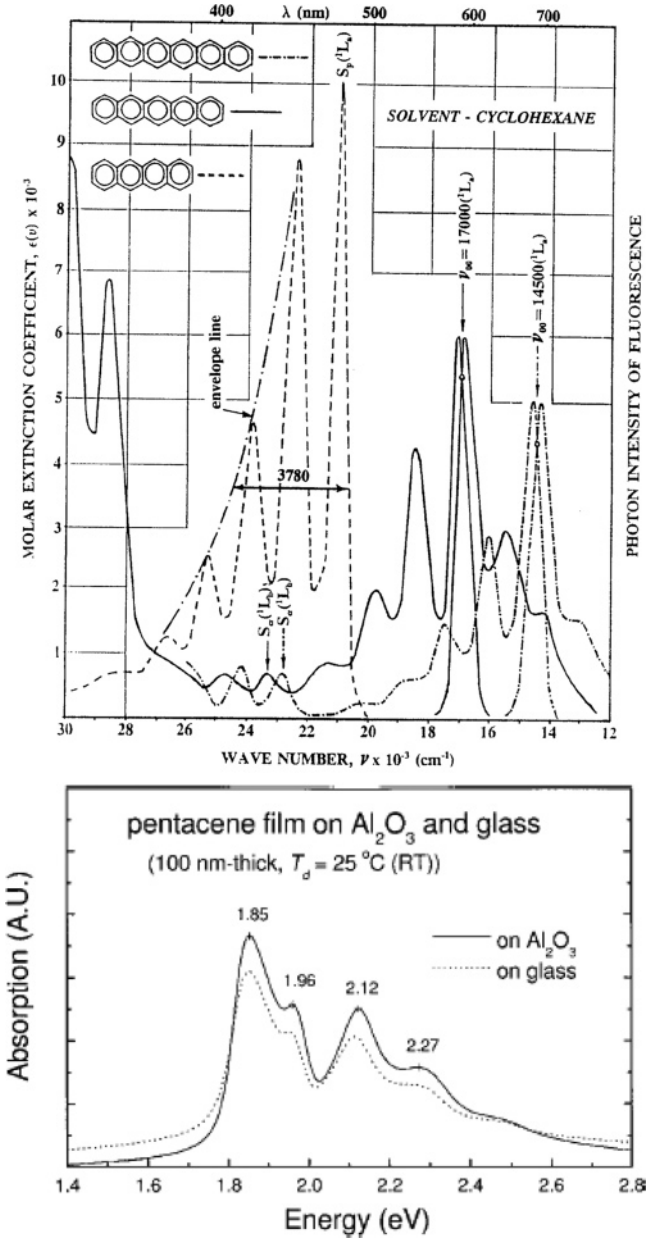

Figure 21. (top) UV−vis absorption and photoluminescence spectra of tetracene **136.4**, pentacene **136.5**, and hexacene **136.6**. (Reproduced with permission from ref 276. Copyright 1997 Elsevier Science Ltd.) (bottom) Absorption spectra of 100 nm thick pentacene **136.5** films on Al_2O_3 and glass near the fundamental HOMO−LUMO transition. (Reproduced with permission from ref 271. Copyright 2002 Plenum Publishing Corporation.)

argon matrix[273,274] the longest wavelength absorption for pentacene is blue-shifted by ~80 nm compared to the solid state [Figure 21 (top)]. Excitation energies of oligoacenes up to heptacene were calculated using a new method based on time-dependent density functional theory (TDDFT).[275]

Table 8. Best Experimental Values for Ionization Potential (IP) and Electron Affinity (EA) and Best Theoretical Values for Vertical Ionization Potential (VIP) and Adiabatic Ionization Potential (AIP) of Acenes[a]

compd	IP^{exp} (ref 18)	VIP^{theor} (OVGF)[b,279]	VIP (best theor est)[280]	AIP (best theor est)[280]	VEA (OVGF)[b,279]	EA (exp)
benzene (**136.1**)	9.24378 ± 0.00007	9.044	9.44(8)	9.22(4)	−2.605	−1.12 ± 0.03[281]
naphthalene (**136.2**)	8.144 ± 0.001	7.847	8.24(1)	8.14(1)	−1.304	−0.19 ± 0.03[281]
anthracene (**136.3**)	7.439 ± 0.006	7.202	7.47(3)	7.41(9)	−0.438	0.530 ± 0.005[282]
tetracene (**136.4**)	6.97 ± 0.05	6.533	6.94(8)	6.91(4)	+0.158	1.04 ± 0.04[283]
pentacene (**136.5**)	6.63 ± 0.05	6.150	6.57(3)	6.55(6)	+0.585	1.35 ± 0.04[283]
hexacene (**136.6**)	6.36−6.44	5.865	6.43	6.42	+0.909	

[a] All energies are expressed in electronvolts. [b] At OVGF/cc-pVDZ//B3LYP/cc-pVDZ.

The fluorescence of acenes was studied in detail, and internal conversion rate constants as well as absorption and fluorescence parameters up to hexacene were determined [Figure 21 (top)].[276]

The proton affinities of benzene, naphthalene, anthracene, and tetracene were measured in 1980,[277] and the values were later reevaluated by Hunter and Lias.[18] Proton affinities at all reactive positions for benzene, naphthalene, and anthracene were calculated at different theoretical levels up to MP2/6-31G*//HF/6-31G*, and the results have been compared to experimental proton affinities.[18,251] The gas-phase basicity and proton affinity of pentacene have been determined to be 225.7 kcal/mol using FT-ICR mass spectrometry.[278]

The best experimental values of ionization potentials of acenes are summarized in Table 8.[18] Computations of ionization potentials for oligoacenes were found to be difficult. Calculations[279] (Table 8) at the OVGF/cc-pVDZ level showed significant discrepancies between the calculated vertical and experimental ionization thresholds especially for longer oligoacenes. The authors suggested that these unusually large discrepancies between the OVGF/cc-pVDZ and experimental ionization potentials of naphthacene (tetracene), pentacene, and hexacene are related to their more strongly electron correlated nature. A focal point analysis of the convergence of the calculated ionization potentials has been performed in order to extrapolate the CCSD(T) results to an asymptotically complete (cc-pV∞Z) basis set. The best estimates for the adiabatic ionization potential of benzene, naphthalene, anthracene, tetracene, pentacene, and hexacene [9.22, 8.14, 7.42, 6.91, 6.56, and 6.42 eV (Table 8)[280]] match, within reason, the benchmark experimental[18] values. Interestingly, at this level of theory, electron affinities for acenes are positive, starting from tetracene (and experimentally they are positive starting from anthracene) (Table 8). Another important observation is a decrease of the difference between vertical and adiabatic ionization potentials with increasing acene length.[280]

The experimental values for the electron affinities of benzene, naphthalene, anthracene, tetracene, and pentacene are −1.12 ± 0.03,[281] −0.19 ± 0.03,[281] 0.530 ± 0.005,[282] 1.04 ± 0.04,[283] and 1.35 ± 0.04 eV,[283] respectively. Experimental values for the EAs of larger oligoacenes, such as hexacene, are not currently known. It is clear that elongation of the oligoacene chain results in a substantial increase in electron affinity. Schaefer III et al. studied the electron affinities of benzene, naphthalene, anthracene, and tetracene computationally using six different exchange correlation density functionals.[252] The BLYP and B3LYP functionals have low average absolute errors of only 0.18 and 0.19 eV, when compared to experimental values, and the authors recommend these functionals in future studies of PAH anions.

3.5. Pentacene as Organic Semiconductors

3.5.1. Crystal Structure of Pentacene

Crystal structures of oligoacenes up to pentacene are known, and the crystal data as well as experimental studies of their electronic structure, available up to 1978, have been summarized in the monograph.[284] It is well-known that, remarkably, all acenes, from benzene[285] through pentacene,[286−288] as well as several oligothiophenes[289] and oligophenylenes[290] crystallize in the herringbone structure (Figure 22 depicts the herringbone structure for

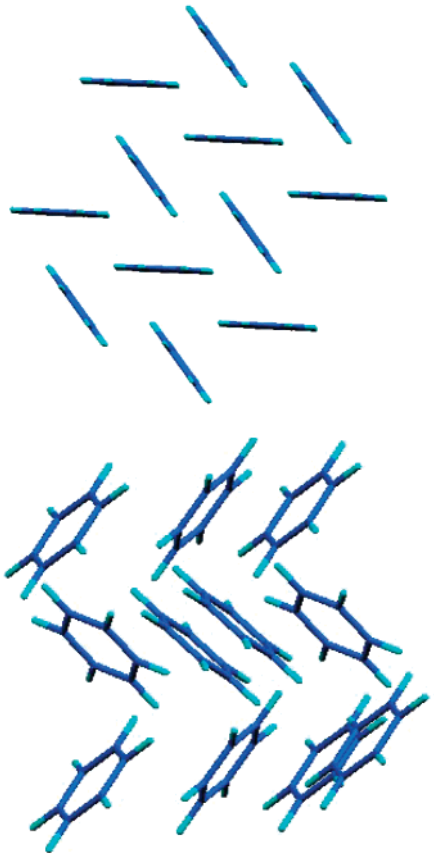

Figure 22. Heringbone structure of pentacene[297] (top: RefCode PENTACEN01 from CCDC) and benzene[285] (bottom: RefCode BENZEN01 from CCDC).

pentacene and benzene). Gavezzotti et al. analyzed the structure of numerous PAHs[291,292] and found that all examined compounds crystallize in layered structures and that the intralayer structure depends on the relative abundance of C−H and C−C interactions. If the C−H interactions dominate (or if the PAH contains a relatively large number of H atoms), a herringbone structure is generally found. With an increasing relative number of C−C interactions, the structure becomes more graphite-like.

The effect of molecular ordering in different polymorphs of pentacene on its electronic properties has been investigated in detail.[293−295] Generally, aromatic hydrocarbons show a great propensity to polymorphism. Indeed several pentacene polymorphs are known, and complete X-ray data are available for the three structures.[296−298] Pentacene single crystals were grown from trichlorobenzene solutions by Campbell et al.,[296] (RefCode PENTACEN from CCDC) and by Holmes et al.[297] (RefCode PENTACEN01 from CCDC). It was recently shown by Siegrist et al.[298] that a new pentacene polymorph with enhanced physical properties (RefCode PENTACEN02 from CCDC) can be obtained by vapor-phase growth. An additional two X-ray structures for polymorphs of pentacene were reported (RefCode PENTACEN03 and PENTACEN04 from CCDC).[299] Venuti et al.[293] argued on the basis of lattice dynamics calculations that phase PENTACEN02 is coincident with phase PENTACEN01 and confirmed that phase PENTACEN is significantly different. Moreover, they suggested that the method of crystal growth (from solution or vapor) is not the determining factor for obtaining either structure and that sample purity or growth temperature is more critical.

Della Valle et al. predicted several hundred distinct minima in the potential energy surface of crystalline pentacene, which should correspond to many polymorph structures, with two deepest minima corresponding to the structures of two observed known polymorphs.[300] Recently, de Wijs et al. analyzed the similarities and differences between the structures of all acenes.[300] Calculations performed by Tiago and co-workers[295] indicated that the electronic energy gaps for the different polymorph structures are slightly different. Intermolecular interactions are more favorable in the vapor-phase grown structure. Recently, solid-state packing in conjugated oligomers including the parent and substituted pentacenes was rationalized in terms of "pitch and roll" inclinations (i.e., two angles determining the distortion from an "ideal" noninclined co-facial π-stack).[301]

Extended Hückel theory calculations of the band electronic structures of the parent and substituted pentacene derivatives were reported by Haddon et al.[302] The results show that the parent pentacene polymorphs are 2-dimensional in their band electronic structure with moderate dispersions. The bandwidths in the 14.1 Å d spacing polymorph (the vapor-phase grown)[297] are noticeably larger (0.09−0.28 eV) than those for the 14.5 Å d spacing polymorph (0.07−0.18 eV, the solution-phase grown),[296] in agreement with the superior physical properties found for the 14.1 Å d spacing polymorph.[298] The dispersion in the highest lying valence band of the 14.1 Å d spacing polymorph is calculated to be about 0.2 eV along the X direction.

Growth dynamics of pentacene thin films have been studied utilizing the real-time imaging capabilities of photoelectron emission microscopy by the low-energy electron microscopy (LEEM) technique.[303] Organic thin-film growth of pentacene closely mimics epitaxial growth of inorganic materials.

Recently, the structure of a monolayer-thick pentacene film grown on amorphous silicon dioxide (a-SiO_2, a commonly used dielectric layer in OTFTs) was studied by grazing-angle incidence X-ray diffraction (GI-XRD) using a synchrotron source.[304] The results confirm that the monolayer is crystalline; however, its structure is different from that of bulk pentacene, which has important implications for carrier transport in pentacene-based OTFTs. The lattice parameters for a monolayer-thick pentacene film grown on amorphous silicon dioxide were significantly different from those reported for bulk pentacene but were consistent with a packing motif resembling the (001) layers in the bulk form, that is, with the pentacene molecules in the monolayer adopting a near-vertical orientation (with the long axis perpendicular to the substrate) on the a-SiO_2 substrate. The energy-minimized monolayer structure using the cell parameters obtained by GI-XRD reveals a herringbone packing of the pentacene molecules similar to that observed in the bulk.

3.5.2. Organic Field-Effect Transistors

Organic semiconductors have been studied since the late 1940s.[305] Despite many efforts invested in this field, until the past decade, OFETs had no significant practical impact in optoelectronic applications. Nowadays organic semiconductor materials are part of a rapidly growing field revolutionizing applications in photovoltaic cells,[150,306] chemical sensors,[307] microelectronic actuators,[308] and TFTs.[194] Organic FETs are very similar to commonly used silicon-based TFT transistors which contain amorphous silicon as the semiconductor material (charge-carrier mobility about 0.5 $cm^2/V{\cdot}s$). Currently, the most developed organic FETs are based on pentacene. Plastic flexible organic-based transistors have already reached the requirements for mass applications in microelectronics[309] as pixel drivers for flexible displays and identification and product tagging purposes. For discussions of organic FETs, see refs 194, 195, 310, 311, and 312. Organic TFT devices are usually prepared in one of two configurations: top-contact device, with source and drain electrodes evaporated onto the organic semiconducting layer, or bottom-contact device, with the organic semiconductor deposited onto the prefabricated source and drain electrodes with the gate usually on top or the side (Figure 23).

The TFTs based on crystalline or amorphous inorganic semiconductors are well-known.[313] The basic equation describing the drain current in FETs is

$$I_d = (W/L)\mu C_i[(V_g - V_T)^2 - {}^1/_2 V_d{}^2]$$

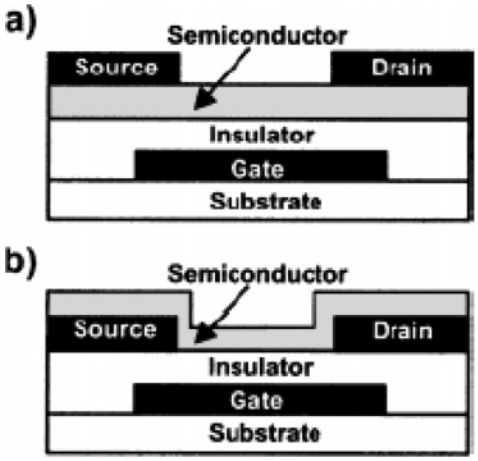

Figure 23. OTFT device configurations: (a) top-contact device, with source and drain electrodes evaporated onto the organic semiconducting layer through a mask; (b) bottom-contact device, with the organic semiconductor deposited onto the gate insulator and the prefabricated source and drain electrodes. (Reproduced with permission from ref 194. Copyright 2002 WILEY−VCH Verlag GmbH.)

where μ is the field-effect carrier mobility, W is the channel width, L is the channel length, C_i is the capacitance per unit area of the insulator layer, V_T is the threshold voltage, V_d is the drain voltage, and V_g is the gate voltage.[312] Thus, to achieve high drain current, the field-effect carrier mobility should be maximized.

Pentacene and tetracene have been used as hole collectors (transporters) in organic photovoltaic cells,[314] but of the electronic applications mentioned, oligoacenes have played a much more important role as active semiconducting materials in OFETs, mostly due to a remarkably low reorganization energy (see below) and an appropriate ionization potential responsible for excellent hole conductance.[315] The energy required for the structural relaxation in pentacene (the reorganization energy), going from the neutral state to the cation radical and the reverse, is small; hence, hole transport through pentacene films is effective. The field-effect mobility in pentacene-based TFTs has been improving to equal that of hydrogenated amorphous silicon (0.5 $cm^2/V·s$) and to supersede it up to 3 $cm^2/V·s$.[194,195,310,316] More recently, an even higher mobility of 5 $cm^2/V·s$[317] was reported for pentacene (achieved using surface modification[318]). A field-effect transistor on a pentacene single crystal has also been fabricated.[319,320] The formation of large single-crystal domains in vacuum-deposited pentacene TFTs and the high degree of molecular ordering that this implies are correlated with the high mobilities obtained from these devices.[321] Unlike oligothiophene-based TFTs,[322] where an impressive increase in mobility was achieved through design of new molecules, the increased performance of pentacene-based TFTs was achieved mainly through the development of device fabrication techniques, including[323] optimization of the film deposition parameters[323,324] and improvement of morphology, dielectric-semiconductor interfacial properties, and purification of materials.[325] Finally, improvement of acene mobility by appropriate chemical modification (substitution) is underway.[326,327]

Another advantage of organic FETs is the possibility of implementation in nanoelectronics. The optimum channel thickness in pentacene-based thin-film transistors was found to be 30 nm,[328] a few times below the limit of silicon (determined by uniformity of doping). Indeed, 30 nm channel-length pentacene transistors have been reported recently.[329]

We note that organic molecular crystals have an upper limit of microscopic mobilities.[194] The weak intermolecular van der Waals interactions may be responsible for this limit. In contrast, in inorganic semiconductors such as Si, Ge, and GaAs, the atoms are held together with very strong covalent bonds. In these semiconductors, charge carriers move as highly delocalized plane waves in wide bands and have a very high mobility at ($\sim 10^3$ $cm^2/V·s$).

3.5.3. Pentacene from Soluble Precursors

The charge mobility achieved in pentacene-based OTFTs satisfies the required value of many applications (1 $cm^2/V·s$). However, one of the main motivations for organic electronic materials, the possibility of solution processing, is hindered by pentacene's insolubility. Vacuum deposition is the most frequently used for pentacene or other acenes. AFM images of pentacene films from high mobility devices showed a high degree of molecular ordering with micrometer-sized and larger dendritic grains, while poorly performing devices showed small grains and higher molecular disorder.[330] Also, the surface roughness of the dielectric layer has a great impact on mobility; increasing the dielectric roughness reduces the free carrier mobility.[331]

The inability to consistently control and reproduce film thickness and order is a drawback associated with the chemical vapor deposition (CVD) technique. On the other hand, one of the greatest advantages of molecular semiconductors is potential solution processing, which is expected to reduce the cost of device fabrication considerably. In this regard, several solution processable pentacene precursors have been synthesized.[332] After spin-coating onto substrates, they give homogeneous films which can be thermolyzed in a vacuum to produce a pentacene layer. The first example of this approach, reported by Müllen et al., included compound **144** as a precursor.[333,270] The latter was synthesized using a Diels−Alder reaction of benzyne followed by oxidation to compound **143** and another Diels−Alder cycloadition (Scheme 14). However, the mobility of the resulting FET was low, 9×10^{-3} $cm^2/V·s$.[333] Later, optimization of conditions for the conversion of the precursor into pentacene led to an improved charge-carrier mobility of 10^{-1} $cm^2/V·s$.[270] Pentacene may also be obtained from precursor **143** by hydrogenation followed by retro-Diels−Alder reaction (Scheme 14).[270]

A similar approach was reported by a group at IBM in 2002.[334] A pentacene derivative **145** (Scheme 15) with a thermally removable group was cast from solution into the active channel. After heating precursor **145** to 130−200 °C, a pentacene film with significantly improved field-effect mobility up to 0.89 $cm^2/V·s$ was formed.[334] One year later, a modified method to obtain a thin film of pentacene was pub-

Scheme 14. Synthesis of Pentacene via Soluble Precursors[270]

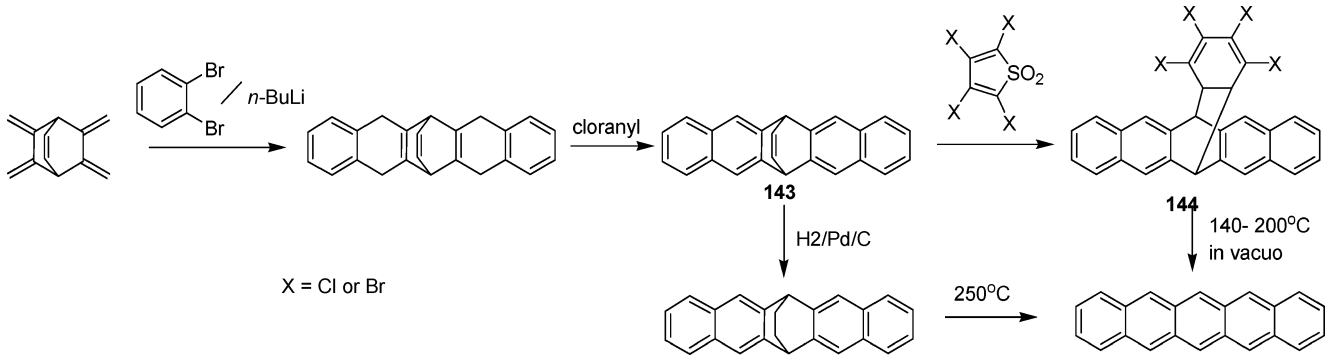

Scheme 15. Synthesis of Soluble Pentacene Precursor 145[334]

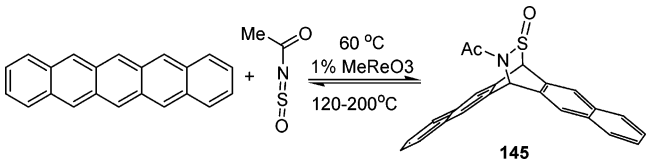

Scheme 16. Synthesis of Soluble Pentacene Precursor 146[335]

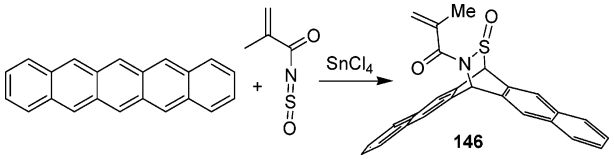

lished.[335] The photosensitive precursor **146** (Scheme 16) can be polymerized via vinyl moieties by irradiation, which allows its patterning. The illuminated areas were polymerized, and nonilluminated areas were removed by dissolution. Heating the polymeric material released pentacene **136.5** incorporated in the poly(*N*-sulfynylacrylamide) matrix. The field-effect mobility of FETs, obtained by this procedure, was relatively low, up to 0.021 $cm^2/V{\cdot}s$; however, this procedure allows direct photopatterning of a pentacene precursor, which is another significant step for low-cost fabrication.

3.5.4. Theoretical Study of Transport Properties of Pentacene[336]

Understanding the charge-carrier transport in organic semiconductor materials such as pentacene is an important topic, not only of fundamental academic interest but also of great technical relevance in such promising fields as organic field-effect transistors, organic light emitting diodes (OLED), or photovoltaic cells. At the microscopic level, the charge-transport mechanism can be described as involving an electron transfer from a charged molecule to an adjacent neutral molecule. The charge-carrier mobility, μ, determines charge-carrier transport for a given semiconducting solid. The charge-transport properties depend on the degree of ordering of the molecules, on the energies and intermolecular overlap of molecular orbitals, and on chemical or structural defects.[343] For a brief review of different experimental methods that can measure charge-carrier mobilities, see ref 337.

Hole- and electron-vibrational couplings to molecular modes in oligoacene crystals were studied experimentally (using high-resolution gas-phase ultraviolet photoelectron spectroscopy, UPS) and computationally (using density functional theory).[338] The first vertical ionization potentials were measured (in gas phase) to be 7.421 eV for anthracene, 6.939 eV for tetracene, and 6.589 eV for pentacene (error $\pm$0.001 eV). Due to high resolution of the method employed for these molecules, several ionization bands, including the first ionization, contain partially resolved vibrational fine structure, providing an experimental determination of reorganization energies. The relaxation energies obtained from UPS spectra are 69.7, 58.8, and 49.6 meV for anthracene, tetracene, and pentacene, respectively. Using these values, the dimensionless hole-vibrational coupling was estimated to give relaxation energies of 0.279, 0.235, and 0.198 for anthracene, tetracene, and pentacene crystals, respectively. The hole-vibrational coupling is inversely proportional to the number of atoms along the π-conjugated backbone. Relaxation energies obtained from UPS spectra are in good agreement with DFT calculated values. Similar calculations predict 0.404, 0.314, and 0.250 for the dimensionless electron-vibrational parameter in anthracene, tetracene, and pentacene, respectively. Thus, the hole-vibrational coupling is found to be significantly smaller than the electron-vibrational coupling in the case of anthracene, tetracene, and pentacene. However, both are predicted to converge to the same limiting value around 0.05 at the limit of infinite conjugation length.

According to semiempirical INDO calculations, in the absence of impurities and defects, electrons can be as mobile as holes in pentacene crystals[339,340] because the interchain transfer integrals are very similar for electrons and holes ($\sim$47 meV). It was also concluded that charge transport in pentacene has a dominant two-dimensional character and takes place within the layers in directions that are nearly perpendicular to the long molecular axes. The valence and conduction bandwidths in pentacene crystals were estimated to be as large as 608 and 588 meV, respectively.[339] Recently, the bandwidths for naphthalene, anthracene, tetracene, and pentacene were calculated to be on the order of 0.1$-$0.5 eV. Furthermore, comparison of the thermal-averaged velocity$-$velocity tensors with the experimental mobility data indicates that the simple band model is applicable for temperatures only up to about 150 K.[341] It is interesting to point out that the theoretical estimates

of the conduction and valence bandwidths in a single crystal of pentacene have the same order of magnitude as the conduction bandwidth characteristic of the widely studied TTF−TCNQ organic charge-transfer complex and its derivatives.[339,342] This is particularly notable if one considers the intermolecular distances and interorbital angles of the two systems; in the former, they are outside van der Waals radii, and in the latter, they are much shorter than the sum of van der Waals radii.

Interestingly, a significant HOMO and LUMO splitting is calculated not only along the a axis but also along the diagonal axes (d_1 and d_2 in Figure 24),

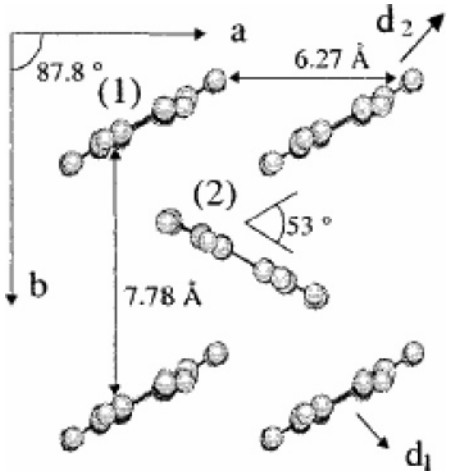

Figure 24. Lattice parameters within the ab layer of a single crystal of pentacene. Labels 1 and 2 refer to the two inequivalent molecules in the layer; axes d_1 and d_2 are those that connect these inequivalent molecules. (Reproduced with permission from ref 194. Copyright 2001 American Chemical Society.)

although the molecular planes of adjacent molecules along the latter form an angle of 53°. A vanishingly small splitting is obtained from interactions between molecules located in adjacent layers (along c),[343] confirming a two-dimensional charge transport in pentacene.

Recently, the effect of an external electric field on the charge-transport parameters in pentacene was investigated using semiempirical calculations.[344] For electric fields below 10^7 V/cm the charge distribution and geometric structure remain nearly unchanged. Pronounced charge redistributions and geometric distortions are observed at higher fields, which lead to a significant modulation of the two components of the reorganization energy.[345] However, these two components have opposite evolutions, so that the global reorganization energy remains nearly unaffected by the application of the field. The transfer integrals are also calculated to remain nearly constant and independent of the field strength.[344]

3.6. Substituted Acenes

3.6.1. Anthracene and Tetracene-Based Materials for FETs

To date, anthracene is not active in FETs; however, rather high mobilities (0.18 cm^2/V·s) were achieved using oligoanthracene **147**.[346]

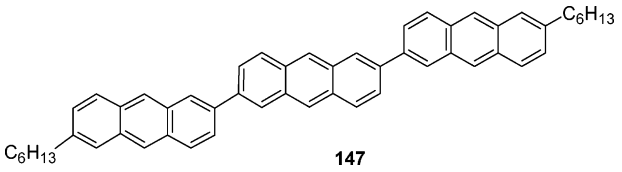

147

Several anthradithiophenes (**148**−**151**) were synthesized by H. Katz et al., and their morphology and field-effect mobility have been studied.[347] All four compounds form highly ordered polycrystalline vacuum-evaporated films with mobilities as high as 0.15 cm^2/V·s. Compound **151** has a mobility of 0.06 cm^2/V·s even though 70% of its molecular volume is occupied by hydrocarbon chains. The alkylated anthradithiophenes combine a pentacene-like intrinsic mobility with greater solubility and oxidative stability.

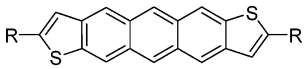

syn and anti isomer mixture

148: R=H
149: R=C_6H_{13}
150: R=$C_{12}H_{25}$
151: R=$C_{18}H_{37}$

FETs of optically transparent free-standing single crystals of unsubstituted tetracene **136.4** have been fabricated.[348] These FETs exhibit effective hole channel mobility μ_{eff} up to 0.15 cm^2/V s and on/off ratios up to 2×10^7. Independently, field-effect transistors on tetracene single crystals have been reported.[349] The mobility of these transistors reaches the room-temperature value of 0.4 cm^2/V s.

Recently, a mobility of 8 cm^2/V·s in organic media was achieved with another member of the acene family, rubrene (5,6,11,12-tetraphenyltetracene, **152**).[350] Single crystals of rubrene were grown by sublimation in an inert gas atmosphere. The crystals are orthorhombic with $a = 7.184(1)$ Å, $b = 14.433(3)$ Å,and $c = 26.897(7)$ Å. The interplanar distance between tetracene units is about 3.7 Å. The crystal structure of rubrene shows π-stacked and herringbone structures.[351] Apparently, good π-overlap is responsible for the observed high mobility. For the synthesis of rubrene, see ref 352.

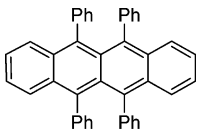

152

A new method of high-performance OFET fabrication on the surface of a free-standing organic single crystal was developed.[320,353] The transistors were constructed by laminating a monolithic elastomeric transistor stamp against the surface of a crystal with the organic crystal placed on top of the source and drain electrodes. Strong field-effect modulation of the channel conductance was observed, with on/off ratios as high as 10^6. Rubrene-based OFETs with charge-carrier mobilities as high as 15 cm^2/V·s (charge-carrier mobilities of 3−15 cm^2/V·s were obtained for

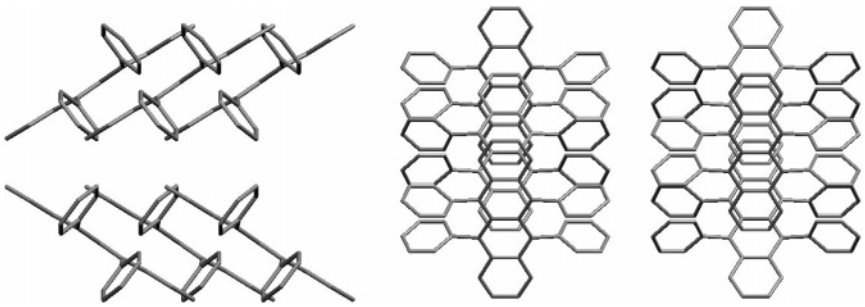

Figure 25. X-ray structure of rubrene, RefCode QQQCIG01 from CCDC: (left) view along the *c* axis; (right) view along the *b* axis.

different rubrene crystals) were fabricated using this method. The first experimental verification of anisotropy of organic single crystals in field-effect experiments also became possible using this new technique. The maximum hole mobility was realized along the *b* axis, for which one might expect a stronger $\pi-\pi$ overlap (Figure 25).

3.6.2. Substituted Pentacenes

Despite the substantial research in pentacene devices, relatively few derivatives of pentacene are known. A first obvious advantage of substituted pentacenes should be their higher solubility, which would simplify their purification and processing. 6,13-Diphenylpentacene (**153**) and tetraphenylpentacene (**154**) were prepared in 1942 using Grignard reagent.[354] The latter was recently prepared by an improved route, and its crystal structure was solved at UCLA.[355] Unfortunately, the crystal structure contains a *p*-xylene molecule of solvation and does not show any π-stacking or herringbone structure.

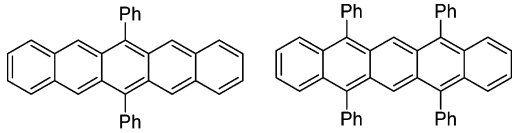

153 **154**

Maulding and Roberts synthesized a series of phenylethynyl-substituted acenes by the reaction of the corresponding ketones (diketones and tetraketone) with lithium phenylacetylide, followed by reduction of the corresponding quinols with stannous chloride.[356] Phenylethynyl substitution results in large shifts of emission and absorption to longer wavelengths and increased fluorescence efficiencies.[356] For example, the parent tetracene **136.4** absorbs at 476 nm (and emits at 483 nm with 21% quantum yield), while **155** absorbs at 548 nm (and emits at 580 nm with 66% quantum yield); the parent pentacene absorbs at 576 nm (and emits at 578 nm with quantum yield <1%), while **156** absorbs at 655 nm (and emits at 680 nm with 34% quantum yield) and **157** absorbs at 705 nm (and emits at 740 nm with 8% quantum yield).

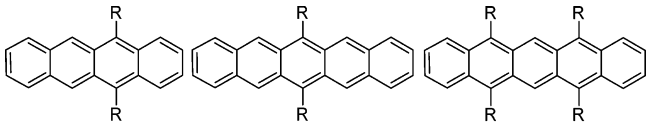

155 R = C≡C−C_6H_5 **156** **157**

A number of soluble pentacene derivatives (**158**−**160**) were synthesized by Anthony et al. in a one-pot reaction from 6,13-pentacenequinone (or its ether derivatives) and 5,14-pentacenequinone (Scheme 17).[326,357,358]

The isopropyl-substituted pentacenes **158f** and **159** show self-assembly of the aromatic moieties into π-stacked arrays, which probably enhance intermolecular overlap, compared to the parent pentacene (Figures 26 and 27). In contrast to unsubstituted pentacene, compounds **158f** and **159**[326] do not adopt the herringbone pattern but stack in two-dimensional columnar arrays with significant overlap of the pentacene rings (the interplanar spacing of the aromatic rings is 3.47 Å for **158f**, compared with 6.27 Å for pentacene). Devices fabricated using **158f** showed a field-effect mobility of 0.4 $cm^2/V{\cdot}s$.[359]

The unique arrangement of molecules **158f** and **159** in the solid state led to significant resistivity anisotropy in the crystal. Conductivity measured along the *b* axis in **158f**, perpendicular to the plane of the pentacene rings, was the highest (4×10^{-7} S/cm), followed by that measured parallel to the long axis of the molecules (the *a* axis, 2×10^{-9} S/cm). The conductivity across the short (*c*) axis was the lowest (3.3×10^{-11} S/cm) due to the insulating barrier created by the substituents.[360] The highest conductivity measured for **159** was 1.2×10^{-10} S/cm, which is just a little higher than the conductivity of **158f** along its least-conductive axis. Temperature-dependent conductivity studies revealed that these materials are semiconductors, with thermal activation energies in the range 0.3−1.5 eV.[361] The photoresponse of the conductivity in functionalized pentacene compounds **158c** and **158f** was also studied.[362]

These materials pack in three general motifs: segregated stacks (such as **158f**, Figure 26), slip-stacks (such as **158c**),[357] and columnar stacks (such as **159**, Figure 27).[326] Segregated stacks result in two-dimensional overlap, producing the best electronic properties. The noticeable solid-state structure differences of substituted pentacenes from that of the parent pentacene herringbone packing are reflected in their electronic band structures.[302] Pentacene **158c** adopts a pronounced one-dimensional structure that leads to a large bandwidth along the stacking direction; **158f** also adopts a stacked structure, but because the molecules are laterally interleaved in the brick-wall fashion, this compound is strongly two-dimensional.

Takahashi synthesized alkyl-substituted pentacene derivative **161** by successive homologation and de-

Scheme 17. Synthesis of Dialkylpentacenes by Anthony et al.[326,357,358]

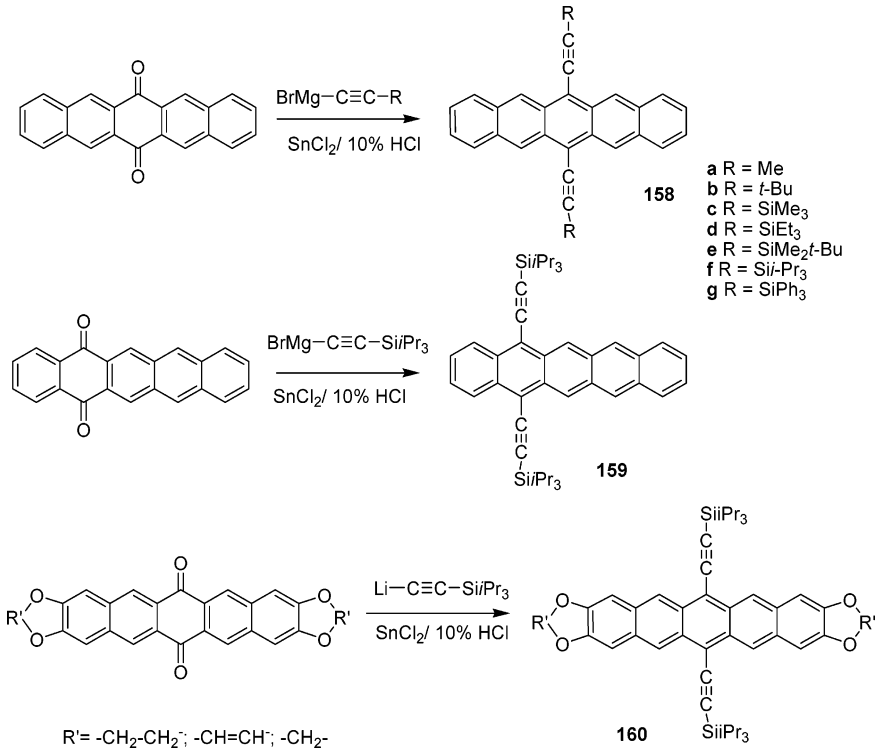

termined its X-ray structure.[363] The pentacene derivative **161** was deep-blue and soluble in organic solvents such as THF, $CHCl_3$, benzene, hexane, ether, AcOEt, and acetone.

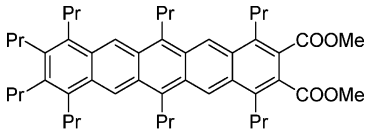

161

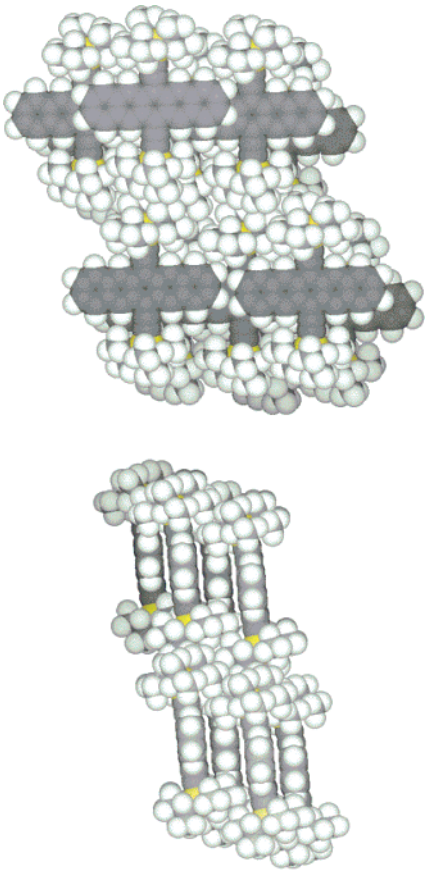

Figure 26. Solid-state ordering of **158f**: (top) view of the *ac* layer (looking down the *b* axis); (bottom) view of the *bc* layer (looking down the *a* axis). (Reproduced with permission from ref 326. Copyright 2001 American Chemical Society.)

The multistep synthesis of 2,3,9,10-tetramethylpentacene (**162**)[327] was performed similarly to the procedures described for pentacene (Scheme 18).[213] Both **162** and **136.5** produce pink solutions in 1,2-diclorobenzene (ODCB) and exhibit a pink-red fluorescence. The longest wavelength band has a characteristic vibronic fingerlike shape, and the maxima were almost unchanged (by less than 2 nm) in going from pentacene to tetramethylpentacene.

Cyclic voltammograms of both pentacene **136.5** and **162** (Figure 28) showed quasi-reversible oxidation and reduction in hot 1,2-dichlorobenzene with nBu$_4$NPF$_6$ electrolyte. The oxidation potentials and reduction potentials ($E^{1/2}$ vs Ag wire, Fc/Fc$^+$ shows 0.47 V under these conditions) are +0.73 V, −1.66 V for **136.5** and +0.58 V, −1.66 V for **162**, respectively. The HOMO−LUMO gaps, determined from the $E^{1/2}$ of oxidation and reduction potentials, were 2.4 and 2.3 eV for **136.5** and **162**, respectively. An OTFT fabicated with compound **162** with a mobility of 0.30 cm^2/V·s renders it the first pentacene derivative with mobility similar to that of the parent pentacene.

Oligoacenes starting from anthracene are good dienes for Diels−Alder reactions.[188,189,380] Much less, however, is known about oligoacene compounds as dienophiles.[364] Recently, an interesting reaction of a pentacene derivative acting as a dienophile was discovered (Scheme 19).[365] Cycloaddition of 2,3,9,10-

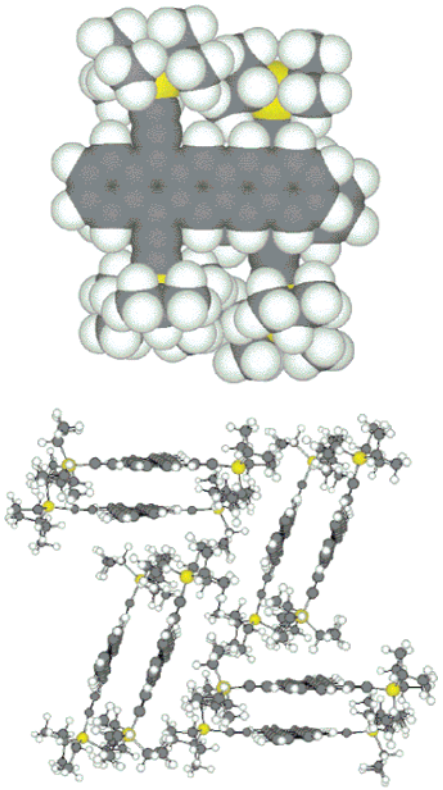

Figure 27. View of the close-packing "dimeric" stacks of **159** (top) and their arrangement in the solid state (bottom). (Reproduced with permission from ref 326. Copyright 2001 American Chemical Society.)

tetrachloropentacene (**163**) with itself followed by dechlorination lead to a novel aromatic ladder polymer—poly(iptycene), which can be converted to a highly conducting carbon at relatively low temperature (600−900 °C).

A relatively long C2−C3 bond length in **163** (calculated value 1.442 Å) is weaker than in typical aromatic compounds and hence more reactive. This opens the possibility for a Diels−Alder reaction between the peripheral double bond (C2−C3) of **163** (acting as dienophile) and the central ring of another **163** molecule (acting as diene), resulting in the [4 + 2] cycloaddition followed by dechlorination, producing an iptycene structure. The calculated overall activation barrier (~50 kcal/mol) seems very reasonable for the reaction occurring at 400 °C. Once the pentacene has undergone cycloaddition, the terminal double bond of the naphthalene fragment loses its dienophilicity, resulting in preferable formation of a linear polymer, the first ladder-type poly(iptycene) described. Loss of the two residual chlorine atoms above 600 °C is accompanied by gradual dehydrogenation, resulting in a highly conducting material (pressed

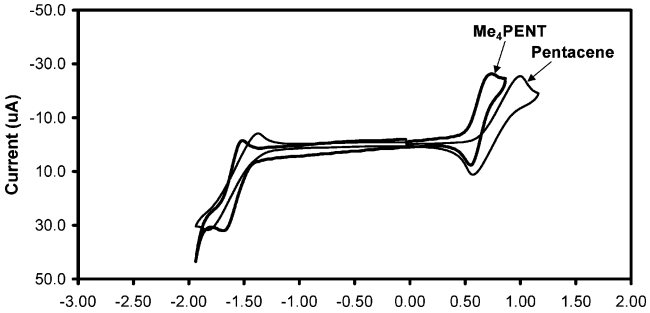

Figure 28. Cyclic voltammograms of pentacene **136.5** and tetramethylpentacene **162** in hot (150 °C) ODCB solutions (0.1 M Bu_4N PF_6). The potentials are vs a Ag wire pseudoreference electrode; Fc/Fc^+ shows 0.47 V under these conditions. The large $E_{p.a.}/E_{p.c.}$ separation is due to uncompensated resistance in low-polar media and was also observed for ferrocene.

pellet $\sigma_{rt} \sim 10^{-3}$ S/cm for material obtained at 730 °C and >5 S/cm for material obtained at 960 °C, two-probe method). This conversion temperature is remarkably lower than the normal graphitization temperatures (2000−3000 °C) and in the range of a graphitization of hexabenzocoronene derivatives.[366] It is possible that the structural similarity between PAH and graphite favors the graphitization process. Interestingly, when the pyrolysis of a number of PAHs is performed under very high pressure, diamond-like carbons can be formed. The pyrolysis of naphthalene, anthracene, pentacene, perylene, and coronene at 8 GPa suggests that the temperature (1280 °C) for diamond formation does not depend on the nature of the starting PAH for all investigated compounds.[367]

Several other substituted pentacene structures, such as 6,13-diethylpentacene,[368] 6,13-dihydroxypentacene,[369] [*b*]-cyclohexenepentacene,[370] 1,4,8,11-tetramethoxypentacene,[371] 1,11,12,13,14-pentahydroxypentacene,[371] 1,11,12,13,14-pentakis(hydroxymethyl)-pentacene,[372] 6,13-dichloropentacene,[373] and 5,6,7,-12,13,14-hexachloropentacene,[374] have been claimed in the literature, but only one of these (1,4,8,11-tetramethoxypentacene) has been fully characterized. To the best of our knowledge, the application of any of these materials in FETs or other electronic devices has not been reported to date.

3.7. Benzannulated Pentacenes and Higher Homologues

Numerous benzannulated pentacenes, hexacenes, and heptacenes were synthesized, mostly by Clar et al. (Chart 20), and crystal structures that revealed completely planar structure were determined for some of these (e.g., compound **164s**[375]). As these compounds have been thoroughly reviewed by Clar[188]

Scheme 18. Synthesis of 2,3,9,10-Substituted Pentacenes 162 and 163

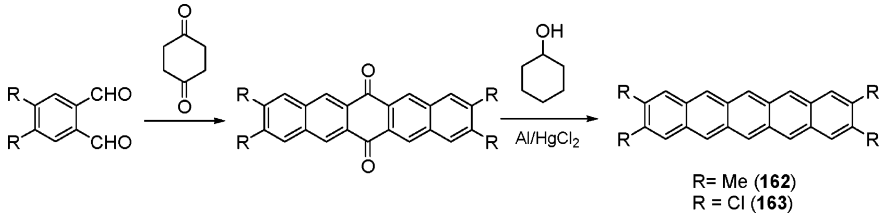

Scheme 19. Thermal Polymerization of 163[365]

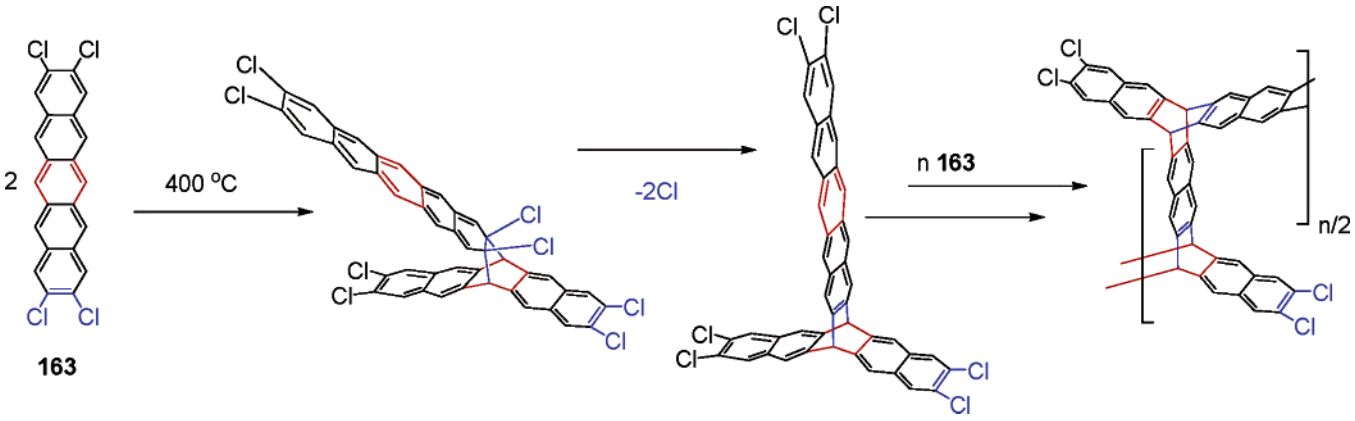

Chart 20. Benzannulated Pentacenes, Hexacenes, and Heptacenes

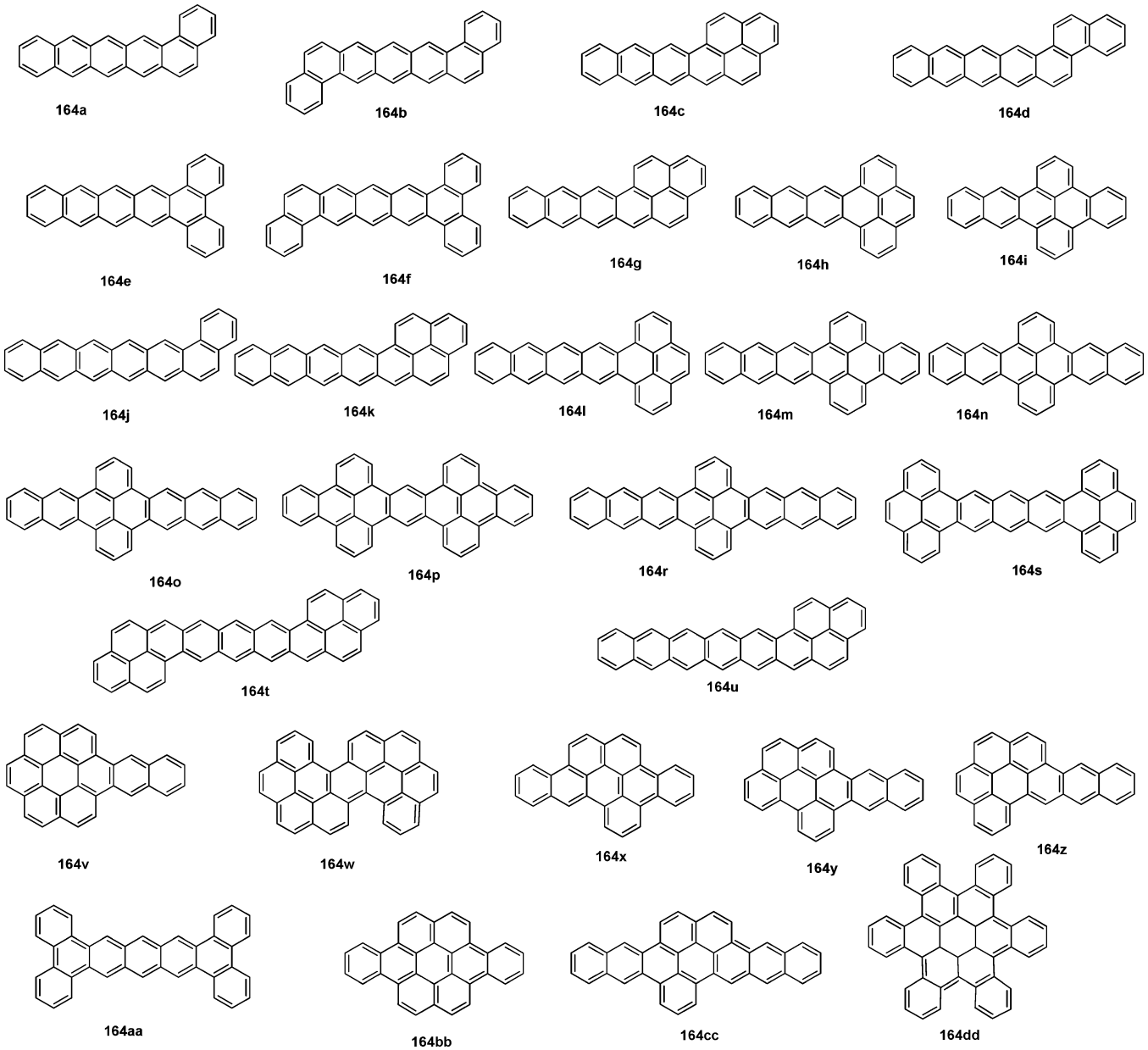

and Harvey,[189] here we only mention recent developments relevant to electronic materials.

Introducing phenyl substituents in the acene fragment of many of compounds **164**, results in puckering the molecules, e.g., twisting. These twisted PAHs are topologically interesting molecules that have been studied in detail, mostly by Pascal's group, who designed, synthesized and characterized many of these contorted molecules up to formal pentacene derivative **165**.[376] Recently, an efficient synthesis of

a novel twisted and stable, electroluminescent "twistacene" **166** was reported using a novel mild bisbenzyne precursor **167** (Scheme 20).[377]

Scheme 20. Synthesis of "Twistacene" 166

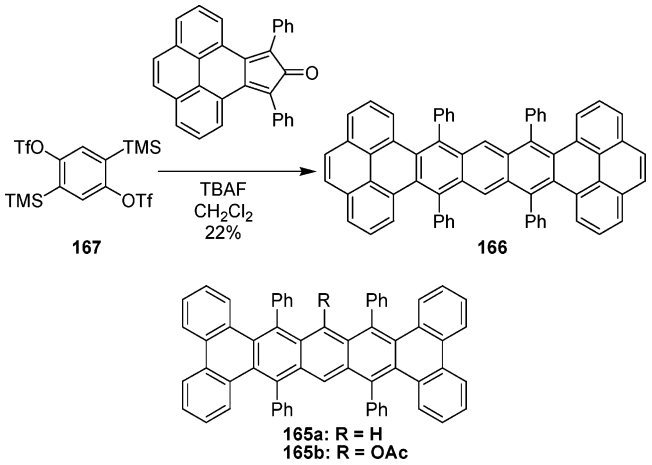

Despite (or perhaps due to) the significant twisting in **166**, its lowest energy electronic absorption (λ_{max} at 530 nm) is red-shifted compared to its parent **164**s (λ_{max} = 506 nm in TCB).[378] The bathochromic effect is most likely a result of a combination of the phenyl substitution and twisting of the π-system. Overall, the λ_{max} of **166** falls between tetracene (475 nm) and pentacene (582 nm), that is, at considerably longer wavelength than anthracene, the longest non-cross-conjugated moiety in **166**. In solution, **166** is strongly fluorescent with 15% quantum efficiency and essentially zero Stokes shift. CV measurements ($E°_{red}$ = −1.79, $E°_{ox}$= 0.72 V vs Ag/Ag$^+$, Figure 29) suggest

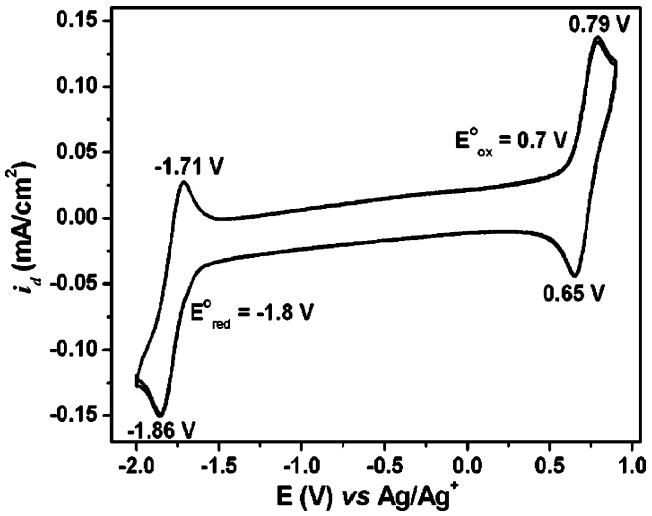

Figure 29. Cyclic voltammetry of **166** in ODCB. (Reproduced with permission from ref 377. Copyright 2003 American Chemical Society.)

a HOMO−LUMO gap of 2.51 eV, in reasonable agreement with the optical gap (2.3 eV) and the calculated $\Delta E_{HOMO-LUMO}$ [2.6 eV, B3LYP/6-31G(d)]. Furthermore, both calculation and experimental results placed the HOMO−LUMO gap of **166** right between tetracene (calcd 2.8 eV, exp 2.6 eV) and pentacene (calcd 2.2 eV, exp 2.1 eV). The combined photoluminescence and CV results render **166** as a potentially interesting material for OLEDs. Indeed, **166** affords excellent white-emitting LEDs with low turn-on voltage and high luminance.[379]

3.8. Acene−Fullerene Clusters

As discussed above, in Diels−Alder reactions of acenes, the most reactive is the central ring and the reactivity increases with an increasing number of rings.[188,189,380] As the dienophilic character of fullerene is well-known,[381,382] the Diels−Alder reaction was used to create a number of diads across these two types of materials. The reaction between anthracene and fullerene was first discovered in 1993,[383] and since then, it was studied in great detail (Scheme 21).

Scheme 21. Synthesis of Anthracene−C_{60} Adduct 169 and Its Solid-State Disproportionation

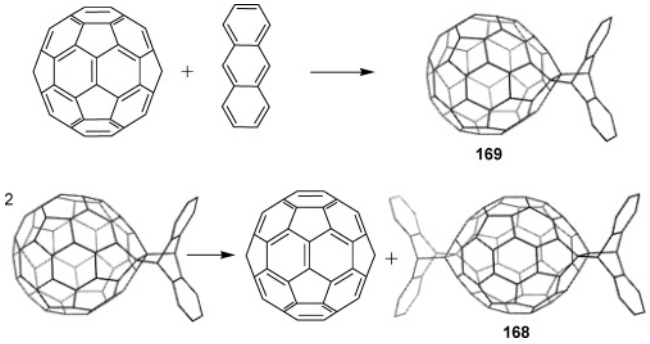

It was demonstrated that the solution-phase cycloaddition of 9,10-dimethylanthracene to fullerene at room temperature proceeds reversibly.[384] It has been shown experimentally that there is an inverse α-secondary isotope effect and the β-secondary isotope effect is close to unity, suggesting a concerted mechanism.[385] A variety of anthracenes have been attached to C_{60} in solution,[386] and an elegant approach was developed for the antipodal bisadduct **168** by a topochemically controlled thermal transformation of the crystalline monoadduct **169** (see Scheme 21).[387]

Interestingly, the cycloaddition efficiency of anthracenes to fullerene is improved when the reaction is performed in solid state using a high-speed vibration milling (HSVM) technique.[388] The HSVM treatment of C_{60} with 9,10-dimethylanthracene, tetracene, or naphtho[2,3-*a*]pyrene also gave the corresponding [4 + 2] cycloadducts in 51−62% yields.[388]

Reversible binding of C_{60} to an anthracene derivative was used to produce a fullerodendrimer **170** (Scheme 22).[389] Good solubility in water, brought by a dendritic poly(amidoamine) substituent, and a possibility of removing the dendritic substituents render this system useful for biomedical applications. It can act as a fullerene reservoir releasing C_{60} intracellularly. This fullerodendrimer also represents a new class of fullerenes and can act as photosensitizer to generate singlet oxygen in water.

The first reaction of fullerene with pentacene was reported in 1997, and its major product, monoadduct **171** (resulted from addition of fullerene across the central 6,13-carbons of pentacene), was isolated in 59% yield after reflux in toluene.[390] A 10-fold excess of C_{60} increases the yield of monoadduct **171** to 86% (based on pentacene consumed). In a solid-phase

Scheme 22. Reversible Diels–Alder Reaction of C_{60} and 170[389]

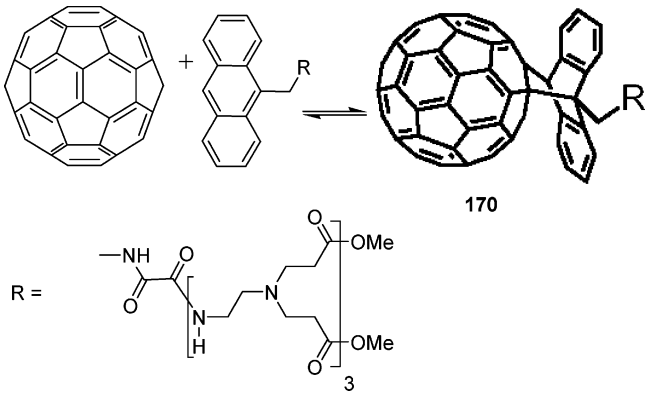

mechanochemical synthesis, a 1:1 mixture (**171**) and 2:1 (**172**) and 1:2 (**173**) addition products were obtained in 19%, 11%, and 15% yields, respectively[388] (Scheme 23). When 2 mol equiv of C_{60} was used, the yield of the *trans*-bisfullerene adduct **172** increased to 16%. The syn–anti stereochemistry of the bis-addition product was not investigated in this study; anti stereochemistry was assumed for the product based on ^{13}C NMR data, but the authors pointed out that the ^{13}C NMR data are also consistent with the syn adduct having C_{2s} symmetry.

Figure 30 shows the packing of **171** in the solid state.[391] It has a packing mode analogous to that found[387] for the fullerene adduct with anthracene. The bent pentacene fragment of the adduct embraces the fullerene portion of a neighboring adduct. Within the region of contact, the shortest nonbonded C···C distances are 3.17 and 3.20 Å. The fold angle of the pentacene (the angle between the least squares planes of the two naphthalene rings in the adduct) is 126.7°. This angle is similar to the fold angle (123.2°) in **174** and also similar to that found in *s*-dipentacene (127.4 Å),[392] the photodimer of pentacene.

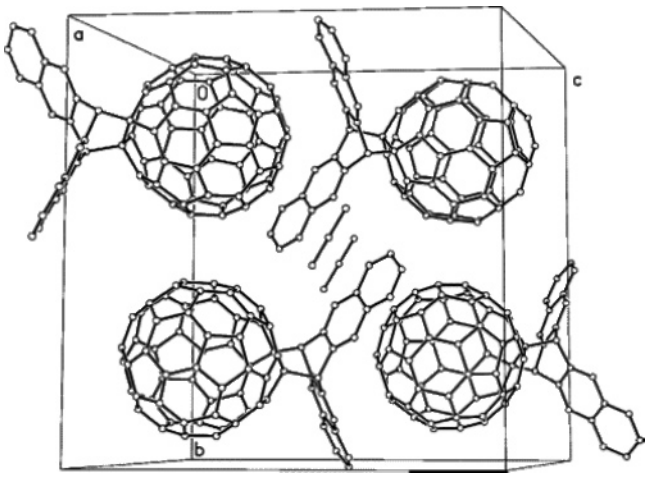

Figure 30. Unit cell of **171**·2CS_2. (Reproduced with permission from ref 391. Copyright 2003 American Chemical Society.)

The insertion of aryl substituents at positions 6 and 13 of pentacene results in formation of bis-adduct only, via addition of two fullerene molecules in positions 5,14 and 7,12 (see ref 393). *cis*-Bisfullerene-[60] adducts **174** and **175** of 6,13-disubstituted pentacenes were synthesized in 75–85% isolated yields under kinetically controlled Diels–Alder conditions (Chart 21). The cycloadditions were completely regio-

Chart 21. Fullerenopentacene Adducts 174 and 175

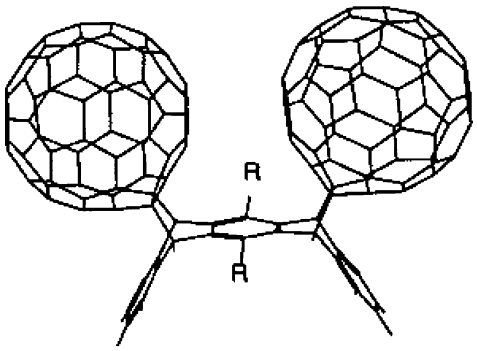

174, R = Ph
175, R = 4-MeOPh

selective and highly stereoselective, with only traces of the diastereomeric *trans*-bisfullerene[60] adducts formed. The cis stereochemistry was established by careful NMR experiments taking advantage of slow rotation of the substituents at the 6,13 positions of pentacene. When **174** and **175** were heated to reflux in $CHCl_3$ (bp 63 °C) for an extended time period, no detectable retro-Diels–Alder reaction results, thereby confirming the kinetically controlled nature of the forward reactions run in refluxing CS_2 (bp 46 °C).[393] Molecular modeling studies suggest that favorable C_{60} π-stacking interactions of two fullerenes account for the high cis stereoselectivities observed in the

Scheme 23. Synthesis of Pentacene–C_{60} Adducts

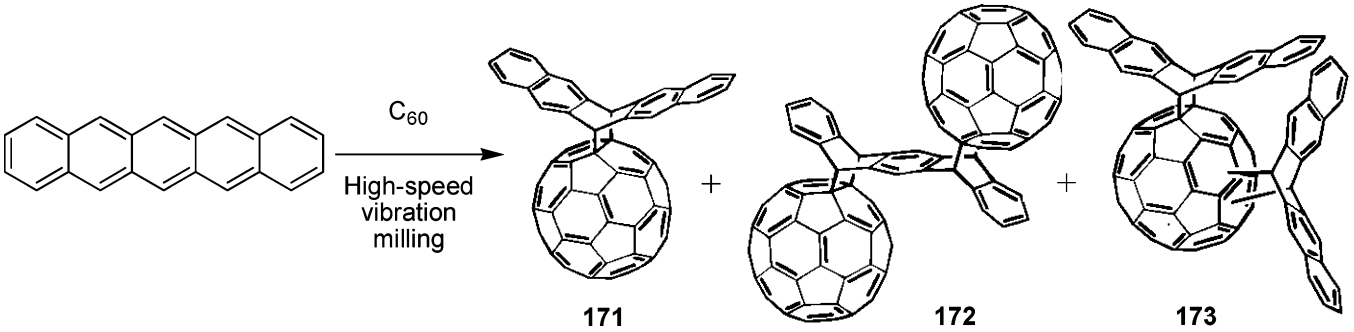

reactions between C_{60} and 6,13-disubstituted pentacenes.[394]

Recently, the structure of **174** was also confirmed by X-ray analysis.[391] Two five-membered rings on adjacent fullerene moieties directly face each other, and the carbon atoms that make the closest contact are as low as 3.065(8) Å (Figure 31). The distance

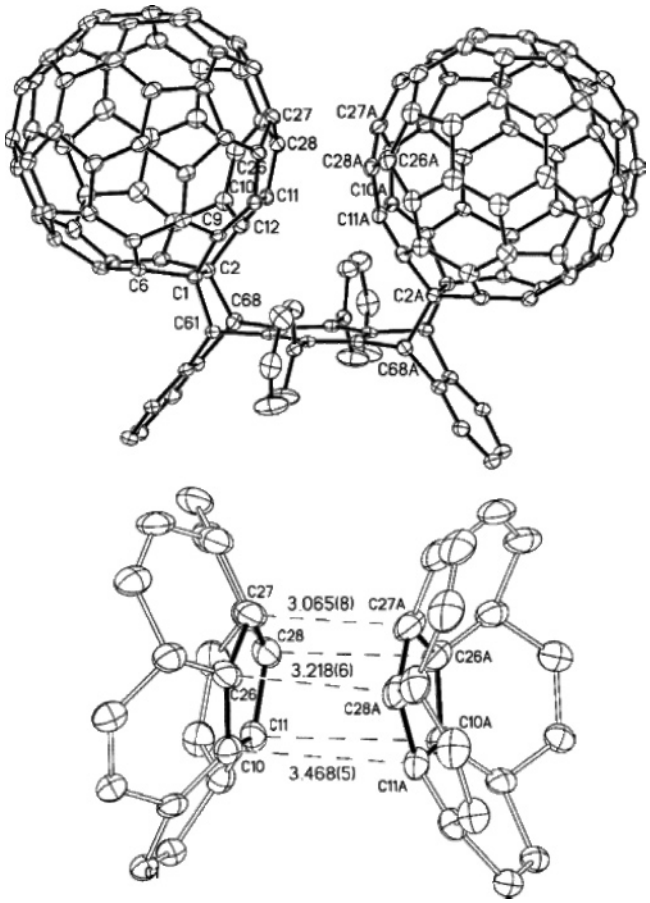

Figure 31. Top: perspective view of **174** in **174**·(4.5 CS_2) showing 50% thermal ellipsoids for all non-hydrogen atoms. Selected bond distances: C1−C2, 1.605(5) Å; C1−C6, 1.534(5) Å; C1−C61, 1.593(5) Å. Bottom: expanded view of the region of contact between the two fullerene moieties with the nonbonding C···C distances. (Reproduced with permission from ref 393. Copyright 2003 American Chemical Society.)

between the centers of the butting pentagons in two fullerenes is 3.284 Å, which is slightly shorter than the 3.35 Å van der Waals spacing between adjacent sheets of graphite. The centroid-to-centroid distance between adjacent fullerenes is 9.805 Å. For comparison, the analogous centroid-to-centroid distance in pristine C_{60} crystal (in which the molecules are orientationally disordered) is 9.94 Å.[395] Molecular mechanics (MM2) calculations predict the structures of **174** with a high degree of accuracy. Semiempirical calculations were far less accurate.[395]

Formally, the cycloadduct of heptacene with three fullerene molecules has been synthesized diastereoselectively starting from C_{60} and 5,7,9,14,16,18-hexahydro-6,8,15,17-tetraphenylheptacene **176**.[396] Heating compound **177** in benzene along with an excess of 2,3-dichloro-5,6-dicyano-1,4-benzoquinone (DDQ) and C_{60} affords compound **176** in 74% crude

Scheme 24. Synthesis of *cis,cis*-Tris[60]fullerene 6,8,15,17-Tetraphenylheptacene Adduct 176[396]

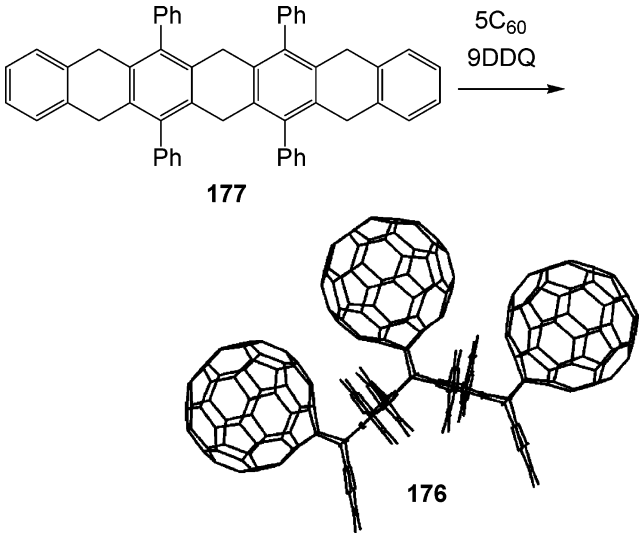

and 20% isolated yield (Scheme 24). It is not necessary that the heptacene molecule is actually formed. The reaction can proceed through sequential oxidation and trapping of each "anthracene" subunit by C_{60}.

As demonstrated above, new materials can be synthesized combining the fullerene and acene chemistry. The complementarity of their properties can also be used to create advanced electronic devices combining the materials in a single device. Recently, a CMOS (complementary metal oxide semiconductor) logic gate circuit was fabricated with C_{60} and pentacene thin-film FETs, using fullerene as an n-channel conductor and pentacene as a p-channel conductor.[397] (An n-channel FET with a thin film of C_{60} was first fabricated in 1995.[398] The mobility of the C_{60} in the FET has recently been improved to 0.56 $cm^2/V{\cdot}s$ by performing the device fabrication and characterization under 10^{-10} Torr without exposure to air.[399])

3.9. Heteroacenes

Heteroarenes are an interesting but much less studied class of π-functional materials. Substitution of one of several carbon atoms in oligoacenes with a heteroatom such as nitrogen in different valence states may deliver many intriguing properties in these π-electron systems, including a zwitterionic structure and lowered HOMO−LUMO gap.

Tetraphenylhexaazaanthracene (**178**) was synthesized in 1998.[400] It has 16 π-electrons and is formally antiaromatic. Yet, it is an atmosphere-stable, highly fluorescent compound, which can be heated to 400 °C without appreciable decomposition. Two resonance structures, **178** and **178a**, can be drawn for this molecule, but the absence of an ESR signal and sharp lines in NMR spectra suggest that a biradical resonance structure **178a** has negligible contribution and a closed-shell zwiterionic resonance structure **178** is dominant. The zwitterionic structure of **178** was also confirmed by X-ray crystallography and theoretical calculations. Thus, **178a**, by converting to **178**, sacrifices the central benzene in favor of two independent cyanine subunits with a total of 16 π-elec-

trons. In cyclic voltammetry, **178** exhibits two (quasi) reversible reductions, $E°_{1red} = -1.36$ V and $E°_{2red} = -1.62$ V, and one irreversible oxidation, $E°_{ox} = +0.55$ V (vs SCE). Only the first reduction is both chemically and electrochemically reversible.

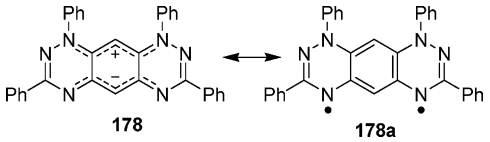

The electronically related heteroacene 5,7-diphenyl-5*H*,12*H*-quinoxalino[2,3-*b*]phenazine (**179a**)[401] also possesses a singlet ground state with zwitterionic structure, which was confirmed by solvent-dependent UV−vis and fluorescence studies.[401] A model compound with hydroden substitution in the 5,7 positions has a calculated dipole moment of 8.15 D (at B3LYP/6-31G(d)).[402] Zwitterionic azaacenes show dramatic HOMO−LUMO gap reduction compared to all-carbon acenes (λ_{max} of phenyl-substituted **179a** is 750−810 nm, depending on the solvent),[401] which makes them promising materials for electronic applications.

A related 5,7-bisoctadecyl derivative **179b** displays interesting high-temperature liquid crystalline properties (Scheme 25).[403] The monolayers of **179b** on a water−air interface form stripelike domains that responded strongly to an applied magnetic field. These stripe domains were transferred as Langmuir−Blodgett (LB) films onto glass substrates, where they were structurally characterized.[404] Tetraazapentacenes with long chain alkyl substituents, **179b** and **179c**, present a unique system because they are zwitterionic yet have an overall molecular structure that promotes a range of possible packing configurations.

Scheme 25. Synthesis of Tetrazapentacenes 179[403]

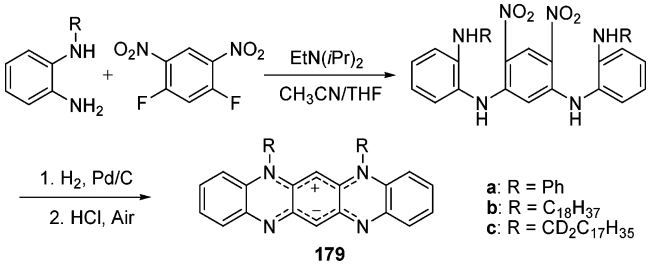

Several dihydrodiazapentacenes which are isostructural to pentacene and dihydrodiazahexacene have been synthesized, and their applications in thin-film transistors have been evaluated.[405] The synthesis of the dihydrodiazapentacenes (**180**, **181**) and dihydrodiazahexacene (**182**) was efficiently achieved through simple condensation reactions between a 1,2-aromatic diamine and a 1,2-aromatic diol (Scheme 26).[405] These materials are expected to be easily derivatized, though these were not reported. They are reported to be somewhat soluble and environmentally stable, though one would expect them to be readily oxidized. Like their acene analogues, these materials behave as organic field-effect transistors; however, their mobilities were relatively low, approaching 10^{-2} cm^2 V^{-1} s^{-1} with on/off ratios about 10^4.

Another heteroacene series, the isoquinolones, was synthesized using a new synthetic method through a zwitterionic aryne-trapping chemistry.[406] The mesoion **183** served as the diene source and provided the thermally labile protective lactam group (Scheme 27). Extrusion of one protecting unit in vacuo at 200 °C from the bislactams **184** and **185** furnished isoquinolinone **186** and **187**.

The most interesting feature of the X-ray structure of **187** is an extraordinarily long N−CO bond (of 1.434 Å). The UV−vis spectrum of **187** (in chloroform) shows the longest absorption at $\lambda_{max} = 588$ nm. It is quite surprising that **187** with a relatively small π-system revealed an optical gap similar to that of pentacene ($\lambda_{max} = 582$ nm, 2.13 eV in chloroform). The redox behavior of **187** is completely reversible with $E°_{red}$ and $E°_{ox}$ potentials of −1.6 and 0.5 V (respectively, vs Ag/Ag^+ in ODCB), and the electrochemical HOMO−LUMO gap (2.1 eV) is in excellent agreement with the optical data.

3.10. Tetrathiotetracene and Related Materials

An interesting and important class of molecular conducting materials was created by introducing

Scheme 26. Synthesis of Dihydrodiazapentacene 180[405]

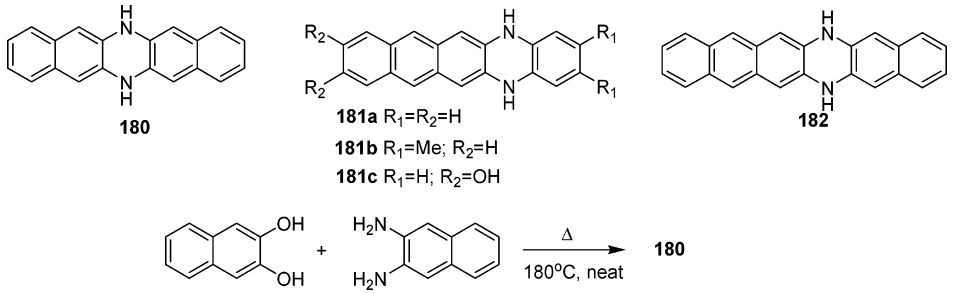

Scheme 27. Synthesis of Isoquinolones 186 and 187[406]

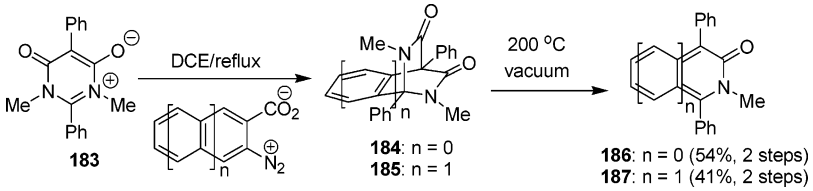

Chart 22. Structures of Chalcogenoacenes

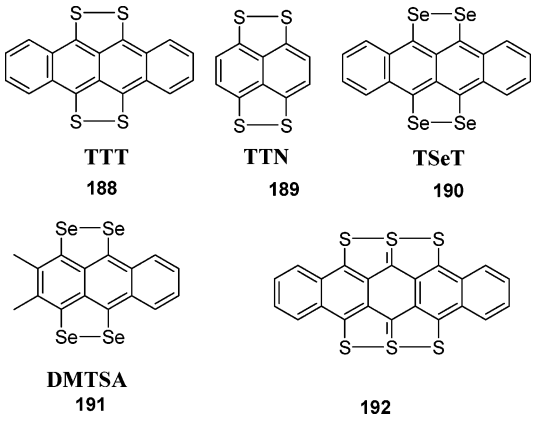

chalcogen substituents on acenes (**188**−**192**). TTT (**188**, Chart 22) is known as a stronger donor than TTF and was first used in formation of conducting charge-transfer complexes in the 1960s before the "TTF era".[407]

The first compounds of this series, TTT (**188**) and TSeT (**189**), were prepared by Marshalk et al.[215,408−410] by different synthetic methods (Scheme 28).

The chalcogenotetracenes are air-sensitive compounds, and the value of the room-temperature conductivity of TTT and TSeT may be used as a criterion of their purity (the higher conductivity corresponds to lower purity). The purification of TTT (**188**) and TSeT (**189**) includes multiple recrystallization followed by gradient sublimation.[407] Both **188** and **189** are strong electron donors and can be easily oxidized to cation radicals. The electrochemical oxidation of **188** exhibits two reversible oxidation steps at $E°_{1ox} = +0.24$ V and $E°_{2ox} = +0.73$ V vs SCE (in DCM)[411] (cf. TTF $E°_{1ox} = +0.37$ V and $E°_{2ox} = +0.67$ V vs SCE in DCM).[11] The ionization potentials of TTT (6.27 eV) and TSeT (6.33 eV)[412] are also lower than those for TTF (6.7−6.9 eV[18]). The electronic structures of tetrathioacenes **188** and **189** were studied by ESCA (electron spectroscopy for chemical analysis).[413] Electronic, infrared, and resonance Raman spectra of TTT and TSeT appeared in several publications.[407] The electronic absorption spectra of TTT and TSeT in solutions are practically identical and contain bands at 315 nm (3.94 eV), 470 nm (2.64 eV), and 700 nm (1.77 eV). The later exhibits a characteristic acene vibrational structure. Thus, the optical gap of TTT and TSeT (1.77 eV) is significantly lower than that of tetracene (2.61 eV)[242] and even pentacene (2.1 eV). The conductivity of TTT strongly depends on the purification method. Matsunaga first reported an anomalously large value, that is, 10^{-4} S/cm in 1965.[414] Obviously, the high conductivity of TTT is associated with the partial oxidation of TTT with oxygen,[411] giving rise to the formation of $TTT^{\bullet+}$. Many different conductivity values for TTT were reported in the literature, with the lowest being on the order of 10^{-7} S/cm.[407] The room-temperature conductivity of TSeT was also measured with values similar to TTT conductivity (7.7×10^{-7} S/cm for vacuum sublimed sample, and 1.1×10^{-4} S/cm for sample exposed to air).[415]

Structural aspects of one-dimensional conductors based on TTT were reviewed previously.[416] Two structural modifications of TTT, orthorhombic and triclinic, were prepared as single crystals, while only the structure of the triclinic phase was completely established.[424,417] The X-ray structure of TSeT is also known.[418] As π-donors, TTT and TSeT form a variety of conducting ion radical salts.

The first of these were obtained by Marshalk et al.[409,419] With inorganic anions such as Cl^-, Br^-, NO_3^-, ClO_4^-, HSO_4^-, CH_3COO^-, and $HCOO^-$, TTT and TSeT form monocation and dication salts.[213,409,419,420] The dication salts are less stable and can be easily reduced to monocation salts.[419] The green color of TTT changes to red upon oxidation and formation of $TTT^{\bullet+}$, which exhibits absorptions around 540, 590, 950, 1100, and 1250 nm.[411] $TTT^{\bullet+}$ inorganic salts are soluble in water, and the solubility is strongly dependent on the anion. Complexes of TTT or TSeT with many organic and organometallic acceptors are known (Chart 23).[414,416,421]

Chart 23. Acceptors Used to Prepare TTT Complexes

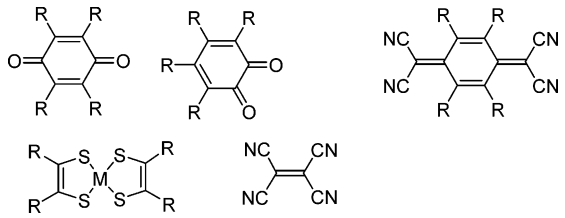

Some of these exhibit metallic properties and have room-temperature conductivity in the range of 10^3

Scheme 28. Synthesis of TTT and TSeT

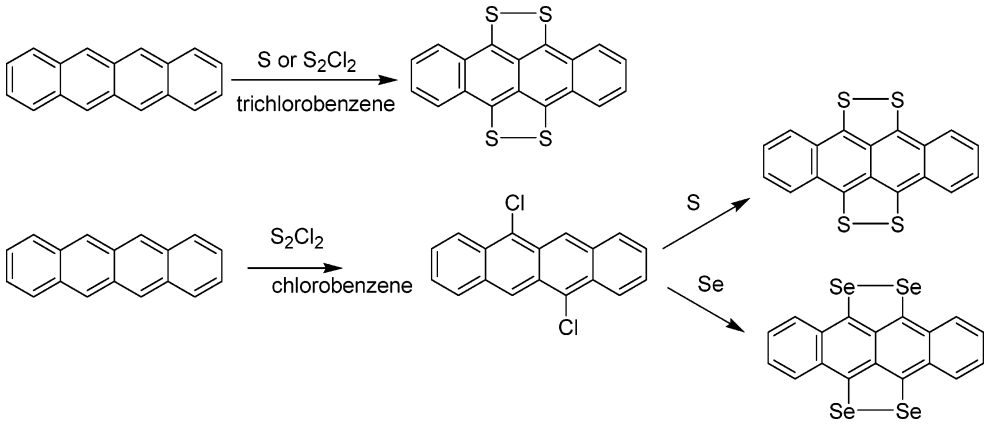

Scheme 29. Synthesis of Hexathiohexacenes 194A and 194b

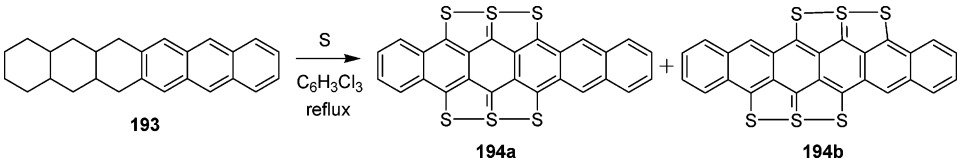

S/cm, rendering these among the most conductive molecular materials. As in TTF-based materials, the partial charge transfer is normally required for high conductivity, for example, $(TTT^{1/2+})_2I_3^-$ ($\sigma_{rt} \approx 10^3$ S/cm). In contrast to TTF derivatives, where spin density is equally delocalized between sulfur and the central carbon atoms, the spin density in TTT cation radical is considerably higher on the four sulfur atoms than on the carbon atoms.[422] CT complexes of TTT were investigated mainly in the 1960s and 1970s.[407] Some 1:1 cation radical salts based on tetraselenaanthracene **191**, in which donor molecules are fully ionized, show metallic behavior.[423] Recently, eight semiconducting cation radical salts of tetrathiotetracene (TTT) with a series of 2-alkoxytetracyanoallyl anions (RO-TCA-; R = Me, Et, Pr^n, Bu^n) were prepared by electrocrystallization.[424] For some of these, and uncommon for TTT 1:2 salts, materials with alternating stack structure and 2+ oxidation state have been observed.

A smaller analogue of TTT, TTN (**189**), also forms a CT salt with TCNQ.[425] The cyclic voltammogram of TTN exhibits two reversible oxidation steps ($E°_{1ox}$ = +0.55 and $E°_{2ox}$ = +0.93 V vs SCE in MeCN) at considerably higher potentials than TTT. The four-probe conductivity of a single crystal of TTN−TCNQ is 40 S/cm between room temperature and ~200 K and is considerably higher than that of TTT−TCNQ (1 S/cm).[425]

Hexathiopentacene **192** was obtained on heating pentacene with sulfur under reflux in 1,2,4-trichlorobenzene.[213] Similar to TTT, it is a scarcely soluble compound and is essentially an insulator ($\sigma_{rt} = 1.2 \times 10^{-13}$ S/cm). In contrast to tetrathiotetracene (TTT, which is doped by air) and the parent pentacene **136.5** (which oxidizes readily in solution), **192** is a completely air-stable compound with an oxidation potential of ~1 V (vs SCE^+).[426] This high oxidation potential stems from the very different electronic structure of **192**. In contrast to TTT, where singly bonded sulfur substituents act as donors, increasing the electron density of the tetracene core, valence considerations in **192** require a quinoid structure to be drawn to two sulfur substituents.[213] Moreover, our recent calculations suggest a pronounced double-bond character of all C−S bonds in **192** with very weak S−S bonding.[426]

The synthesis of hexathiohexacene **194** from a mixture of hydrogenated hexacenes **193** was also reported, but the exact structure of the product (**194a** or **194b** isomer) was not established (Scheme 29).[213]

3.11. Acene Ion Radical Salts

Interestingly and not unexpectedly, the electrical resistivity of acenes can be decreased drastically by both p- and n-doping.[427,428] Exposure of pentacene films and crystals to iodine vapor results in intercalation (p-doping) of iodine between the pentacene layers. The resulting I_3^- doped films exhibited an electrical conductivity of 110 S/cm, which is 11 orders of magnitude larger than that of the hydrocarbon.[427] A structural model[429] for intercalation stages of iodine-doped pentacene was proposed. Doped pentacene behaves as a typical low-dimensional organic metal, with electrical conductivity in the pentacene layer plane 10^7 times higher than that in the perpendicular direction.[430]

Somewhat lower but still pronounced conductivity ($\sigma_{rt} \sim 1$ S/cm) can be achieved in alkali-metal (rubidium) n-doped pentacene.[428,431] Minakata et al. studied the conductivity of a pentacene with a range of alkali metals and showed that the highest room-temperature conductivity decreases with decrease of the intercalant atom size (and also donor ability), in the range Rb (2.8 S/cm) > K (0.3 S/cm) > Na (10^{-5} S/cm).[428] This conclusion needs additional controls such as correlation with structure, doping level, and so forth. With that in mind, recent studies of Cs-doped pentacene (which has the largest ionic radius) revealed a conductivity of ~0.12 S/cm, close to that of K-doped material.[432] Attempts to dope tetracene films with Na, K, and Rb did not cause a conductivity increase, which might be due to the low negative reduction potential of the former, preventing electron-transfer reaction.[428] The absorption spectra of neutral pentacene and its radical cation and anion isolated in solid Ne, Ar, and Kr have been measured from the ultraviolet to the near-infrared.[274]

3.12. Acene-Based Light-Emitting Diodes

Acenes have also found use as electroluminescent materials in organic light-emitting diodes (OLEDs), due to their high fluorescence efficiency. Functionalized anthracene has been reported to yield efficient blue OLEDs.[433] Tetracene derivatives (mostly rubrene) are quite frequently used compounds for OLEDs. Rubrene was used as a dopant[434] in the hole-transporting layer in OLEDs due to its high photoluminescence (PL, 100%) quantum yield and absorption spectrum peaks at 460, 490, and 529 nm which overlap with the emission of many hosts.[435]

Recently, a series of functionalized tetracene derivatives **195a−d** were prepared in search of a suitable material as a guest dye in OLEDs. A number of compounds of type **195** with functionalization on the alkyne and/or the acene ring were prepared by addition of a lithium acetylide to tetracenequinone, followed by deoxygenation with stannous chloride.[436] Solution fluorescence maxima at 540−637 nm with good quantum efficiencies were observed for these compounds. By changing the substituents on the tetracene backbone, the photoluminescence and elec-

troluminescence emission can be shifted to the red, while simultaneously improving the stability and solubility of the emissive molecules. Compound **195b** (R = OMe) shows a relatively sharp electroluminescence emission peak at 656 nm and produces a deep red emission.

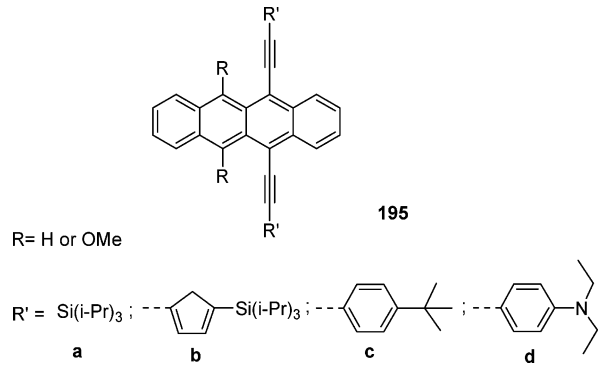

A substituted pentacene, 6,13-diphenylpentacene (**153**), was used as a guest dye to produce red electroluminescence.[437] **153** exhibits a narrow emission spectrum giving rise to a saturated red peak, centered around 625 nm, and shows a strong absorption in the 500−620 nm region, which overlaps well with the emission spectrum of the host most frequently used for the OLED tris(8-hydroxyquinolinato)aluminum (Alq3). An absolute photoluminescence quantum yield of 30% was achieved for a composite film of 0.55 mol % **153** doped into Alq3. An electroluminescence quantum efficiency of 1.3% at 100 A/m^2 was reported.

4. Conclusions

The π-functional molecular materials, based on derivatives of TTFs, oligo(acene)s, and fullerenes, are still an area of fervent chemical research, and numerous examples of complex and beautiful molecular structures with tunable electronic properties have been synthesized to date, within and across these classes of compounds. The past decade witnessed the field of organic electronics transcending from the area of molecular metals and superconductors to organic light-emitting diodes, photovoltaics, and field-effect transistors, where many molecular semiconducting materials have already been commercialized. The new applications, such as unimolecular electronics and nanotechnology in general, although still in their infancy, have attracted a new generation of organic synthetic chemists to the design of new properties in organic media.

The principles of HOMO−LUMO gap control in organic molecules and synthetic approaches to such systems have been elaborated in this review. Numerous examples of molecular materials with HOMO−LUMO gaps in the range of ~2−0.2 eV were demonstrated. At the same time, the fragility of many of these molecules still stands up as a major limitation toward their application in real-world electronic devices. The issue of stability should become one of the major objectives in the future search for π-functional molecular materials.

5. Glossary

A	π-electron acceptor
BQ	benzoquinone
C_{60}	buckminsterfullerene
CCDC	Cambridge Crystallographic Data Center (http://www.ccdc.cam.ac.uk/)
CCSD	coupled cluster calculations, using single and double substitutions from the Hartree−Fock determinant
CT	charge transfer
CV	cyclic voltammetry
D	π-electron donor
DCM	dichloromethane
DFT	density functional theory
DMF	*N,N*-dimethylformamide
EA	electron affinity
EFISH	electric field induced second harmonic
$E°$	thermodynamic redox potential (for reversible processes determined as the $E^{1/2} = (E_{p.a.} + E_{p.c.})/2$, where p.a. and p.c. are anodic and cathodic peaks, respectively)
E_g	electrochemical HOMO−LUMO gap ($E_g = E°_{1ox} - E°_{1red}$)
FET	field-effect transistor
GC	glassy carbon electrode
HOMO	highest occupied molecular orbital
$h\nu_{ICT}$	optical gap for D−A compounds, determined as the energy of the ICT band in electronic absorption spectra
ICT	intramolecular charge transfer
IP	ionization potential
LB	Langmuir−Blodgett (films, technique)
LED	light-emitting diode
LUMO	lowest unoccupied molecular orbital
MO	molecular orbital
NICS	nucleus independent chemical shifts
NHE	normal hydrogen electrode
NLO	nonlinear optical
ODCB	1,2-dichlorobenzene
OFET	organic field-effect transistor
OLED	organic light-emitting diode
OTFT	organic thin-film field-effect transistor
OVGF	outer valence Green's function
PA	polyacene
PAH	polycyclic aromatic hydrocarbons
PI	pyromellitic diimide
RE	reference electrode
SHG	second-harmonic generation
SCE	saturated calomel electrode
TCNQ	tetracyanoquinodimethane
TCNAQ	11,11,12,12-tetracyano(9,10-anthraquinodimethane)
TFT	thin-film field-effect transistor
THF	tetrahydrofuran
toln	toluene
TTF	tetrathiafulvalene
TTFAQ	9,10-bis(1,3-dithiol-2-ylidene)-9,10-dihydroanthracene (anthracene-TTF)
TTT	5,6,11,12-tetrathiotetracene
UPS	ultraviolet photoelectron spectroscopy

6. Acknowledgments

The UCLA group is indebted to the Office of Naval Research and the Air Force Office for Scientific Research for support. D.F.P. acknowledges support from the National Science and Engineering Research Council of Canada and the Fond de Recherche sur la Nature et les Technologies du Québec.

7. References

(1) Engler, E. M.; Patel, V. V. *J. Am. Chem. Soc*. **1974**, *96*, 7376.
(2) Bechgaard, K.; Cowan, D. O.; Bloch, A. N. *J. Chem. Soc., Chem. Commun.* **1974**, 937.
(3) (a) Lerstrup, K.; Talham, D.; Bloch, A.; Poehler, T.; Cowan, D. *J. Chem. Soc., Chem. Commun.* **1982**, 336. (b) McCullough, R. D.; Kok, G. B.; Lerstrup, K. A.; Cowan, D. O. *J. Am. Chem. Soc.* **1987**, *109*, 4115.
(4) Carroll, P. J.; Lakshmikantham, M. V.; Cava, M. P.; Wudl, F.; Aharon-Shalom, E.; Cox, S. D. *J. Chem. Soc., Chem. Commun.* **1982**, 1316.
(5) Otsubo, T.; Takimiya, K. *Bull. Chem. Soc. Jpn.* **2004**, *77*, 43.
(6) Wudl, F.; Wobschall, D.; Hufnagel, E. J. *J. Am. Chem. Soc.* **1972**, *94*, 670.
(7) Ferraris, J.; Cowan, D. O.; Walatka, V. V., Jr.; Perlstein, J. H. *J. Am. Chem. Soc.* **1973**, *95*, 948.
(8) Bryce, M. R. *Adv. Mater.* **1999**, *11*, 11.
(9) Nielsen, M. B.; Lomholt, C.; Becher, J. *Chem. Soc. Rev.* **2000**, *29*, 153.
(10) Bryce, M. R. *J. Mater. Chem.* **2000**, *10*, 589.
(11) Segura, J. L.; Martín, N. *Angew. Chem., Int. Ed.* **2001**, *40*, 1372.
(12) Hurtley, W. R. H.; Smiles, S. *J. Chem. Soc.* **1926**, 2263.
(13) Prinzbach, H.; Berger, H.; Lüttringhaus, A. *Angew. Chem., Int. Ed. Engl.* **1965**, *4*, 435.
(14) Coffen, D. L.; Chambers, J. Q.; Williams, D. R.; Garrett, P. E.; Canfield, N. D. *J. Am. Chem. Soc.* **1971**, *93*, 2258.
(15) Hünig, S.; Kiesslich, G.; Sceutzow, D.; Zhrandik, R.; Carsky, P. *Int. J. Sulfur Chem., Part C* **1971**, 109.
(16) Wudl, F.; Smith, G. M.; Hufnagel, E. J. *J. Chem. Soc., Chem. Commun.* **1970**, 1453.
(17) Lichtenberger, D. L.; Johnston, R. L.; Hinkelmann, K.; Suzuki, T.; Wudl, F. *J. Am. Chem. Soc.* **1990**, *112*, 3302.
(18) Hunter, E. P.; Lias, S. G. *Chemistry WebBook*; NIST Standard Reference Database http://webbook.nist.gov/chemistry/.
(19) (a) Schukat, G.; Richter, A. M.; Fanghaenel, E. *Sulfur Rep.* **1987**, *7*, 155. (b) Schukat, G.; Fanghaenel, E. *Sulfur Rep.* **1993**, *14*, 245. (c) Schukat, G.; Fanghaenel, E. *Sulfur Rep.* **1995**, *18*, 1.
(20) (a) Simonsen, K. B.; Svenstrup, N.; Lau, J.; Simonsen, O.; Mørk, P.; Kristensen, G. J.; Becher, J. *Synthesis* **1994**, 809. (b) Simonsen, K. B.; Becher, J. *Synlett* **1997**, 1211.
(21) (a) Green, D. C. *J. Org. Chem.* **1979**, *44*, 1476. (b) Garín, J.; Orduna, J.; Uriel, S.; Moore, A. J.; Bryce, M. R.; Wegener, S.; Yufit, D. S.; Howard, J. A. K. *Synthesis* **1994**, 489.
(22) Jeppesen, J. O.; Becher, J. *Eur. J. Org. Chem*. **2003**, 3245.
(23) Jigami, T.; Takimiya, K.; Otsubo, T. *J. Org. Chem.* **1998**, *63*, 8865.
(24) Schukat, G.; Fanghaenel, E. *J. Prakt. Chem.* **1979**, *321*, 675.
(25) Fanghänel, E.; van Hinh, L.; Schukat, G. *J. Prakt. Chem.* **1993**, *335*, 599.
(26) (a) Lahlil, K.; Moradpour, A.; Bowlas, C.; Menou, F.; Cassoux, P.; Bonvoisin, J.; Launay, J.-P.; Dive, C.; Dehareng, D. *J. Am. Chem. Soc.* **1995**, *117*, 9995. (b) Fanghänel, E.; Alsleben, I.; Gebler, B.; Herrmann, A.; Herrmann, R.; Palmer, T.; Strunk, K.; Ullrich, A. *Phosphorus, Sulfur Silicon Relat. Elem.* **1997**, *120*, 121.
(27) Watson, W. H.; Eduok, E. E.; Kashyap, R. P.; Krawiec, M. *Tetrahedron* **1993**, *49*, 3035.
(28) Frenzel, S.; Baumgarten, M.; Müllen, K. *Synth. Met*. **2001**, *118*, 97.
(29) Siquot, Y.; Frère, P.; Nozdryn, T.; Cousseau, J.; Sallé, M.; Jubault, M.; Orduna, J.; Garín, J.; Gorgues, A. *Tetrahedron Lett.* **1997**, *38*, 1919.
(30) Chen, W.; Cava, M. P.; Takassi, M. A.; Metzger, R. M. *J. Am. Chem. Soc.* **1988**, *110*, 7903.
(31) Jeppesen, J. O.; Takimiya, K.; Jensen, F.; Brimert, T.; Nielsen, K.; Thorup, N.; Becher, J. *J. Org. Chem.* **2000**, *65*, 5794.
(32) Rovira, C.; Veciana, J.; Santaló, N.; Tarrés, J.; Cirujeda, J.; Molins, E.; Llorca, J.; Espinosa, E. *J. Org. Chem.* **1994**, *59*, 3307.
(33) Ketcham, R.; Hörnfeldt, A.B.; Gronowitz, S. *J. Org. Chem.* **1984**, *49*, 1117.
(34) (a) Mas-Torrent, M.; Durkut, M.; Hadley, P.; Ribas, X.; Rovira, C. *J. Am. Chem. Soc.* **2004**, *126*, 984. (b) Mas-Torrent, M.; Hadley, P.; Bromley, S. T.; Ribas, X.; Tarrés, J.; Mas, M.; Molins, E.; Veciana, J.; Rovira, C. *J. Am. Chem. Soc.* **2004**, *126*, 8546.
(35) (a) Sato, M.; Gonnella, N. C.; Cava, M. P. *J. Org. Chem.* **1979**, *44*, 930. (b) Sugimoto, T.; Awaji, H.; Sugimoto, I.; Misaki, Y.; Yoshida, Z.-I. *Synth. Met.* **1987**, *19*, 569.
(36) (a) Hansen, T. K.; Lakshmikantham, M. V.; Cava, M. P.; Metzger, R. M.; Becher, J. *J. Org. Chem.* **1991**, *56*, 2720. (b) Moore, A. J.; Bryce, M. R.; Ando, D. J.; Hursthouse, M. B. *J. Chem. Soc., Chem. Commun.* **1991**, 320.
(37) Roncali, J. *J. Mater. Chem.* **1997**, *7*, 2307.
(38) Frank, W.; Gompper, R. *Tetrahedron Lett.* **1987**, *28*, 3083.
(39) Khan, T.; Skabara, P. J.; Frère, P.; Allain, M.; Coles, S. J.; Hursthouse, M. B. *Tetrahedron Lett.* **2004**, *45*, 2535.
(40) Takahashi, K.; Nihira, T. *Tetrahedron Lett.* **1989**, *30*, 5903.
(41) (a) Hansen, T. K.; Lakshmikantham, M. V.; Cava, M. P.; Niziurski-Mann, R. E.; Jensen, F.; Becher, J. *J. Am. Chem. Soc.* **1992**, *114*, 5035. (b) Benahmed-Gasmi, A. S.; Frère, P.; Garrigues, B.; Gorgues, A.; Jubault, M.; Carlier, R.; Texier, F. *Tetrahedron Lett.* **1992**, *33*, 6457.
(42) Frère, P.; Allain, M.; Elandaloussi, E. H.; Levillain, E.; Sauvage, F.-X.; Riou, A.; Roncali, J. *Chem. Eur. J.* **2002**, *8*, 784.
(43) Elandaloussi, E.; Frère, P.; Roncali, J. *Tetrahedron Lett.* **1996**, *37*, 6121.
(44) Guerro, M.; Carlier, R.; Boubekeur, K.; Lorcy, D.; Hapiot, P. *J. Am. Chem. Soc.* **2003**, *125*, 3159.
(45) Martín, N.; Orti, E. In *Handbook of Advanced Electronic and Photonic Materials and Devices*; Nalwa, H. S., Ed.; John Wiley & Sons: New York, 2000; Vol. 3, p 245.
(46) Yamashita, Y.; Kobayashi, Y.; Miyashi, T. *Angew. Chem., Int. Ed. Engl.* **1989**, *28*, 1052.
(47) Ueno, Y.; Bahry, M.; Okawara, M. *Tetrahedron Lett.* **1977**, 4607.
(48) Sato, M.; Laksmikantham, M. V.; Cava, M. P.; Garito, A. F. *J. Org. Chem.* **1978**, *43*, 2084.
(49) Bryce, M. R.; Moore, A. J. *Tetrahedron Lett.* **1988**, *29*, 1075.
(50) Akiba, K.; Ishikawa, K.; Inamoto, N. *Bull. Chem. Soc. Jpn.* **1978**, *51*, 2674.
(51) Bryce, M. R.; Moore, A. J. *Synth. Met.* **1988**, *25*, 203.
(52) Saito, K.; Sugiura, C.; Tanimoto, E.; Saito, K.; Yamashita, Y. *Heterocycles* **1994**, *38*, 2153.
(53) Moore, A. J.; Bryce, M. R. *Synthesis* **1991**, 26.
(54) Bryce, M. R.; Coffin, M. A.; Hursthouse, M. B.; Karaulov, A. I.; Müllen, K.; Scheich, H. *Tetrahedron Lett.* **1991**, *32*, 6029.
(55) As registered in major databases such as Beilstein and Chemical Abstracts.
(56) However, a reversible two-electron oxidation of TTFAQ was occasionally observed at low scan rates in highly polar solvents, e.g., for **11a** on Au (but not on Pt or glassy carbon electrodes): Liu, S.-C.; Perèz, I.; Martín, N.; Echegoyen, L. *J. Org. Chem.* **2000**, *65*, 9092.
(57) Moore, A. J.; Bryce, M. R. *J. Chem. Soc., Perkin Trans. 1* **1991**, 157.
(58) Bryce, M. R.; Moore, A. J.; Hasan, M.; Ashwell, G. J.; Frraser, A. T.; Clegg, W.; Hursthouse, M. B.; Karaulov, A. I. *Angew. Chem., Int. Ed. Engl.* **1990**, *29*, 1450.
(59) Kai, H.; Evans, D. H. *J. Electroanal. Chem.* **1997**, *423*, 29.
(60) Perepichka, D. F.; Bryce, M. R.; Perepichka, I. F.; Lyubchik, S. B.; Godbert, N.; Christensen, C. A.; Batsanov, A. S.; Levillain, E.; McInnes, E. J. L.; Zhao, J. P. *J. Am. Chem. Soc.* **2002**, *124*, 14227.
(61) (a) Triki, S.; Ouahab, L.; Lorcy, D.; Robert, A. *Acta Crystallogr., C* **1993**, *49*, 1189. (b) Bryce, M. R.; Finn, T.; Batsanov, A. S.; Kataky, R.; Howard, J. A. K.; Lyubchik, S. B. *Eur. J. Org. Chem.* **2000**, 1199.
(62) Jones, A. E.; Christensen, C. A.; Perepichka, D. F.; Batsanov, A. S.; Beeby, A.; Low, P. J.; Bryce, M. R.; Parker, A. W. *Chem. Eur. J.* **2001**, *7*, 973.
(63) Guldi, D. M.; Sánchez, L.; Martín, N. *J. Phys. Chem. B* **2001**, *105*, 7139.
(64) Martín, N.; Sánchez, L.; Seoane, C.; Ortí, E.; Viruela, P. M.; Viruela, R. *J. Org. Chem.* **1998**, *63*, 1268.
(65) Tsuda, A.; Osuka, A. *Science* **2001**, *293*, 79.
(66) (a) Le Paillard, M. P.; Robert, A.; Garrigou-Lagrange, C.; Delhaes, P.; Le Maguerès, P.; Ouahab, L.; Toupet, L. *Synth. Met.* **1993**, *58*, 223. (b) Khodorkovsky, V.; Becker, J. Y. In *Organic Conductors. Fundamentals and Applications*; Farges, J.-P., Ed.; Marcel Dekker: New York−London−Hong Kong, 1994; p 75. (c) Yamashita, Y.; Tomura, M. *J. Mater. Chem.* **1998**, *8*, 1933.
(67) Dumur, F.; Gautier, N.; Gallego-Planas, N.; Sahin, Y.; Levillain, E.; Mercier, N.; Hudhomme, P.; Masino, M.; Girlando, A.; Lloveras, V.; Vidal-Gancedo, J.; Veciana, J.; Rovira, C. *J. Org. Chem.* **2004**, *69*, 2164−2177.
(68) Frenzel, S.; Müllen, K. *Synth. Met.* **1996**, *80*, 175.
(69) Gautier, N.; Mercier, N.; Riou, A.; Gorgues, A.; Hudhomme, P. *Tetrahedron Lett.* **1999**, *40*, 5997.
(70) Christensen, C. A.; Bryce, M. R.; Batsanov, A. S.; Howard, J. A. K.; Jeppesen, J. O.; Becher, J. *Chem. Commun.* **1999**, 2433.
(71) Coffin, M. A.; Bryce, M. R.; Clegg, W. *J. Chem. Soc., Chem. Commun.* **1992**, 401.
(72) Aqad, E.; Ellern, A.; Shapiro, L.; Khodorkovsky, V. *Tetrahedron Lett.* **2000**, *41*, 2983.
(73) Neilands, O.; Belyakov, S.; Tilika, V.; Edžina, A. *J. Chem. Soc., Chem. Commun.* **1995**, 325.
(74) Andreu, R.; de Lucas, A. I.; Garín, J.; Martín, N.; Orduna, J.; Sánchez, L.; Seoane, C. *Synth. Met.* **1997**, *86*, 1817.
(75) González, M.; Segura, J. L.; Seoane, C.; Martín, N.; Garín, J.; Orduna, J.; Alcalá, R.; Villacampa, B.; Hernández, V.; Navarrete, J. T. L. *J. Org. Chem.* **2001**, *66*, 8872.
(76) Bryce, M. R.; Green, A.; Moore, A. J.; Perepichka, D. F.; Batsanov, A. S.; Howard, J. A. K.; Ledoux-Rak, I.; González, M.; Martín, N.; Segura, J. L.; Garín, J.; Orduna, J.; Alcalá, R.; Villacampa, B. *Eur. J. Org. Chem.* **2001**, 1927.

(77) González, M.; Martín, N.; Segura, J. L.; Seoane, C.; Garín, J.; Orduna, J.; Alcalá, R.; Sánchez, C.; Villacampa, B. *Tetrahedron Lett.* **1999**, *40*, 8599.
(78) Garín, J.; Orduna, J.; Rupérez, J. I.; Alcalá, R.; Villacampa, B.; Sánchez, C.; Martín, N.; Segura, J. L.; Gonzalez, M. *Tetrahedron Lett.* **1998**, *39*, 3577.
(79) Hansen, J. A.; Becher, J.; Jeppesen, J. O.; Levillain, E.; Nielsen, M. B.; Petersen, B. M.; Petersen, J. C.; Şahin, Y. *J. Mater. Chem.* **2004**, *14*, 179.
(80) Pérez, I.; Liu, S.-G.; Martín, N.; Echegoyen, L. *J. Org. Chem.* **2000**, *65*, 3796.
(81) Herranz, M. A.; Martín, N.; Sanchez, L.; Garín, J.; Orduna, J.; Alcalá, R.; Villacampa, B.; Sánchez, C. *Tetrahedron* **1998**, *54*, 11651.
(82) Otero, M.; Herranz, M. A.; Seoane, C.; Martín, N.; Garín, J.; Orduna, J.; Alacalá, R.; Villacampa, B. *Tetrahedron* **2002**, *58*, 7463.
(83) *Nonlinear Optics of Organic Molecules and Polymers*; Nalwa, H. S., Miyata, S., Eds.; CRC Press: Boca Raton−New York, 1997.
(84) Tanaka, H.; Okano, Y.; Kobayashi, H.; Suzuki, W.; Kobayashi, A. *Science* **2001**, *291*, 285.
(85) Cassox, P.; Valade, L.; Kobayashi, H.; Kobayashi, A.; Clark, R. A.; Underhill, A. E. *Coord. Chem. Rev.* **1991**, *110*, 115.
(86) Engler, E. M.; Patel, V. V.; Schumaker, R. R. *J. Chem. Soc., Chem. Commun.* **1979**, 184.
(87) Fujiwara, E.; Kobayashi, A.; Kobayashi, H. *Synth. Met.* **2003**, *135−136*, 535.
(88) Ueda, K.; Goto, M.; Sugimoto, T.; Endo, S.; Toyota, N.; Yamamoto, K.; Fujita, H. *Synth. Met.* **1997**, *85*, 1679.
(89) Ueda, K.; Goto, M.; Iwamatsu, M.; Sugimoto, T.; Endo, S.; Toyota, N.; Yamamoto, K.; Fujita, H. *J. Mater. Chem.* **1998**, *8*, 2195.
(90) Tanaka, H.; Kobayashi, H.; Kobayashi, A. *Synth. Met.* **2003**, *135−136*, 549.
(91) Le Narvor, N.; Rebrtson, N.; Wallace, E.; Kilburn, J. D.; Underhill, A. E.; Bartlett, P. N.; Webster, M. *J. Chem. Soc., Dalton Trans.* **1996**, 823.
(92) Kobayashi, A.; Suzuki, W.; Fujiwara, E.; Tanaka, H.; Fujishiro, Y.; Nishibori, E.; Takata, M.; Sakata, M.; Okanao, Y.; Kobayashi, H. *Synth. Met.* **2003**, *135−136*, 511.
(93) Bian, G.-Q.; Dai, J.; Zhu, Q.-Y.; Yang, W.; Yan, Z.-M.; Munakata, M.; Maekawa, M. *Chem. Commun.* **2002**, 1474.
(94) McCullough, R. D.; Belot, J. A.; Rheingold, A. L.; Yap, G. P. A. *J. Am. Chem. Soc.* **1995**, *117*, 9913.
(95) Liu, S.-X.; Dolder, S.; Franz, P.; Neels, A.; Stoeckli-Evans, H.; Decurtins, S. *Inorg. Chem.* **2003**, *42*, 4801.
(96) Yoneda, T.; Kamata, Y.; Ueda, K.; Sugimoto, T.; Tada, T.; Shiro, M.; Yoshino, H.; Murata, K. *Synth. Met.* **2003**, *135−136*, 573.
(97) Kubo, K.; Nakano, M.; Tamura, H.; Matsubayashi, G.; Nakamoto, M. *J. Organomet. Chem.* **2003**, *669*, 141.
(98) Kobayashi, A.; Sasa, M.; Suzuki, W.; Fujiwara, E.; Tanaka, H.; Tokumoto, M.; Okano, Y.; Fijiwara, H.; Kobayashi, H. *J. Am. Chem. Soc.* **2004**, *126*, 426.
(99) Kumasaki, M.; Tanaka, H.; Kobayashi, A. *J. Mater. Chem.* **1998**, *8*, 301.
(100) Kobayashi, A.; Tanaka, H.; Kumasaki, M.; Torii, H.; Narymbetov, B.; Adachi, T. *J. Am. Chem. Soc.* **1999**, *121*, 10763.
(101) Aviram, A.; Ratner, M. *Chem. Phys. Lett.* **1974**, *29*, 277.
(102) For a recent review on molecular rectification, see: Metzger, R. M. *Chem. Rev.* **2003**, *103*, 3803.
(103) Stokbro, K.; Taylor, J.; Brandbyge, M. *J. Am. Chem. Soc.* **2003**, *125*, 3674.
(104) Le Paillard, M. P.; Robert, A. *Bull. Soc. Chim. Fr.* **1992**, *129*, 205.
(105) Goldenberg, L. M.; Becker, J. Y.; Paz-Tal Levi, O.; Khodorkovsky, V. Y.; Bryce, M. R.; Petty, M. C. *J. Chem. Soc., Chem. Commun.* **1995**, 475.
(106) Simonsen, K. B.; Zong, K.; Rogers, R. D.; Cava, M. P.; Becher, J. *J. Org. Chem.* **1997**, *62*, 679.
(107) Simonsen, K. B.; Thorup, N.; Cava, M. P.; Becher, J. *Chem. Commun.* **1998**, 901.
(108) Ploug-Sørensen, A.; Nielsen, M. B.; Becher, J. *Tetrahedron Lett.* **2003**, *44*, 2979.
(109) Nielsen, M. B.; Nielsen, S. B.; Becher, J. *Chem. Commun.* **1998**, 475.
(110) Collier, C. P.; Mattersteig, G.; Wong, E. W.; Luo, Y.; Beverly, K.; Sampaio, J.; Raymo, F. M.; Stoddart, J. F.; Heath, J. R. *Science* **2000**, *289*, 1172.
(111) Nielsen, M. B.; Lomholt, C.; Becher, J. *Chem. Soc. Rev.* **2000**, *29*, 153.
(112) Nielsen, M. B.; Hansen, J. G.; Becher, J. *Eur. J. Org. Chem.* **1999**, 2807.
(113) Hamilton, D. G.; Montalti, M.; Prodi, L.; Fontani, M.; Zanello, P.; Sanders, J. K. M. *Chem. Eur. J.* **2000**, *6*, 608.
(114) Hansen, J. G.; Bang, K. S.; Thorup, N.; Becher, J. *Eur. J. Org. Chem.* **2000**, 2135.
(115) Guo, X.; Zhang, D.; Xu, W.; Zhu, D. *Synth. Met.* **2003**, *137*, 981.
(116) Guo, X.; Zhang, D.; Zhang, H.; Fan, Q.; Xu, W.; Ai, X.; Fan, L.; Zhu, D. *Tetrahedron* **2003**, *59*, 4843.
(117) Blower, M. A.; Bryce, M. R.; Devonport, W. *Adv. Mater.* **1996**, *8*, 63.
(118) Wang, C.; Bryce, M. R.; Batsanov, A. S.; Stanley, C. F.; Beeby, A.; Howard, J. A. K. *J. Chem. Soc., Perkin Trans. 2* **1997**, 1671.
(119) Cook, M. J.; Cooke, G.; Jafari-Fini, A. *Chem. Commun.* **1996**, 1925.
(120) Wang, C.; Bryce, M. R.; Batsanov, A. S.; Howard, J. A. K. *Chem. Eur. J.* **1997**, *3*, 1679.
(121) Farren, C.; Christensen, C. A.; FitzGerald, S.; Bryce, M. R.; Beeby, A. *J. Org. Chem.* **2002**, *67*, 9130.
(122) Li, H.; Jeppesen, J. O.; Levillain, E.; Becher, J. *Chem. Commun.* **2003**, 846.
(123) Zhang, G.; Zhang, D.; Guo, X.; Zhu, D. *Org. Lett.* **2004**, *6*, 1209.
(124) Becher, J.; Brimert, T.; Jeppesen, J. O.; Pedersen, J. Z.; Zubarev, R.; Bjørnholm, T.; Reitzel, N.; Jensen, T. R.; Kjaer, K.; Levillain, E. *Angew. Chem., Int. Ed.* **2001**, *40*, 2497.
(125) For a review on TCNQ acceptors, see: Martín, N.; Segura, J. L.; Seoane, C. *J. Mater. Chem.* **1997**, *7*, 1661.
(126) Panetta, C. A.; Heimer, N. E.; Hussey, C. L.; Metzger, R. M. *Synlett* **1991**, 301.
(127) Hertler, W. R. *J. Org. Chem.* **1976**, *41*, 1412.
(128) Panetta, C. A.; Baghdadchi, J.; Metzger, R. M. *Mol. Cryst. Liq. Cryst.* **1984**, *107*, 103.
(129) de Miguel, P.; Bryce, M. R.; Goldenberg, L. M.; Beeby, A.; Khodorkovsky, V.; Shapiro, L.; Niemz, A.; Cuello, A. O.; Rotello, V. *J. Mater. Chem.* **1998**, *8*, 71.
(130) Perepichka, D. F.; Bryce, M. R.; Batsanov, A. S.; Howard, J. A. K.; Cuello, A. O.; Gray, M.; Rotello, V. M. *J. Org. Chem.* **2001**, *66*, 4517.
(131) Herranz, M. A.; González, S.; Pérez, I.; Martín, N. *Tetrahedron* **2001**, *57*, 725.
(132) (a) Segura, J. L.; Martín, N.; Seoane, C.; Hanack, M. *Tetrahedron Lett.* **1996**, *37*, 2503. (b) González, M.; Illescas, B.; Martín, N.; Segura, J. L.; Seoane, C.; Hanack, M. *Tetrahedron* **1998**, *54*, 2853.
(133) Tsiperman, E.; Regev, T.; Becker, J.; Bernstein, J.; Ellern, A.; Khodorkovsky, V.; Shames, A.; Shapiro, L. *Chem. Commun.* **1999**, 1125.
(134) Moriarty, R. M.; Tao, A.; Gilardi, R.; Song, Z.; Tuladhar, S. M. *Chem. Commun.* **1998**, 157.
(135) Scheib, S.; Cava, M. P.; Baldwin, J. W.; Metzger, R. M. *J. Org. Chem.* **1998**, *63*, 1198.
(136) Scheib, S.; Cava, M. P.; Baldwin, J. W.; Metzger, R. M. *Thin Solid Films* **1998**, *327−329*, 100.
(137) Perepichka, D. F.; Bryce, M. R.; Pearson, C.; Petty, M. C.; McInnes, E. J. L.; Zhao, J. P. *Angew. Chem., Int. Ed.* **2003**, *42*, 4635.
(138) Perepichka, I. F.; Kuz'mina, L. G.; Perepichka, D. F.; Bryce, M. R.; Goldenberg, L. M.; Popov, A. F.; Howard, J. A. K. *J. Org. Chem.* **1998**, *63*, 6484 and references therein.
(139) (a) Perepichka, D. F.; Bryce, M. R.; McInnes, E. J. L.; Zhao, J. P. *Org. Lett.* **2001**, *3*, 1431. (b) Perepichka, D. F.; Bryce, M. R.; Batsanov, A. S.; McInnes, E. J. L.; Zhao, J. P.; Farley, R. D. *Chem. Eur. J.* **2002**, *8*, 4656.
(140) Zheng, Z.-R.; Evans, D. H. *J. Am. Chem. Soc.* **1999**, *121*, 2941.
(141) Kroto, H. W.; Heath, J. R.; O'Brien, S. C.; Curl, R. F.; Smalley, R. E. *Nature* **1985**, *318*, 162.
(142) Margadonna, S.; Prassides, K. *J. Solid State Commun.* **2002**, *168*, 639. Margadonna, S.; Prassides, K. In *Organic Conductors, Superconductors and Magnets: From Synthesis to Molecular Electronics*; Ouhab, L., Yagubskii, E., Eds.; NATO Science Series II. Mathematics, Physics and Chemistry; Kluwer Academic Publisher: Dordrecht−Boston−London, 2004; Vol. 139, p 157.
(143) Brabec, C. J.; Sariciftci, N. S.; Hummelen, J. C. *Adv. Funct. Mater.* **2001**, *11*, 15.
(144) Wudl, F. *J. Mater. Chem.* **2002**, *12*, 1959.
(145) Haddon, R. C. *Science* **1993**, *261*, 1545.
(146) Ajie, H.; Alvarez, M. M.; Anz, S. J.; Beck, R. D.; Diedrich, F.; Fostiropoulos, K.; Huffman, D. R.; Krätschmer, W.; Rubin, Y.; Schriver, K. E.; Sensharama, D.; Whetten, R. L. *J. Phys. Chem.* **1990**, *94*, 8630.
(147) Bruno, C.; Doubitski, I.; Marcaccio, M.; Paolucci, F.; Paolucci, D.; Zaopo, A. *J. Am. Chem. Soc.* **2003**, *125*, 15738.
(148) Allemand, P.-M.; Koch, A.; Wudl, F.; Rubin, Y.; Diedrich, F.; Alvarez, M. M.; Anz, S. J.; Whetten, R. L. *J. Am. Chem. Soc.* **1991**, *113*, 1050.
(149) Xie, Q.; Pèrez-Cordero, E.; Echegoyen, L. *J. Am. Chem. Soc.* **1992**, *114*, 3978.
(150) Review: Martín, N.; Sánchez, L.; Illescas, B.: Pèrez, I. *Chem. Rev.* **1998**, *98*, 2527.
(151) (a) Wudl, F. *Acc. Chem. Res.* **1992**, *25*, 157. (b) Hirsch, A. *Top. Curr. Chem.* **1999**, *199*, 1. (c) Yurovskaya, M. A.; Trushkov, I. V. *Russ. Chem. Bull. Int. Ed.* **2000**, *51*, 367.
(152) Prato, M.; Maggini, M.; Giacometti, C.; Scorrano, G.; Sandonà, G.; Farnia, G. *Tetrahedron* **1996**, *52*, 5221.
(153) Martín, N.; Sánchez, L.; Seoane, C.; Andreu, R.; Garín, J.; Orduna, J. *Tetrahedron Lett.* **1996**, *37*, 5979.
(154) Martín, N.; Sánchez, L.; Herranz, M. A.; Guldi, D. M. *J. Phys. Chem. A* **2000**, *104*, 4648.

(155) Simonsen, K. B.; Konovalov, V. V.; Konovalova, T. A.; Kawai, T.; Cava, M. P.; Kispert, L. D.; Metzger, R. M.; Becher, J. *J. Chem. Soc., Perkin Trans. 2* **1999**, 657.
(156) Guldi, D. M.; González, S.; Martín, N.; Antón, A.; Garín, J.; Orduna, J. *J. Org. Chem.* **2000**, *65*, 1978.
(157) Allard, E.; Delaunay, J.; Cheng, F.; Cousseau, J.; Orduna, J.; Garín, J. *Org. Lett.* **2001**, *22*, 3503.
(158) Llacay, J.; Mas, M.; Molins, E.; Veciana, J.; Powell, D.; Rovira, C. *Chem. Commun.* **1997**, 659.
(159) Llacay, J.; Veciana, J.; Vidal-Gancedo, J.; Bourdelande, J. L.; González-Moreno, R.; Rovira, C. *J. Org. Chem.* **1998**, *63*, 5201.
(160) (a) Boulle, C.; Rabreau, J. M.; Hudhomme, P.; Cariou, M.; Jubault, M.; Gorgues, A.; Orduna, J.; Garín, J. *Tetrahedron Lett.* **1997**, *38*, 3909. (b) Hudhomme, P.; Boulle, C.; Rabreau, J. M.; Cariou, M.; Jubault, M.; Gorgues, A. *Synth. Met.* **1998**, *94*, 73.
(161) Kreher, D.; Cariou, M.; Liu, S.-G.; Levillain, E.; Veciana, J.; Rovira, C.; Gorgues, A.; Hudhomme, P. *J. Mater. Chem.* **2002**, *12*, 2137.
(162) Liu, S.-G.; Echegoyen, L. *Eur. J. Org. Chem.* **2000**, 1157.
(163) Ravaine, S.; Delhaès, P.; Leriche, P.; Sallé, M. *Synth. Met.* **1997**, *87*, 93.
(164) Zeng, P.; Liu, Y.; Zhang, D.; Yang, C.; Li, Y.; Zhu, D. *J. Phys. Chem. Solids* **2000**, *61*, 1111.
(165) Keshavarz-K, M.; Knight, B.; Haddon, R. C.; Wudl, F. *Tetrahedron* **1996**, *52*, 5149.
(166) Herranz, M. A.; Illescas, B.; Martín, N.; Luo, C.; Guldi, D. M. *J. Org. Chem.* **2000**, *65*, 5728.
(167) Segura, J. L.; Priego, E. M.; Martín, N. *Tetrahedron Lett.* **2000**, *41*, 7737.
(168) Segura, J. L.; Priego, E. M.; Martín, N.; Luo, C.; Guldi, D. M. *Org. Lett.* **2000**, *2*, 4021.
(169) Ellenbogen, J. C.; Love, J. C. *Proc. IEEE* **2000**, *88*, 386.
(170) Martín, N.; Pérez, I.; Sánchez, L.; Seoane, C. *J. Org. Chem.* **1997**, *62*, 5690.
(171) Herranz, M. A.; Martín, N.; Sánchez, L.; Seoane, C.; Guldi, D. M. *J. Organomet. Chem.* **2000**, *599*, 2.
(172) Sánchez, L.; Pérez, I.; Martín, N.; Guldi, D. *Chem. Eur. J.* **2003**, *9*, 2457.
(173) Herranz, M. A.; Martín, N. *Org. Lett.* **1999**, *1*, 2005.
(174) Martín, N.; Sánchez, L.; Guldi, D. M. *Chem. Commun.* **2000**, 113.
(175) González, S.; Martín, N.; Swartz, A.; Guldi, D. M. *Org. Lett.* **2003**, *5*, 557.
(176) Herranz, M. A.; Martín, N.; Ramey, J.; Guldi, D. M. *Chem. Commun.* **2002**, 2968.
(177) González, S.; Martín, N.; Guldi, D. *J. Org. Chem.* **2003**, *68*, 779.
(178) Liddell, P. A.; Kodis, G.; de la Garza, L.; Bahr, J. L.; Moore, A. L.; Moore, T. A.; Gust, D. *Helv. Chim. Acta* **2001**, *84*, 2765.
(179) Kodis, G.; Liddell, P. A.; de la Garza, L.; Moore, A. L.; Moore, T. A.; Gust, D. *J. Mater. Chem.* **2002**, *12*, 2100.
(180) Keshavarz-K, M.; Knight, B.; Srdanov, G.; Wudl, F. *J. Am. Chem. Soc.* **1995**, *117*, 11371.
(181) Taylor, R. *Chem. Eur. J.* **2001**, *7*, 4075.
(182) Yoshida, Y.; Otsuka, A.; Drozdova, O. O.; Saito, G. *J. Am. Chem. Soc.* **2000**, *122*, 7244.
(183) Liu, N.; Touhara, H.; Morio, Y.; Komichi, D.; Okino, F.; Kawasaki, S. *J. Electrochem. Soc.* **1996**, *143*, L216.
(184) Zhou, F.; Van Berkel, G. J.; Donovan, B. T. *J. Am. Chem. Soc.* **1994**, *116*, 5485.
(185) Translations of the redox potentials between different reference electrodes are not always accurate. The reduction potential of $C_{60}F_{48}$ was reported to be only 0.02 V more positive than that of $C_{60}F_{46}$ (see ref 155, Table 7).
(186) Ohkubo, K.; Taylor, R.; Boltalina, O. V.; Ogo, S.; Fukuzumi, S. *Chem. Commun.* **2002**, 1952.
(187) Burley, G. A.; Avent, A. G.; Boltalina, O. V.; Gol'dt, I. V.; Guldi, D. M.; Marcaccio, M.; Paolucci, F.; Paolucci, D.; Taylor, R. *Chem. Commun.* **2003**, 148.
(188) Clar, E. *Polycyclic Hydrocarbons*; Academic Press: London, 1964; Vols. 1 and 2.
(189) Havey, R. G. *Polycyclic Aromatic Hydrocarbons*; Wiley-VCH: New York, 1997.
(190) Chung, D. D. L. *J. Mater. Sci.* **2002**, *37*, 1475.
(191) Iijima, S.; Ichihashi, T. *Nature* **1993**, *363*, 603.
(192) For a short overview, see: Geerts, Y.; Klärner, G.; Müllen, K. In *Electronic Materials: The Oligomer Approach*; Müllen, K., Wagner, G., Eds.; Wiley-VCH: Weinheim, Germany, 1998; p 48.
(193) For a short overview of polyacenes as a part of a discussion on ladder polymers, see: Roncali, J. *Chem. Rev.* **1997**, *97*, 173.
(194) Dimitrakopoulos, C. D.; Malenfant, P. R. L. *Adv. Mater.* **2002**, *14*, 99.
(195) Dimitrakopoulos, C. D.; Mascaro, D. J. *IBM J. Res. Dev.* **2001**, *45*, 11.
(196) Faraday, M. *Philos. Trans. R. Soc. London* **1825**, 440. See also: Schleyer, P. v. R. *Chem. Rev.* **2001**, *101*, 1115.
(197) See the special issue on aromaticity in: *Chem. Rev.* **2001**, *101*, 1115−1566.
(198) For a discussion of aromaticity in acenes, see: Krygowski, T. M.; Cyrański, M. K. *Chem. Rev.* **2001**, *101*, 1385.
(199) For a discussion of aromaticity in large PAH, see: Watson, M. D.; Fechtenkötter, A.; Müllen, K. *Chem. Rev.* **2001**, *101,* 1267.
(200) Schleyer, P. v. R.; Manoharan, M.; Jiao, H.; Stahl, F. *Org. Lett.* **2001**, *3*, 3643.
(201) Angliker, H.; Rommel, E.; Wirz, J. *Chem. Phys. Lett.* **1982**, *87*, 208.
(202) (a) Honer, A. *Polycyclic aromatic hydrocarbon (PAH) metabolite*; Technische Universitat Berlin: Berlin, 2001; pp 99−121. (b) Harayama, S. *Curr. Opin. Biotechnol.* **1997**, *8*, 268.
(203) Schön, J. H.; Kloc, C.; Batlogg, B. *Nature* **2000**, *406*, 702. For a retraction, see: *Nature* **2003**, *422*, 93.
(204) Schön, J. H.; Berg, S.; Kloc, C.; Batlogg, B. *Science* **2000**, *287*, 1022. For a retraction, see: *Science* **2002**, *298*, 961.
(205) Schön, J. H.; Kloc, C.; Dodabalapur, A.; Batlogg, B. *Science* **2000**, *289*, 599. For a retraction, see: *Science* **2002**, *298*, 961.
(206) Schön, J. H.; Kloc, C.; Batlogg, B. *Science* **2000**, *288*, 2338. For a retraction, see: *Science* **2002**, *298*, 961.
(207) For a complete list of retracted papers in *Science* and *Nature*, see: *Science* **2002**, *298*, 961; *Nature* **2003**, *422*, 93.
(208) Beasley, M. R.; Datta, S.; Kogelnik, H.; Kroemer, H.; Monroe, D. *Report of the Investigation Committee on the Possibility of Scientific Misconduct in the Work of Hendrik Schön and Coauthors*; http://publish.aps.org/reports/ (doi: 10.1103/aps.reports.lucent); Lucent Technologies/American Physical Society: September 2002.
(209) See also: www.lucent.com/news_events/researchreview.html.
(210) Representative syntheses of pentacene and its derivatives: (a) Luo, J.; Hart, H. *J. Org. Chem.* **1987**, *52*, 4833. (b) Satchell, M. P.; Stacey, B. E. *J. Chem. Soc.* **1971**, 468. (c) Laquindanum, J. G.; Katz, H. E.; Lovinger, A. J. *J. Am. Chem. Soc.* **1998**, *120*, 664. (d) Wartini, A. R.; Staab, H. A.; Neugebauer, F. A. *Eur. J. Org. Chem.* **1998**, 1161.
(211) Goldfinger, M. B.; Crawford, K. B.; Swager, T. M. *J. Am. Chem. Soc.* **1997**, *119*, 4578. Goldfinger, M. B.; Crawford, K. B.; Swager, T. M. *J. Org. Chem.* **1998**, *63*, 1676. Goldfinger, M. B.; Swager, T. M. *J. Am. Chem. Soc.* **1994**, *116*, 7895 and references therein.
(212) Clar, E.; John, F. *Chem. Ber.* **1929**, *62*, 3027. Clar, E.; John, F. *Chem. Ber.* **1930**, *63*, 2987. Clar, E.; John, F. *Chem. Ber.* **1931**, *64*, 2194.
(213) Goodings, E. P.; Mitchard, D. A.; Owen, G. *J. Chem. Soc., Perkin Trans. 1* **1972**, *11*, 1310.
(214) Bailey, W. J.; Madoff, M. *J. Am. Chem. Soc.* **1953**, *75*, 5603.
(215) Marschalk, Ch. *Bull. Soc. Chim.* **1939**, *6*, 1112.
(216) Clar, E. *Chem. Ber.* **1939**, *72B*, 2137.
(217) Bailey, W. J.; Liaio, C.-W. *J. Am. Chem. Soc.* **1955**, *77*, 992.
(218) (a) Stacey, B. E.; Satchell, M. P. *J. Chem. Soc. C: Org.* **1971**, *3*, 468. (b) Lang, K. F.; Zander, M. *Chem. Ber.* **1963**, *96*, 707.
(219) Clar, E. *Chem. Ber.* **1942**, *75B*, 1283.
(220) See ref 188, Vol. 1, p 460.
(221) Clar, E. *Chem. Ber.* **1942**, *75B*, 1330.
(222) See also: Marschalk, Ch. *Bull. Soc. Chim.* **1943**, *10*, 511.
(223) (a) Boggiano, B.; Clar, E. *J. Chem. Soc.* **1957**, 2681. (b) Also see: ref 220.
(224) Notario, R.; Abbound, J.-L. M. *J. Phys. Chem. A* **1998**, *102*, 5290.
(225) (a) Duong, H. Ph.D. Thesis, University of California, Los Angeles, 2003. (b) Fang, T. Ph.D. Thesis, University of California, Los Angeles, 1986.
(226) Biermann, D.; Schmidt, W. J. *J. Am. Chem. Soc.* **1980**, *102*, 3163.
(227) (a) Dresselhaus, M. S.; Dresselhaus, G.; Eklund, P. C. *Science of Fullerenes and Carbon Nanotubes*; Academic Press: San Diego, CA, 1996; pp 1−985. (b) Saito, R.; Dresselhaus, S.; Dresselhaus, M. S. *Physical Properties of Carbon Nanotubes*; Imperial College Press: London, 1998.
(228) Choi, H. S.; Kim, K. S. *Angew Chem., Int. Ed.* **1999**, *38*, 2256. Tonmunphean, S.; Wijitkosoom, A.; Tantirungrotechai, Y.; Nuttavut, N.; Limtrakul, J. *Bull. Chem. Soc. Jpn.* **2003**, *76*, 1537. Türker, L. *THEOCHEM* **2000**, *531*, 333. Yang, S. W.; Zhang, H.; Soon, J. M.; Lim, C. W.; Wu, P.; Loh, K. P. *Diamond Relat. Mater.* **2003**, *12*, 1194. Loh, K. P.; Yang, S. W.; Soon, J. M.; Zhang, H.; Wu, P. *J. Phys. Chem. A* **2003**, *107,* 5555.
(229) Stoddart, J. F. *Nature* **1988**, *334*, 10 and references therein.
(230) For the most recent experimental attempts, see: (a) Neudorff, W. D.; Lentz, D.; Anibarro, M.; Schlüter, A. D. *Chem. Eur. J.* **2003**, *9*, 2745. (b) Godt, A.; Enkelmann, V.; Schlüter, A. D. *Angew. Chem., Int. Ed. Engl.* **1989**, *28*, 1680. (c) Kintzel, O.; Luger, P.; Weber, M.; Schlüter, A. D. *Eur. J. Org. Chem.* **1998**, 99 and references therein.
(231) Chiang, C. K.; Fincher, C. R., Jr.; Park, Y. W.; Heeger, A. J.; Shirakawa, H.; Louis, E. J.; Gau, S. C.; MacDiarmid, A. G. *Phys. Rev. Lett.* **1979**, *39*, 1098.
(232) For a detailed, most recent discussion of the Peierls instability in polyacene and oligoacenes, see: Raghu, C.; Patil, Y. A.; Ramasesha, S. *Phys. Rev. B* **2002**, *65*, 155204/1.
(233) Brédas, J. L.; Chance, R. R.; Baughman, R. H. *J. Chem. Phys.* **1982**, *76*, 3673.
(234) Pomerantz, M.; Cardona, R.; Rooney, P. *Macromolecules* **1989**, *22*, 304.
(235) A low band gap of 0.2 eV for polyacene was predicted in: Kao, J.; Lilly, A. C., Jr. *J. Am. Chem. Soc.* **1987**, *109*, 4149.

(236) Cizek, J.; Paldus, J. *J. Chem. Phys.* **1970**, *53*, 821.
(237) Lowe, J. P.; Kafafi, S. A.; LaFemina, J. P. *J. Phys. Chem.* **1986**, *90*, 6602.
(238) Kivelson, S.; Chapman, O. L. *Phys. Rev. B* **1983**, *28*, 7236.
(239) For early calculations, see: Boon, M. R. *Theor. Chim. Acta* **1971**, *23*, 109. Tanaka, K.; Ozeki, K.; Nankai, S.; Yamabe, T.; Shirakawa, H. *J. Phys. Chem. Solids* **1983**, *44*, 1069.
(240) Longuett Higgins, H. C.; Salem, L. *Proc. R. Soc. London, Ser. A* **1959**, *251*, 172. Longuett Higgins, H. C.; Salem, L. *Proc. R. Soc. London, Ser. A* **1960**, *255*, 435.
(241) Kertesz, M.; Hoffmann, R. *Solid State Commun.* **1983**, *47*, 97.
(242) Houk, K. N.; Lee, P. S.; Nendel, M. *J. Org. Chem.* **2001**, *66*, 5107.
(243) Srinivasan, B.; Ramasesha, S. *Phys. Rev. B* **1998**, *57*, 8927.
(244) Yamabe, T.; Tonaka, K.; Ohzeki, K.; Yata, S. *Solid State Commun.* **1982**, *44*, 823.
(245) Whangbo, M. H.; Hoffmann, R.; Woodward, R. B. *Proc. R. Soc. London, Ser. A* **1979**, *366*, 23.
(246) Kertesz, M.; Lee, Y. S.; Stewart, J. J. P. *Int. J. Quantum Chem.* **1989**, *35*, 304.
(247) Chandrasekhar, J.; Das, P. K. *J. Phys. Chem.* **1992**, *96*, 679.
(248) Cioslowski, J. *J. Chem. Phys* **1993**, *98*, 473.
(249) Bendikov, M.; Duong, H. M.; Starkey, K.; Houk, K. N.; Carter, E. A.; Wudl, F. *J. Am. Chem. Soc.* **2004**, *126*, 7416.
(250) Wiberg, K. *J. Org. Chem.* **1997**, *62*, 5720.
(251) Wang, D. Z.; Streitwieser, A. *Theor. Chem. Acc.* **1999**, *102*, 78.
(252) Rienstra-Kiracofe, J. C.; Barden, C. J.; Brown, S. T.; Schaefer, H. F. *J. Phys. Chem. A* **2001**, *105*, 524.
(253) Suresh, C. H.; Gadre, S. R. *J. Org. Chem.* **1999**, *64*, 2505 and references therein.
(254) The aromaticity in polyacenes was also studied by Cyrański et al.: Cyrański, M. K.; Stepien, B. T.; Krygowski, T. M. *Tetrahedron* **2000**, *56*, 9663.
(255) Similar results were also reported in: Cheng, M.-F.; Li, W.-K. *Chem. Phys. Lett.* **2003**, *368*, 630.
(256) Schleyer, P. v. R.; Maerker, C.; Dransfeld, A.; Jiao, H.; Hommes, N. J. R. v. E. *J. Am. Chem. Soc.* **1996**, *118*, 6317.
(257) Raghu, C.; Anusooya Pati, Y.; Ramasesha, S. *Phys. Rev. B* **2002**, *66*, 035116/1.
(258) Gao, Y.; Liu, C.-G.; Jiang, Y.-S. *J. Phys. Chem. A* **2002**, *106*, 2592.
(259) Aihara, J. *Phys. Chem. Chem. Phys.* **1999**, *1*, 3193.
(260) Angliker, H.; Rommel, E.; Wirz, J. *Chem. Phys. Lett.* **1982**, *87*, 208.
(261) Open-shell ground-state singlet disjoint diradicals have been discussed in detail by Borden, Davidson, and others: (a) Borden, W. T.; Davidson, E. R. *J. Am. Chem. Soc.* **1977**, *99*, 4587. (b) Du, P.; Borden, W. T. *J. Am. Chem. Soc.* **1987**, *109*, 930. (c) Du, P.; Hrovat, D. A.; Borden, W. T.; Lahti, P. M.; Rossi, A. R.; Berson, J. A. *J. Am. Chem. Soc.* **1986**, *108*, 5072. (d) Hrovat, D. A.; Borden, W. T. *J. Am. Chem. Soc.* **1994**, *116*, 6327. (e) Bally, T.; Borden, W. T. *Rev. Comput. Chem.* **1999**, *13*, 1. (f) Filatov, M.; Shaik, S. *J. Phys. Chem. A* **1999**, *103,* 8885. (g) Clifford, E. P.; Wenthold, P. G.; Lineberger, W. C.; Ellison, G. B.; Wang, C. X.; Grabowski, J. J.; Vila, F.; Jordan, K. D. *J. Chem. Soc., Perkin Trans. 2* **1998**, 1015.
(262) Borden, W. T.; Iwamura, H.; Berson, J. A. *Acc. Chem. Res.* **1994**, *27*, 109.
(263) Heeger, A. J.; Kivelson, S.; Schrieffer, J. R.; Su, W.-P. *Rev. Mod. Phys.* **1988**, *60*, 781.
(264) (a) Hochstrasser, R. M.; Wesel, J. E. *Chem. Phys. Lett.* **1974**, *24*, 1. (b) Wunsch, L.; Metz, F.; Neusser, H. J.; Schlag, E. W. J. *Chem. Phys*. **1976**, *66*, 386. (c) Friedrich, D. M.; McClain, W. M. *Chem. Phys. Lett.* **1975**, *32*, 541.
(265) Haas, Y.; Zilberg, S. *J. Am. Chem. Soc.* **1995**, *117*, 5387.
(266) Mikami, N.; Ito, M. *Chem. Phys*. **1977**, *23*, 141. Swiderek, P.; Hohlneicher, G.; Maluendes, S. A.; Dupuis, M. *J. Chem. Phys.* **1993**, *98*, 974.
(267) Zilberg, S.; Samuni, U.; Fraenkel, R.; Haas, Y. *Chem. Phys.* **1994**, *186*, 303. Zilberg, S.; Haas, Y.; Shaik, S. *J. Phys. Chem.* **1995**, *99*, 16558.
(268) Shaik, S.; Zilberg, S.; Haas, Y. *Acc. Chem. Res.* **1996**, *29*, 211.
(269) Shaik, S.; Shurki, A.; Danovich, D.; Hiberty, P. C. *Chem. Rev.* **2001**, *101*, 1501.
(270) Herwig, P. T.; Müllen, K. *Adv. Mater*. **1999**, *11*, 480−483.
(271) Kim, K.; Yoon, Y. K.; Mun, M.-O.; Park, S. P.; Kim, S. S.; Im, S.; Kim, J. H. *J. Supercond.* **2002**, *15*, 595.
(272) *UV Atlas of Organic Compounds*; Plenum Press: New York, 1966; Vol. 3.
(273) Szczepanski, J.; Wehlburg, C.; Vala, M. *Chem. Phys. Lett.* **1995**, *232*, 221.
(274) Halasinski, T. M.; Hudgins, D. M.; Salama, F.; Allamandola, L. J.; Bally, T. *J. Phys. Chem. A* **2000**, *104*, 7484.
(275) Heinze, H. H.; Görling, A.; Rösch, N. *J. Chem. Phys.* **2000**, *113*, 2088.
(276) Nijegorodov, N.; Ramachandran, V.; Winkoun, D. P. *Spectrochim. Acta, A* **1997**, *53*, 1813.
(277) Meot-Ner (Mautner), M. *J. Phys. Chem.* **1980**, *84*, 2716.
(278) Notario, R.; Abboud, J.-L. M. *J. Phys. Chem. A* **1998**, *102,* 5290.
(279) Deleuze, M. S.; Trofimov, A. B.; Cederbaum, L. S. *J. Chem. Phys.* **2001**, *115*, 5859. Deleuze, M. S. *J. Chem. Phys.* **2002**, *116*, 7012.
(280) Deleuze, M. S.; Claes, L.; Kryachko, E. S.; François, J.-P. *J. Chem. Phys.* **2003**, *119*, 3106.
(281) Burrow, P. D.; Michejda, J. A.; Jordan, K. D. *J. Chem. Phys.* **1987**, *86*, 9.
(282) Schiedt, J.; Weinkauf, R. *Chem. Phys. Lett.* **1997**, *266*, 201.
(283) Crocker, L.; Wang, T.; Kebarle, P. *J. Am. Chem. Soc.* **1993**, *115*, 7818.
(284) Silinsh, E. A. *Organic molecular crystals: their electronic states*; Springer series in solid-state sciences, Vol. 16; Springer-Verlag: Berlin−New York, 1980.
(285) Bacon, G. E.; Curry, N. A.; Wilson, S. A. *Proc. R. Soc. London, Ser. A* **1964**, *279*, 98.
(286) Search of a Cambridge database for benzene, naphthalene, anthracene, tetracene, and pentacene.
(287) Desiraju, G. R.; Gavezzotti, A. *Acta Crystallogr., Sect. B* **1989**, *45*, 473.
(288) Silinsh, E. A. *Organic Molecular Crystals*; Springer-Verlag: Berlin, 1980.
(289) Hotta, S.; Waragai, K. *Adv. Mater.* **1993**, *5*, 896. Horowitz, G.; Bachet, B.; Yassar, A.; Lang, P.; Demanze, F.; Fave, J. L.; Garnier, F. *Chem. Mater.* **1995**, *7*, 1337. Siegrist, T.; Fleming, R. M.; Haddon, R. C.; Laudise, R. A.; Lovinger, A. J.; Katz, H. E.; Bridenbaugh, P.; Davis, D. D. *J. Mater. Res.* **1995**, *10*, 2170. Servet, B.; Ries, S.; Trotel, M.; Alnot, P.; Horowitz, G.; Garnier, F. *Adv. Mater.* **1993**, *5*, 461.
(290) Charbonneau, G.-P.; Delugeard, Y. *Acta Crystallogr., Sect. B* **1977**, *33*, 1586.
(291) Desiraju, G. R.; Gavezzotti, A. *Acta Crystallogr., Sect. B* **1989**, *45*, 473.
(292) Gavezzotti, A.; Desiraju, G. R. *Acta Crystallogr., Sect. B* **1988**, *44*, 427.
(293) Venuti, E.; Valle, R. G. D.; Brillante, A.; Masino, M.; Girlando, A. *J. Am. Chem. Soc.* **2002**, *124*, 2128.
(294) Mattheus, C. C.; de Wijs, G. A.; de Groot, R. A.; Palstra, T. T. M. *J. Am. Chem. Soc.* **2003**, *125*, 6323.
(295) Tiago, M. L.; Northrup, J. E.; Louie, S. G. *Phys. Rev. B* **2003**, *67*, 115212.
(296) Campbell, R. B.; Roberston, J. M.; Trotter, J. *Acta Crystallogr*. **1962**, *15*, 289.
(297) Holmes, D.; Kumaraswamy, S.; Matzger, A. J.; Vollhardt, K. P. *Chem. Eur. J*. **1999**, *5*, 3399.
(298) Siegrist, T.; Kloc, Ch.; Schön, J. H.; Batlogg, B.; Haddon, R. C.; Berg, S.; Thomas, G. A. *Angew. Chem., Int. Ed*. **2001**, *40*, 1732.
(299) Mattheus, C. C.; Dros, A. B.; Baas, J.; Meetsma, A.; de Boer, J. L.; Palstra, T. T. M. *Acta Crystallogr., Sect. C* **2001**, 57, 939.
(300) Della Valle, R. G.; Venuti, E.; Brillante, A.; Girlando, A. *J. Chem. Phys.* **2003**, *118*, 807.
(301) Curtis, M. D.; Cao, J.; Kampf, J. W. *J. Am. Chem. Soc.* **2004**, *126*, 4318.
(302) Haddon, R. C.; Chi, X.; Itkis, M. E.; Anthony, J. E.; Eaton, D. L.; Siegrist, T.; Mattheus, C. C.; Palstra, T. T. M. *J. Phys. Chem. B* **2002**, *106*, 8288.
(303) zu Heringdorf, F.-J. M.; Ruter, M. C.; Tromp, B. M. *Nature* **2001**, *412*, 517.
(304) Fritz, S. E.; Martin, S. M.; Frisbie, C. D.; Ward, M. D.; Toney, M. F. *J. Am. Chem. Soc.* **2004**, *126*, 4084.
(305) Pope, M.; Swenberg, C. E. *Electronic Processes in Organic Crystals and Polymers*, 2nd ed.; Oxford University Press: Oxford, 1999; pp 337−340.
(306) (a) Sariciftci, N. S. *Curr. Opin. Solid State Mater. Sci.* **1999**, *4*, 373. (b) Guldi, D. K.; Prato, M. *Acc. Chem. Res.* **2000**, *33*, 695. (c) Guldi, D. M. *Chem. Commun.* **2000**, 321. (d) Segura, J. L.; Martín, N. *Chem. Soc. Rev.* **2000**, *29*, 13. (e) Diederich, F.; Gómez-López, M. *Chem. Soc. Rev*. **1999**, *28*, 263. (f) Echegoyen, L.; Echegoyen, L. E. *Acc. Chem. Res.* **1998**, *31*, 593. (g) Yu, G.; Gao, J.; Hummelen, J. C.; Wudl, F.; Heeger, A. J. *Science* **1995**, *270*, 1789. (h) Sariciftci, N. S.; Smilowitz, L.; Heeger, A. J.; Wudl, F. *Science* **1992**, *258*, 1474. (i) Chirvase, D.; Chiguvare, Z.; Knipper, M.; Parisi, J.; Dyakonov, V.; Hummelen, J. C. *J. Appl. Phys.* **2003**, *93*, 3376.
(307) McQuade, D. T.; Pullen, A. E.; Swager, T. M. *Chem. Rev.* **2000**, *100*, 2537.
(308) (a) Marsella, M. J.; Reid, R. J.; Estassi, S.; Wang, L. S. *J. Am. Chem. Soc.* **2002**, *124*, 12507. (b) Marsella, M. J.; Reid, R. J. *Macromolecules* **1999**, *32*, 5982. (c) Pede, D.; Smela, E.; Johansson, T.; Johansson, M.; Inganäs, O. *Adv. Mater.* **1998**, *10*, 233. (d) Marsella, M. J. *Acc. Chem. Res.* **2002**, *35*, 944. (e) Baughman, R. H.; Cui, C. X.; Zakhidov, A. A.; Iqbal, Z.; Barisci, J. N.; Spinks, G. M.; Wallace, G. G.; Mazzoldi, A.; De Rossi, D.; Rinzler, A. G.; Jaschinski, O.; Roth, S.; Dertesz, M. *Science* **1999**, *284*, 1340. (f) Pei, Q.; Inganäs, O. *J. Phys. Chem.* **1992**, *96*, 10507. (g) Jager, E. W. H.; Smela, E.; Inganäs, O. *Science* **2000**, *290*, 1540. (h) Smela, E.; Gadegaard, N. *Adv. Mater.* **1999**, *11*, 953.
(309) Wurthner, F. *Angew. Chem., Int. Ed*. **2001**, *40*, 1037.
(310) Horowitz, G. *J. Mater. Res.* **2004**, *19*, 1946.
(311) For other reviews on organic FETs, see: Katz, H. E. *J. Mater. Chem.* **1997**, *7*, 369. Horowitz, G. *Adv. Mater.* **1998**, *10*, 365.

Katz, H. E.; Bao, Z. *J. Phys. Chem. B* **2000**, *104*, 671. Katz, H. E.; Bao, Z.; Gilat, S. L. *Acc. Chem. Res.* **2001**, *34*, 359.
(312) Garnier, F. *Chem. Phys.* **1998**, *227*, 253.
(313) Sze, S. M. *Physics of Semiconductor Devices*; Wiley: New York, 1981.
(314) (a) Senadeera, G. K. R.; Jayaweera, P. V. V.; Perera, V. P. S.; Tennakone, K. *Solar Energy* **2002**, *73*, 103. (b) Videlot, C.; Fichou, D.; Garnier, F. *J. Chim. Phys. Phys.-Chim. Biol.* **1998**, *95*, 1335. (c) Dahlberg, S. C.; Musser, M. E. *J. Chem. Phys.* **1979**, *71*, 2806. (d) Matsumura, M.; Uohashi, H.; Furusawa, M.; Yamamoto, N.; Tsubomura, H. *Bull. Chem. Soc. Jpn.* **1975**, *48*, 1965.
(315) Gruhn, N. E.; da Silva Filho, D. A.; Bill, T. G.; Malagoli, M.; Coropceanu, V.; Kahn, A.; Brédas, J. L. *J. Am. Chem. Soc.* **2002**, *124*, 7918.
(316) Klauk, H.; Halik, M.; Zschieschang, U.; Schmid, G.; Radlik, W. *J. Appl. Phys.* **2002**, *92*, 5259.
(317) Kelley, T. W.; Muyres, D. V.; Baude, P. F.; Smith, T. P.; Jones, T. D. *MRS Symp. Proc.* **2003**, *771*, 169.
(318) Kelley, T. W.; Boardman, L. D.; Dunbar, T. D.; Muyres, D. V.; Pellerite, M. J.; Smith, T. P. *J. Phys. Chem. B* **2003**, *107*, 5877.
(319) Butko, V. Y.; Chi, X.; Lang, D. V.; Ramirez, A. P. *Appl. Phys. Lett.* **2003**, *83*, 4773.
(320) de Boer, R. W. I.; Gershenson, M. E.; Morpurgo, A. F.; Podzorov, V. Los Alamos National Laboratory, Preprint Archive, Condensed Matter **2004**, 1−23, http://xxx.lanl.gov/pdf/cond-mat/0404100
(321) Laquindanum, J. G.; Katz, H. E.; Lovinger, A. J.; Dodabalapur, A. *Chem. Mater.* **1996**, *8*, 2542.
(322) (a) Garnier, F. *Chem. Phys.* **1998**, *227*, 253. (b) Katz, H. E.; Dodabalapur, A.; Bao, Z. In *Handbook of Oligo- and Polythiophenes*; Fichou, D., Ed.; Wiley-VCH: Weinheim, Germany, 1999; p 459. (c) Horowitz, G.; Peng, X.; Fichou, D.; Garnier, F. *J. Appl. Phys.* **1990**, *67*, 528. (d) Horowitz, G. *Adv. Mater.* **1998**, *10*, 365. (e) Horowitz, G.; Hajlaoui, R.; Bouchriha, R. B.; Hajlaoui, M. *Adv. Mater.* **1998**, *10*, 923.
(323) Lin, Y.; Gundlach, D. J.; Nelson, S. F.; Jackson, T. N. *IEEE Trans. Electron Devices* **1997**, *44*, 1325.
(324) Koch, N.; Ghijsen, J.; Johnson, R. L.; Schwartz, J.; Pireaux, J.-J.; Kahn, A. *J. Phys. Chem. B* **2002**, *106*, 4192.
(325) Kymissis, I.; Dimitrakopoulos, C. D.; Purushothaman, S. *IEEE Trans. Electron Devices* **2001**, *48*, 1060.
(326) Anthony, J. E.; Brooks, J. S.; Eaton, D. L.; Parkin, S. R. *J. Am. Chem. Soc.* **2001**, *123*, 9482.
(327) Meng, H.; Bendikov, M.; Mitchell, G.; Helgeson, R.; Wudl, F.; Bao, Z.; Siegrist, T.; Kloc, C.; Chen, C.-H. *Adv. Mater.* **2003**, *15*, 1090.
(328) Lee, J.; Kim, K.; Kim, J. H.; Im, S.; Jung, D.-Y. *Appl. Phys. Lett.* **2003**, *82*, 4169−4171.
(329) Zhang, Y.; Petta, J. R.; Ambily, S.; Shen, Y.; Ralph, D. C.; Malliaras, G. G. *Adv. Mater.* **2003**, *15*, 1632.
(330) Gundlach, D. J.; Lin, Y.-Y.; Jackson, T. N.; Nelson, S. F.; Schlom, D. G. *IEEE Electron Device Lett.* **1997**, *18*, 87.
(331) Knipp, D.; Street, R. A.; Volkel, A. R. *Appl. Phys. Lett.* **2003**, *82*, 3907.
(332) There is a preliminary report for the first inkjet-printed organic transistors fabricated using a soluble pentacene precursor using a retro Diels−Alder reaction. Although mobilities are lower [>0.01 cm^2/(V s)] than those in vacuum deposited films, solution-based processing is the key for ultralow-cost circuit fabrication, and development of new soluble pentacene precursors is of great promise for the future of organic FETs: Volkman, S. K.; Molesa, S.; Mattis, B.; Chang, P. C.; Subramanian, V. *MRS Symp. Proc.* **2003**, *771*, 391.
(333) Brown, A. R.; Pomp, A.; Hart, C. M.; de Leeuw, D. M.; Klassen, D. B. M.; Havinga, E. E.; Herwig, P.; Müllen, K. *J. Appl. Phys.* **1996**, *79*, 2136.
(334) Afzali, A.; Dimitrakopoulos, C. D.; Breen, T. L. *J. Am. Chem. Soc.* **2002**, *124*, 8812.
(335) Afzali, A.; Dimitrakopoulos, C. D.; Graham, T. O. *Adv. Mater.* **2003**, *15*, 2066.
(336) For a review on computations of transport properties in organic materials, see: Brédas, J. L.; Beljonne, D.; Cornil, J.; Calbert, J. Ph.; Shuai, Z.; Silbey, R. *Synth. Met.* **2002**, *125*, 107.
(337) Karl, N. *Synth. Met.* **2003**, *133−134*, 649 and references therein.
(338) Coropceanu, V.; Malagoli, M.; da Silva Filho, D. A.; Gruhn, N. E.; Bill, T. G.; Brédas, J. L. *Phys. Rev. Lett.* **2002**, *89*, 275503/1−275503/4. See also: Gruhn, N. E.; da Silva Filho, D. A.; Bill, T. G.; Malagoli, M.; Coropceanu, V.; Kahn, A.; Brédas, J.-L. *J. Am. Chem. Soc.* **2002**, *124*, 7918.
(339) Cornil, J.; Calbert, J. Ph.; Brédas, J. L. *J. Am. Chem. Soc.* **2001**, *123*, 1250.
(340) For a review see: Cornil, J.; Beljonne, D.; Calbert, J.-P.; Brédas, J.-L. *Adv. Mater.* **2001**, *13*, 1053.
(341) Cheng, Y. C.; Silbey, R. J.; da Silva Filho, D. A.; Calbert, J. P.; Cornil, J.; Brédas, J. L. *J. Chem. Phys.* **2003**, *118*, 3764.
(342) Heeger, A. J. In *Highly Conducting One-Dimensional Solids*; Devreese, J. T., Evrard, R. P., van Doren, V. E., Eds.; Plenum Press: New York, 1979; p 69 and references therein.
(343) Brédas, J. L.; Calbert, J. P.; Da Silva Filho, D. A.; Cornil, J. *Proc. Natl. Acad. Sci. U.S.A.* **2002**, *99*, 5804.
(344) Sancho-Garcia, J. C.; Horowitz, G.; Brédas, J. L.; Cornil, J. *J. Chem. Phys.* **2003**, *119*, 12563.
(345) The reorganization energy (λ) for self-exchange corresponds to the sum of the geometry relaxation energies upon going from the neutral-state geometry to the charged-state geometry and vice versa. These two portions of λ are typically nearly identical; see: Malagoli, M.; Brédas, J. L. *Chem. Phys. Lett.* **2000**, *327*, 13.
(346) Ito, K.; Suzuki, T.; Sakamoto, Y.; Kubota, D.; Inoue, Y.; Sato, F.; Tokito, S. *Angew. Chem., Int. Ed.* **2003**, *42*, 1159.
(347) Laquindanum, J. G.; Katz, H. E.; Lovinger, A. J. *J. Am. Chem. Soc.* **1998**, *120*, 664.
(348) Butko, V. Y.; Chi, X.; Ramirez, A. P. *Solid State Commun.* **2003**, *128*, 431.
(349) de Boer, R. W. I.; Klapwijk, T. M.; Morpurgo, A. F. *Appl. Phys. Lett.* **2003**, *83*, 4345.
(350) Podzorov, V.; Sysoev, S. E.; Loginova, E.; Pudalov, V. M.; Gershenson, M. E. *Appl. Phys. Lett.* **2003**, *83*, 3504. See also: Podzorov, V.; Pudalov, V. M.; Gershenson, M. E. *Appl. Phys. Lett.* **2003**, *82*, 1739.
(351) Bulgarovskaya, I.; Vozzhennikov, V.; Aleksandrov, S.; Bel'skii, V. *Latv. PSR Zinat. Akad. Vestis, Kim. Ser.* **1983**, *4*, 53. The same unit cell parameters were reported in: Henn, D. E.; Williams, W. G.; Gibbons, D. J. *J. Appl. Crystallogr.* **1971**, *4*, 256.
(352) Dodge, J. A.; Bain, J. D.; Chamberlin, A. R. *J. Org. Chem.* **1990**, *55*, 4190.
(353) Sundar, V. C.; Zaumseil, J.; Podzorov, V.; Menard, E.; Willett, R. L.; Someya, T.; Gershenson, M. E.; Rogers, J. A. *Science* **2004**, *303*, 1644.
(354) Allen, C. F. H.; Bell, A. *J. Am. Chem. Soc.* **1942**, *64*, 1253.
(355) Chen, Y.; Wudl, F. Unpublished.
(356) Maulding, D. R.; Roberts, B. G. *J. Org. Chem.* **1969**, *34*, 1734.
(357) Anthony, J. E.; Eaton, D. L.; Parkin, S. R. *Org. Lett.* **2002**, *4*, 15.
(358) Payne, M. M.; Delcamp, J. H.; Parkin, S. R.; Anthony, J. E. *Org. Lett.* **2004**, *6*, 1609.
(359) Sheraw, C. D.; Jackson, T. N.; Eaton, D. L.; Anthony, J. E. *Adv. Mater.* **2003**, *15*, 2009.
(360) We could not locate the recent reliable value of resistivity of parent pentacene. A value of 10^{14} Ω cm was reported by Schön et al. (Schön, J. H.; Kloc, Ch.; Batlogg, B. *Appl. Phys. Lett.* **2000**, *77*, 2473); however, many of the papers by Schön et al. were the subject of independent investigations[208] and latter retracted. Anthony et al.[326] cited, on the basis of the same work of Schön et al., the value of 10^{12} Ω cm for the resistivity of pentacene. The conductivity of pentacene was estimated to be below 10^{-9} S cm^{-1} by Minakata et al.[427]
(361) Brooks, J. S.; Eaton, D. L.; Anthony, J. E.; Parkin, S. R.; Brill, J. W.; Shusko, Y. *Curr. Appl. Phys.* **2001**, *1*, 301.
(362) Tokumoto, T.; Brooks, J. S.; Clinite, R.; Wei, X.; Anthony, J. E.; Eaton, D. L.; Parkin, S. R. Los Alamos National Laboratory, Preprint Archive, Condensed Matter, **2002**, 1−18, http://xxx.lanl.gov/pdf/cond-mat/0203522.
(363) Takahashi, T.; Kitamura, M.; Shen, B.; Nakajima, K. *J. Am. Chem. Soc.* **2000**, *122*, 12876.
(364) One example of *intra*molecular [4 + 2] cyclization of a 1,2 double bond of one anthracene moiety acting as a dienophile toward the 9,10 diene of another anthracene is known: Becker, H.-D.; Anderson, K. *Tetrahedron Lett.* **1983**, *24*, 3273.
(365) Perepichka, D. F.; Bendikov, M.; Meng, H.; Wudl, F. *J. Am. Chem. Soc.* **2003**, *125*, 10190.
(366) Recently, graphitization of predefined polycyclic aromatic hydrocarbons at 800 °C was reported. Gherghel, L.; Kübel, C.; Lieser, G.; Räder, H.-J.; Müllen, K. *J. Am. Chem. Soc.* **2002**, *124*, 13130.
(367) High-quality 5−40 μm size single crystals of diamonds can be formed from the PAH. Davydov, V. A.; Rakhmanina, A. V.; Agafonov, V.; Narymbetov, B.; Boudou, J.-P.; Szwarc, H. *Carbon* **2004**, *42*, 261.
(368) Anderson, J. E.; Bettels, B. R. *J. Chem. Soc., Perkin Trans. 2* **1990**, *7*, 1121.
(369) Kudryasheva, N. S.; Val'kova, G. A.; Shigorin, D. N.; Gorelik, M. V. *Russ. J. Phys. Chem. (Engl. Transl.)* **1989**, *63*, 91.
(370) Lang, K. F.; Zander, M. *Chem. Ber.* **1963**, *96*, 707.
(371) Brzezinski, B.; Zundel, G. *J. Phys. Chem.* **1994**, *98*, 2271.
(372) Brzezinski, B.; Zundel, G. *Chem. Phys. Lett.* **1991**, *178*, 138.
(373) Clar, E. *Chem. Ber.* **1932**, *65*, 503.
(374) Medne, R. S.; Livdane, A. D.; Neiland, O. Ya. Patent SU 2077069, 1977 (in Russian); *Ref. Zh. Khim.* **1978**, *14*, N204P.
(375) Ferguson, G.; Parvez, M. *Acta Crystallogr.* **1979**, *B35*, 2419.
(376) (a) Smyth, N.; Engen, V. D.; Pascal, R. A., Jr. *J. Org. Chem.* **1990**, *55*, 1937. (b) Pascal, R. A., Jr.; McMillan, W. D.; Engen, V. D.; Eason, R. G. *J. Am. Chem. Soc.* **1987**, *109*, 4660. (c) Schuster, I. I.; Cracium, L.; Ho, D. M.; Pascal, R. A., Jr. *Tetrahedron* **2002**, *58*, 8875. (d) Zhang, J.; Ho, D. M.; Pascal, R.

A., Jr. *Tetrahedron Lett.* **1999**, *40*, 3859. (e) Qiao, X.; Ho, D. M.; Pascal, R. A., Jr. *Angew. Chem., Int. Ed. Engl.* **1997**, *36*, 1531.
(377) Duong, H. M.; Bendikov, M.; Steiger, D.; Zhang, Q.; Sonmez, G.; Yamada, J.; Wudl, F. *Org. Lett.* **2003**, *5*, 4433.
(378) Clar, E. *Polycyclic Hydrocarbons*; Academic Press: London, 1964; Vol. 2, p 200.
(379) Yang, Y.; Xu, Q.; Duong, H. M.; Wudl, F. *Appl. Phys. Lett.*, in press.
(380) For a theoretical study of reaction of acenes with ethylene, see ref 200 and also ref 255.
(381) For a comprehensive review of cycloaddition reactions of fullerenes, see: Yurovskaya, M. A.; Trushkov, I. V. *Russ. Chem. Bull.* **2002**, *51*, 367.
(382) Martín, N.; Segura, J. L.; Wudl, F. *Dev. Fullerene Sci.* **2002**, *4*, 81.
(383) Schlüter, J. A.; Seaman, J. M.; Taha, S.; Cohen, H.; Lykke, K. R.; Wang, H. H.; Williams, J. M. *J. Chem. Soc., Chem. Commun*. **1993**, 972. Komatsu, K.; Murata, Y.; Sugita, N.; Takeuchi, K.; Wan, T. S. M. *Tetrahedron Lett*. **1993**, *34*, 8473. Tsuda, M.; Ishida, T.; Nogami, T.; Kurono, S.; Ohashi, M. *J. Chem. Soc., Chem. Commun*. **1993**, 1296.
(384) Lamparth, I.; Maichle-Moessmer, C.; Hirsch, A. *Angew. Chem., Int. Ed. Engl*. **1995**, *34*, 1607. Wang, G. W.; Saunders, M.; Cross, R. J. *J. Am. Chem. Soc*. **2001**, *123*, 256.
(385) Chronakis, N.; Orfanopoulos, M. *Tetrahedron Lett*. **2001**, *42*, 1201.
(386) Kräutler, B.; Müller, T.; Duarte-Ruiz, A. *Chem. Eur. J.* **2001**, *7*, 3223.
(387) Kräutler, B.; Müller, T.; Maynollo, J.; Gruber, K.; Kratky, C.; Ochsenbein, P.; Schwarzenbach, D.; Bürgi, H.-B. *Angew. Chem., Int. Ed. Engl.* **1996**, *35*, 1204.
(388) Murata, Y.; Kato, N.; Fujiwara, K.; Komatsu, K. *J. Org. Chem.* **1999**, *64*, 3483.
(389) Takaguchi, Y.; Tajima, T.; Ohta, K.; Motoyoshiya, J.; Aoyama, H.; Wakahara, T.; Akasaka, T.; Fujitsuka, M.; Ito, O. *Angew. Chem., Int. Ed*. **2002**, *41*, 817.
(390) Mack, J.; Miller, G. P. *Fullerene Sci. Technol.* **1997**, *5*, 607.
(391) Miller, G. P.; Briggs, J.; Mack, J.; Lord, P. A.; Olmstead, M. M.; Balch, A. L. *Org. Lett.* **2003**, *5*, 4199.
(392) Berg, O.; Chronister, E. L.; Yamashita, T.; Scott, G. W.; Sweet, R. M.; Calabrese, J. *J. Phys. Chem. A* **1999**, *103*, 2451.
(393) Miller, G. P.; Mack, J. *Org. Lett.* **2000**, *2*, 3979.
(394) Miller, G. P.; Mack, J.; Briggs, J. *Org. Lett.* **2000**, *2*, 3983.
(395) Bürgi, H.-B.; Blanc, E.; Schwarzenbach, D.; Liu, S.; Lu, Y.; Kappes, M.. M.; Ibers, J. A. *Angew. Chem., Int. Ed*. **1992**, *31*, 640.
(396) Miller, G. P.; Briggs, J. *Org. Lett.* **2003**, *5*, 4203.
(397) Kanbara, T.; Shibata, K.; Fujiki, S.; Kubozono, Y.; Kashino, S.; Urisu, T.; Sakai, M.; Fujiwara, A.; Kumashiro, R.; Tanigaki, K. *Chem. Phys. Lett.* **2003**, *379*, 223.
(398) Haddon, R. C.; Perel, A. S.; Morris, R. C.; Palstra, T. T. M.; Hebard, A. F.; Fleming, R. M. *Appl. Phys. Lett.* **1995**, *67*, 121.
(399) Kobayashi, S.; Takenobu, T.; Mori, S.; Fujiwara, A.; Iwasa, Y. *Appl. Phys. Lett.* **2003**, *82*, 4581.
(400) Hutchison, K.; Srdanov, G.; Hicks, R.; Yu, H.; Wudl, F.; Strassner, T.; Nendel, M.; Houk, K. N. *J. Am. Chem. Soc*. **1998**, *120*, 2989.
(401) (a) Wudl, F.; Koutentis, P. A.; Weitz, A.; Ma, B.; Strassner, T.; Houk, K. N.; Khan, S. I. *Pure Appl. Chem.* **1999**, *71*, 295. (b) Koutentis, P. A. *ARKIVOC* **2002**, 175.
(402) Bendikov, M.; Wudl, F. Unpublished.
(403) Riley, A. E.; Mitchell, G. W.; Koutentis, P. A.; Bendikov, M.; Kaszynki, P.; Wudl, F.; Tolbert, S. H. *Adv. Funct. Mater.* **2003**, *13*, 531.
(404) Choi, H.; Yang, X.; Mitchell, G. W.; Collier, C. P.; Wudl, F.; Heath, J. R. *J. Phys. Chem. B* **2002**, *106*, 1833.
(405) Miao, Q.; Nguyen, T.-Q.; Someya, T.; Blanchet, G. B.; Nuckolls, C. *J. Am. Chem. Soc.* **2003**, *125*, 10284.
(406) To be published (Wudl, F.; Starkey, K.; Duong, H. An isoquinolone approach to polyacenes. *Abstracts of Papers*, 221st National Meeting of the American Chemical Society, 2001; ORGN-423).
(407) Shchegolev, I. F.; Yagubskii, E. B. Cation radical salts of tetrathiotetracene and tetraselenotetracene: synthetic aspects and physical properties. In *Extended Linear Chain Compounds*; Miller, J. S., Ed.; Plenum Press: New York, 1982; Vol. 2, pp 385−434.
(408) Marshalk, C.; Stumm, C. *Bull. Soc. Chim. Fr.* **1948**, 418.
(409) Marshalk, C. *Bull. Soc. Chim. Fr.* **1952**, 800.
(410) These methods were later improved by Perez-Albuerne: Perez-Albuerne, B. A. U. S. Patent 3,723,417, 1973.
(411) Geiger, W. B. *J. Phys. Chem.* **1973**, *77*, 1862.
(412) Chibisova, T. A.; Redchenko, V. V.; Semenov, S. G.; Kramarenko, S. S.; Solomentseva, T. I. *J. Gen. Chem. USSR* **1990**, 364.
(413) Riga, J.; Verbist, J. J.; Wudl, F.; Kruger, A. *J. Chem. Phys.* **1978**, *69*, 3221.
(414) Matsunaga, Y. *J. Chem. Phys.* **1965**, *42*, 2248.
(415) Shirotani, I.; Kamura, Y.; Inokuchi, H.; Hirooka, I. *Chem. Phys. Lett.* **1976**, *40*, 257.
(416) Shibaeva, R. P. In *Extended Linear Chain Compounds*; Miller, J. S., Ed.; Plenum Press: New York, 1982; Vol. 2, pp 435−67.
(417) Dideberg, O.; Toussaint, J. *Acta Crystallogr., Ser. B* **1974**, *30*, 2481. Shibaeva, R. P.; Rozenberg, L. P. *Kristallografiya* **1975**, *20*, 943.
(418) Hilti, D.; Mayer, C. W.; Rihs, G. *Helv. Chim. Acta* **1978**, *61*, 1462. Sandman, D. J.; Stark, J. C.; Hamill, G. P.; Burke, W. A.; Foxman, B. M. *Mol. Cryst. Liq. Cryst.* **1982**, *86*, 1819.
(419) Marshalk, C.; Niederhauser, J. P. *Bull. Soc. Chim. Fr.* **1952**, 151.
(420) Perez-Albuerne, B. A.; Johnson, H.; Trevoy, D. J. *J. Chem. Phys.* **1971**, *55*, 1547.
(421) Wheland, R. C.; Gillson, J. L. *J. Am. Chem. Soc.* **1976**, *98*, 3916.
(422) Bramwell, F. B.; Haddon, R. C.; Wudl, F.; Kaplan, M. L.; Marshall, J. H. *J. Am. Chem. Soc.* **1978**, *100*, 4612.
(423) Takimiya, K.; Ohnishi, A.; Aso, Y.; Otsubo, T.; Ogura, F.; Kawabata, K.; Tanaka, K.; Mizutani, M. *Bull. Chem. Soc. Jpn.* **1994**, *67*, 766.
(424) Sekizaki, S.; Tada, C.; Yamochi, H.; Saito, G. *J. Mater. Chem.* **2001**, *11*, 2293.
(425) Wudl, F.; Schafer, D. B.; Miller, D. *J. Am. Chem. Soc.* **1976**, *98*, 252.
(426) Perepichka, D. F.; Kondratenko, M.; Hong, M. To be published.
(427) Minakata, T.; Nagoya, I.; Ozaki, M. *J. Appl. Phys.* **1991**, *69*, 7354.
(428) Minakata, T.; Ozaki, M.; Imai, H. *J. Appl. Phys.* **1993**, *74*, 1079.
(429) Ito, T.; Mitani, T.; Takenobu, T.; Iwasa, Y. *J. Phys. Chem. Solids* **2004**, *65*, 609.
(430) Matsuo, Y.; Sasaki, S.; Ikehata, S. *Synth. Met.* **2001**, *121*, 1383.
(431) Matsuo, Y.; Sasaki, A.; Yoshida, Y.; Ikehata, S. *Mol. Cryst. Liq. Cryst. Sci. Technol., Sect. A* **2000**, *340*, 223.
(432) Matsuo, Y.; Suzuki, T.; Yokoi, Y.; Ikehata, S. *J. Phys. Chem. Solids* **2004**, *65*, 619.
(433) (a) Zhang, Z. L.; Jiang, X. Y.; Zhu, W. Q.; Zheng, X. Y.; Wu, Y. Z.; Xu, S. H. *Synth. Met.* **2003**, *137*, 1141. (b) Kondakov, D. Y.; Sandifer, J. R.; Tang, C. W.; Young, R. H. *J. Appl. Phys.* **2003**, *93*, 1108. (c) Danel, K.; Huang, T.-H.; Lin, J. T.; Tao, Y.-T.; Chuen, C.-H. *Chem. Mater.* **2002**, *14*, 3860. (d) Jiang, X.-Y.; Zhang, Z.-L.; Zheng, X.-Y.; Wu, Y.-Z.; Xu, S.-H. *Thin Solid Films* **2001**, *401*, 251. (e) Yu, M. X.; Duan, J.-P.; Lin, C. H.; Cheng, C.-H.; Tao, Y. T. *Chem. Mater.* **2002**, *14*, 3958. (f) Shen, W.-J.; Dodda, R.; Wu, C.-C.; Wu, F.-I.; Liu, T.-H.; Chen, H.-H.; Chen, C.-H.; Shu, C.-F. *Chem. Mater.* **2004**, *16*, 930. (g) Kan, Y.; Wang, L.; Duan, L.; Hu, Y.; Wu, G.; Qiua, Y. *Appl. Phys. Lett.* **2004**, *84*, 1513.
(434) Aziz, H.; Popovic, Z. D. *Appl. Phys. Lett.* **2002**, *80*, 2180. Li, G.; Shinar, J. *Appl. Phys. Lett.* **2003**, *83*, 5359.
(435) Mattoussi, H.; Murata, H.; Merritt, C. D.; Iizumi, Y.; Kido, J.; Kafafi, Z. H. *J. Appl. Phys.* **1999**, *86*, 2642.
(436) Odom, S. A.; Parkin, S. R.; Anthony, J. E. *Org. Lett.* **2003**, *5*, 4245.
(437) Picciolo, L. C.; Murata, H.; Kafafi, Z. H. *Appl. Phys. Lett*. **2001**, *78*, 2378.

CR030666M